Bacillus circulans XYLANASE: STABILITY AND MECHANISM OF ACTION

by

Jamshid Davoodi

Thesis submitted to the School of Graduate Studies, University of Ottawa in partial fulfilment of the requirements for the Degree of Doctor of Philosophy in Biochemistry

ISBN 0-612-16433-0

Canada

ABSTRACT

The stability and mechanism of the action of the enzyme *Bacillus circulans* xylanase (1,4-β-D-xylanohydrolase, EC 3.2.1.8) were investigated by various biophysical techniques. On the basis of the sequence homology between *B. circulans* xylanase and xylanase A from *Schizophyllum commune*, a disulphide bond was introduced between the residues 100 and 148, S100C/N148C (DS1 mutant). The presence of this covalent cross-link leads to a 5 °C increase in the melting point of the protein, as verified by differential scanning calorimetry. Introduction of another disulphide bond in a similar position, V98C/A152C, the DS2 mutant also enhances the stability of the protein by as much as 4 °C. On the basis of the notion that the increase in the stability of a protein is proportional to the number of residues encompassed by the cross-link, the N and C-termini were joined, A1GC/G187,C188, to form the circular xylanase (cXI) mutant. This mutant also acquired a 3.8 °C elevated melting point. A combination of S100C/N148C and A1GC/G187,C188 mutations is accompanied by a 12.3 °C increase in the melting point, which is 3.5 °C more than expected. Thus, the stabilization effect of the two disulphide bonds appears to be cooperative rather than additive. Moreover, the thermodynamic data obtained from differential scanning calorimetry under reversible conditions support previous findings that the stabilizing effect of disulphide bonds is a consequence of a decreased conformational entropy of the unfolded state. Furthermore, the results of this study support the notion that the introduction of a disulphide bond can be used as a strategy to prevent the aggregation of proteins by restricting the exposure of some elements required for this process.

The active site of *Bacillus circulans* xylanase contains two acidic residues, glutamic acids 78 and 172, which are crucial for the catalytic activity of the enzyme. Fourier-transform infrared and near-UV circular dichroism

spectroscopies were used to determine the pK_a of these residues. For the wild type enzyme, a titration of one of carboxylate groups occurs at pH 6.8, as evidenced by FT-IR spectroscopy. This titration is absent in the E78Q or E172Q variants of the enzyme. This, taken with crystallographic data, indicates that glutamic acid at position 172 has an abnormally high pK_a of 6.8. The high pK_a value of Glu 172 is caused largely by electrostatic interactions of this residue with a proximal glutamic acid at position 78. Furthermore, the circular dichroism spectrum of the wild type xylanase shows a structural transition at pH 4.9 in the near-UV region which is absent for the E78C mutant. This taken with the fact that glutamic acid 78 forms a network of hydrogen bonds with tyrosine 69 and tryptophan 71 indicate that the transition with pK_a 4.9 should be attributed to glutamic acid 78. The presence of two proximal carboxyl groups, from glutamic acids 78 and 172, results in a pH-dependent destabilization of the protein structure as evidenced by differential scanning calorimetry experiments with the wild type xylanase and a number of mutant proteins.

Dedication

I am proud to dedicate my thesis to the great nation of Iran without its support this could not be accomplished.

Whether at Naishapour or Babylon,

Whether the Cup with sweet or bitter run,

The Wine of Life keeps oozing drop by drop,

The Leaves of Life kep falling one by one.

Hakim Omar Khayyam (~1050 A.D.)

Translated from Farsi by **Edward FitzGerald** (1859)

Acknowledgements

It is my privilege to thank Drs. Paul R. Carey and Witold K. Surrewicz for their excellent supervision, support and friendship during the course of this study. I have enjoyed working with and learning from such distinguished scientists.

I am indebted to Dr. Waren Wakarchuck for providing various mutants of the enzyme and Dr. Robert Campbell for providing colour views of the protein. Their constructive opinions have certainly enhanced the quality of the research described in the following pages.

I am grateful to Iranian Ministry of Culture and Higher Education for financial support, and to National Research Council of Canada for allowing me to conduct research in their laboratories.

Finally, I would like to express my sincere thanks to my father, mother, and my wife for their continuous support and encouragement.

TABLE OF CONTENTS

CHAPTER I

GENERAL INTRODUCTION

CHAPTER II

THE EFFECT OF A DISULPHIDE BOND ON THE RATE LIMITING STEP IN THE THERMAL DENATURATION PATHWAY OF *Bacillus circulans* XYLANASE: DIFFERENTIAL SCANNING CALORIMETRIC AND THERMAL INACTIVATION STUDIES

CHAPTER III

COOPERATIVE STABILIZATION EFFECT UPON THE INTRODUCTION OF DISULPHIDE BONDS IN *Bacillus circulans* XYLANASE

CHAPTER IV

ON THE ROLE OF CERTAIN ACTIVE SITE RESIDUES OF *Bacillus circulans* XYLANASE

List of Tables

List of Figures

Abbreviations

B. circulans xylanase	*Bacillus circulans* xylanase
CD	Circular dichroism spectroscopy
cDS1 (circular DS1)	S100C, N148C, A1GC, G187, C188
C_p	Heat capacity at constant pressure
cXI (circular xylanase)	A1GC, G187, C188
DS1	S100C, N148C
DS2	V98C, A152C
DSC	Differential scanning calorimetry
E	Activation energy
FTIR	Fourier Transformed Infrared spectroscopy
GdmHCl	Guanidinium chloride
I	Irreversibly denatured state of protein
K_{app}	Apparent kinetic rate constant of the thermal denaturation
N	Native state of the protein
NMR	Nuclear magnetic resonance
NRC	National Research Council of Canada
Q	The heat of partial denaturation
Q_t	The total heat of the calorimetric transition
t_m	Melting point in °C
T_m	Melting point in Kelvin
U	Unfolded state of protein
WT	Wild type
$[E_0]$	The concentration of enzyme at time zero
[E]	The concentration of active enzyme at time t
ν	Scanning rate
Θ	Elipticity

CHAPTER I

GENERAL INTRODUCTION

I.1. OVERVIEW

Xylans are composed of a backbone of 1,4-linked β-D-xylopyranose residues. According to their origin, xylans of hardwoods, softwoods, or grasses have different substituents that are covalently linked to the backbone (Puls, *et al.*, 1989). These substituents may include *O*-acetyl, α-L-arabionfuranosyl, α-D-glucopyranosyluronic acid and 4-*O*-methyl-α-D-glucopyranosyluronic acid.

Birchwood xylan, for instance, can be composed of up to 35% *O*-acetyl-4-*O*-methylglucorono-xylan (Timell, 1967). The substituents of xylan may be further linked to lignin via ether or ester bonds (Dekker 1989; Azuma & Tetsuo 1988).

The degradation of β-1,4 bonds of xylans involves xylanolytic systems which include β-1,4 xylanases (1,4-β-D-xylan xylanohydrolase; EC 3.2.1.8) and β-xylosidases (1,4-β-D-xylan xylohydrolase; EC 3.2.1.37). The former is generally considered to hydrolyse the xylan backbone whereas the latter enzyme is implicated in the hydrolysis of the xylo-oligomers (Dekker & Richards 1976). Cellulases and xylanases have been grouped into at least eight families on the basis of amino acid sequence identities in their putative catalytic domains (Henrissat, *et al.*, 1995; Gilkes, *et al.*, 1991). Xylanases themselves can be grouped into two families, family F and family G, on the basis of primary structure similarity (Henrissat, 1992). The former is composed of high molecular weight xylanases, whereas the latter comprises small molecular weight xylanases (Gilkes *et al.*, 1991; Henrissat, 1992). No significant homology in the catalytic residues could be detected between the two families (Henrissat, 1992).

The potential for biotechnological applications of xylanases has accelerated research aimed at understanding and manipulating the action of these enzymes. The use of xylanases has been proposed as food thickeners (Zeikus, *et al.*, 1991), for increasing the quality of breads (Maat, *et al.*, 1992),

extracting coffee (Biely, 991), clarifying juices and wine (Biely, 1985), and more importantly for prebleaching kraft pulps (Nissen, *et al.*, 1992; Farrell & Skerker, 1992; Wong & Saddler, 1992). In the latter case, to remove the coloured lignin component, pulp is usually treated with chlorine or chlorine containing chemicals at high temperatures and alkaline conditions. This process is normally associated with the production of toxic chloro-organic compounds (Wong & Saddler 1992). Therefore for bleaching kraft pulps, it is of considerable importance to replace, or at least reduce, chlorine charges with environmentally safe substances, biocatalysts. Xylanases are biocatalysts capable of hydrolysing xylan and thereby releasing lignin. These enzymes, in order to be applicable in the bleach boosting process, have to meet the following conditions; firstly, to avoid any damage to pulp strength, they should not have cellulase activity (Wong & Saddler 1992). Furthermore, they should be stable at high temperatures and finally, should show high activity at alkaline conditions. The small size of the *Bacillus circulans* xylanase protein, which facilitates its diffusion, and its lack of cellulotic activity fulfil two requirements for an application in pulp bleaching.

I.2. BACKGROUND ON *Bacillus circulans* XYLANASE

The *B. circulans*. xylanase (1,4-β-D-xylan xylanohydrolase, EC 3.2.1.8) gene was cloned and hyperexpressed in *Escherichia coli* (Yang *et al.*, 1988, Yang *et al.*, 1989; Sung *et al.*, 1993) at the National Research Council of Canada (NRC). This small globular protein, with a molecular weight of 20 kDa and isoelectric point of about 10 (Wakarchuk, unpublished data), belongs to family G xylanases (Fig. I.1, Gilkes *et al.*, 1991). It contains 185 amino acids (Yang *et al.*, 1988) with a sequence identical to *Bacillus subtilis*, except at position 147 (Yaguchi, *et al.*, 1992). Large numbers of aromatic residues can be detected in the primary structure; 11 tryptophans, 16 tyrosines, and 4 phenylalanines. Seven aspartic and two glutamic acids are also present in the protein. Moreover, five lysines and seven arginines form the basic amino acids of the enzyme. It is of note that the wild type protein does not contain any cysteine residues. *B. circulans* xylanase is considered to be an endoxylanase involved in the random hydrolysis of xylosidic bonds in xylan to xylo-oligosaccharides.

The three-dimensional structure of the *B. circulans* xylanase was determined by X-ray crystallography at 1.6 Å resolution (Campbell, *et el.*, 1993). The structure of this enzyme consists of a single domain containing three β-sheets and one α-helix (Fig.I.2). The β-sheets are almost entirely comprised of anti-parallel strands. Two sheets are each composed of five

strands, while the third one contains six strands. The third sheet folds over one side of the only α-helix present in the structure. The active site of the *B. circulans* xylanase is dominated by aromatic residues; six tyrosines, three tryptophans, and one phenylalanine (Campbell, *et el.*, 1993).

The application of *B. circulans* xylanase to the prebleaching of kraft pulp, is unfortunately hampered by its low thermal stability. The availability of different mutants, the high expression level of the enzyme, and detailed structural knowledge provide an opportunity to undertake biophysical studies directed at understanding the thermodynamic and kinetic aspects of the stability of the wild type xylanase and a number of mutant proteins. Thus, while the purpose of this thesis is not to produce stable xylanase variants for immediate industrial application it does set out to provide the fundamental understanding of stability which can be used by other workers in the design of thermostable mutants.

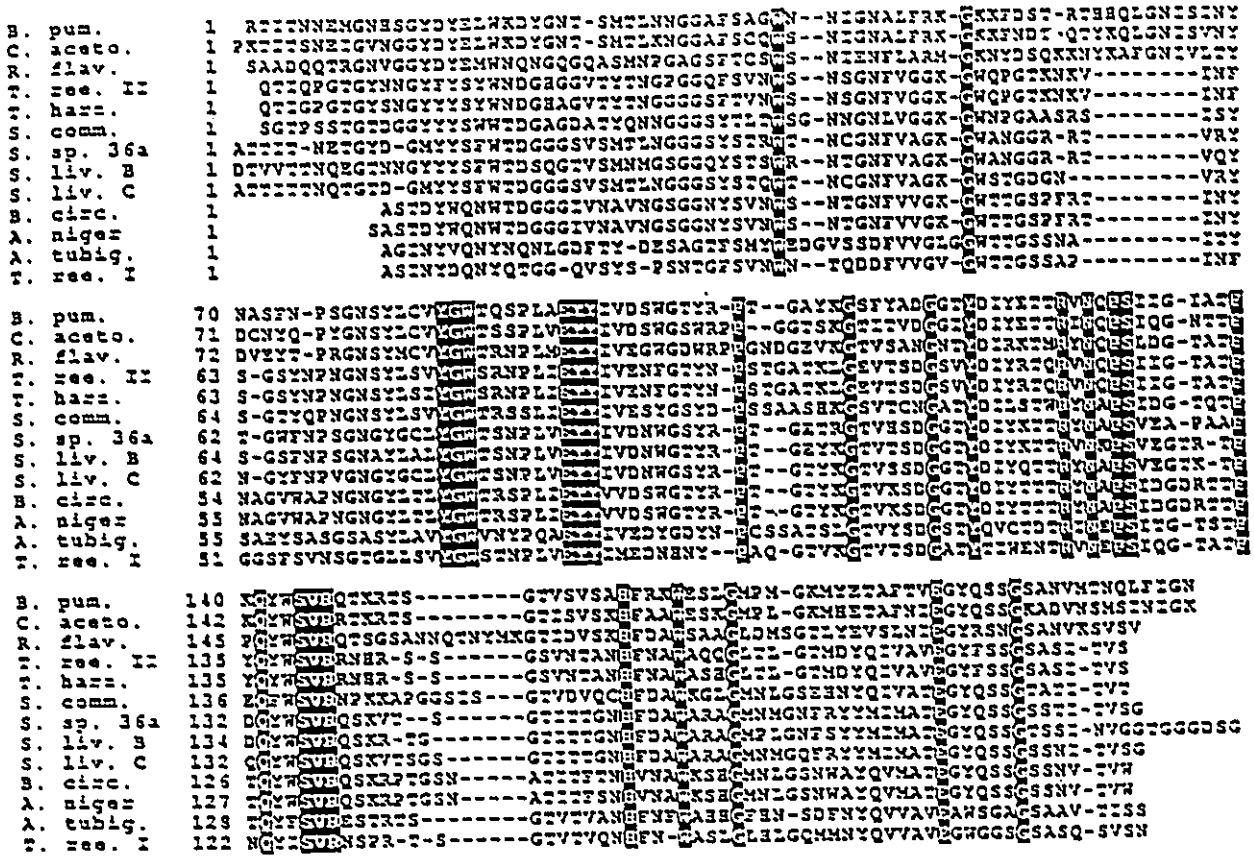

Fig.I.1. Amino acid sequence alignment of low molecular weight xylanases (taken from Wakarchuk *et al.*, 1994a with permission). The sequence of *Bacillus subtilis* and *Trichoderma viride* have not been shown because the *B. subtilis* sequence is identical to *B. circulans* except at position 147, and *T. viride* is essentially identical to *T. reesei* except at positions 9, 143, 144. The sequences are B. pum. = *Bacillus pumilis,* C. aceto. = *Clostridium acetobutylicum,* R. flav. = *Ruminococcus flavefaciens,* T. ree. II = *T. reesi* XYN II, T. harz. = *Trichoderma harzianum,* S. comm. = *Schizophyllum commune,* S. sp 36a = *Streptomyces sp.* 36a, S. liv. B = *Streptomyces lividans* XYN B, S. liv. C = *S. lividans* XYN C, B. circ. = *B. circulans,* A. niger = *Aspergillus niger,* A. tubig. = *Aspergillus tubigenesis,* T. ree. I = *T. reesei* XYN I.

Fig. 1.2. The cartoon structure of the *B. circulans* xylanase from two views.

a)

b)

I.3. PROTEIN STABILIZATION

Due to the harsh physical conditions encountered in industrial processes, a more widespread application of enzymes in biotechnology depends on our ability to produce highly stable proteins. Increases in stability of enzymes are associated with reduced enzyme charges that lowers the cost of their application. Moreover, various advantages arise by carrying out enzymatic reactions at high temperatures;

(a) high conversion rates,

(b) reduction of possibility of microbial growth,

(c) in general, solubility of substrates increases with temperature,

(d) viscosity of the reaction medium decreases with increase in temperature and consequently reduction in diffusion constraints will lead to higher reaction rates (Gupta, 1991).

Over the years, various strategies have been developed to enhance the stability of proteins. Addition of substances, chemical modification, chemical cross-linking, enzyme immobilization, replacement of water with organic solvents, and protein engineering are among the approaches that have been used to stabilize proteins. Protein engineering perhaps is the most powerful technique available to enhance protein stability. This approach provides a tool to alter the stability of proteins by changing amino acids that affect either stabilizing interactions in the folded protein or destabilizing interactions in the

unfolded form, or both (Nosoh & Sekiguchi 1990). In site-directed mutagenesis the underlying strategies to thermostabilize proteins can be classified as follows:

(a) decreasing the conformational entropy of unfolding by substitution of Gly with Ala (Mathews, 1987)

(b) replacement of a poor helix former with a good helix former (Margarit, *et al.*, 1992)

(c) creation of appropriate charges at the end of helices (Mitchison & Baldwin, 1986)

(d) addition of new interactions in the rigid parts of the structure (Mathews, 1987)

(e) elimination of interior cavities (Margarit, *et al.*, 1992)

(f) substituting asparagine with another suitable residue (Ahern, *et al.* 1987)

(g) removal of unfavourable interactions inside the proteins (Inoue, *et al.*, 1992a)

(h) introduction of disulphide bonds (Kanaya, *et al.*, 1991; Takagi, *et al.*, 1990; Matsumura, *et al.*, 1989a)

The assumption that disulphide bonds provide additional stability in globular proteins mainly arises from the fact that the disruption of disulphide cross-links is often accompanied by a dramatic decrease in thermodynamic stability of proteins. For instance, selective reduction and carboxymethylation of one of the

disulphide bonds of hen lysozyme resulted in a 24 °C decrease in thermal stability of the enzyme (Radford, *et al.*, 1991). This knowledge has, therefore, stimulated several attempts to introduce new disulphide bonds to improve protein stability (Matsumura, *et al.*, 1989b; Clarke & Fersht 1993; Wetzel, *et al.*, 1988). In the case of *E. coli* ribonuclease H for example, 11.8 °C increase of the melting point was achieved (Kanaya, *et al.*, 1991). Consequently, a similar strategy was employed to increase the stability of the *B. circulans* xylanase.

A theory originally proposed by Wyman (1964) predicts that the presence of an acidic group with abnormally high pK_a (or a basic group with abnormally low pK_a) should destabilize the protein. This abnormality in the pK_a values is a result of unfavourable interactions inside the proteins, for instance electrostatic repulsion or the presence of charged residues in an hydrophobic environment. The proximity of some acidic residues in the active site cleft of the *B. circulans* xylanase and the presence of number of aromatic residues in the active site suggest that an acidic residue with abnormally high pK_a may be present. It therefore might be possible to substitute one of these residues with an uncharged residues in order to increase the stability of the enzyme, although it must be borne in mind that such a substitution could be deleterious to catalytic activity.

Understanding the detailed kinetic and thermodynamic aspects of stability

of the engineered mutants demands the application of suitable techniques to explore the molecular aspects of stabilization. Differential scanning calorimetry (DSC) is undoubtedly the most potent approach to achieve that goal.

I.4. DSC AND THERMAL STABILITY STUDIES

The study of the unfolding of proteins induced by heat or chemicals can shed light on aspects of protein stability. In addition to providing basic mechanistic insight, such investigations can be of high practical value since the increasing applications of enzymes in biotechnology require an understanding and manipulation of protein stability. In turn, information on the mechanism of protein unfolding can provide insight into the reverse process, i.e. protein folding.

Differential scanning calorimetry (DSC) is the technique of choice in studying the thermal stability of proteins. The basis of the experiment is to measure the heat absorption in a system as the temperature is being raised through the point where the sample changes from its native state to where it is completely denatured. Measurements of heat absorption of the sample in one cell and the buffer alone in a second cell are taken simultaneously so that any heat changes of the buffer are cancelled out. The resulting data are plotted as heat capacity at constant pressure (C_p) versus temperature to give the so called thermograms. The area under the curve corresponds to the calorimetric enthalpy

(ΔH) of the transition (Cantor & Schimmel 1980). It is therefore possible to determine overall thermodynamic parameters such as transition enthalpies, entropies and transition temperatures. Moreover, based on the shape of the thermograms and the calorimetric enthalpy one can determine the number of discrete domains in a macromolecule or the number of subunits that are strongly bound together. This information is of particular importance for proteins that are too large for crystallographic studies (Privalov, 1982, 1989). The information can be easily extracted from DSC data if an equilibrium exists between the folded and unfolded form(s) of the protein under the conditions of the experiment. Sometimes, however, complications arise when irreversible denaturation of a sample coincides with reversible unfolding. In such cases additional information is required in order to interpret the DSC data. Irreversible denaturation of proteins can be attributed to several factors. Many enzymes, once unfolded, become insoluble and form aggregates. As a protein unfolds, hydrophobic residues are exposed to water. Such hydrophobic surfaces may form intermolecular interfaces via aggregation in an attempt to maximize the entropy of the solvent. Other processes like incorrect refolding, disulphide exchange, peptide chain hydrolysis, amino acid and disulphide linkage destruction should be also taken into account as the causes of irreversible denaturation (Ahern & Klibanov, 1987).

I.5. MECHANISM OF ACTION OF XYLANASES

Analysis of the primary sequence alignment of 15 family G xylanases indicates that only two glutamic acid residues are absolutely conserved in this family (Fig.I.1, Wakarchuk, *et al.*, 1994a). This suggests an important role for these two acidic residues in the catalytic process. A site directed mutagenesis study of the *Bacillus pumilus* xylanase, a G family xylanase, showed that two glutamic acid residues are intimately involved in the catalytic mechanism (Ko, *et al.* 1992). Furthermore, a preliminary examination of the glutamic acid residues of *Bacillus subtilis* xylanase suggested their critical participation in catalysis (Wakarchuk, *et al.*, 1992). In this respect they are similar to acidic side chains in hen egg-white lysozyme where two acidic residues Glu 35 and Asp 52 play a major role in the hydrolysis of the substrate. Studies of other glycosidases, specially xylanases and cellulases, have supported the notion that all glycosidases share a common mechanism with hen egg-white lysozyme in which carboxyl groups are involved in catalysis (Bray & Clarke, 1990, and references therein).

All glycosidases examined to date catalyze stereoselective hydrolysis; the configuration about the anomeric centre is either inverted (single displacement reaction) or retained (double displacement reaction) upon hydrolysis of the glycosidic linkage (Gebler, *et al.* 1992). An NMR study has demonstrated that two members of the G family xylanases, *Bacillus subtilis* and *Schizophyllum*

commune xylanases, hydrolyse their substrate by retention of configuration (double displacement reaction) (Gebler, *et al.*, 1992). The primary sequence of the *B. subtilis* is exactly the same as *B. circulans* xylanase except that a serine in the former is replaced with threonine in the latter. It is therefore reasonable to consider that the hydrolysis reaction catalyzed by *B. circulans* xylanase proceeds with retention of the anomeric configuration and a double displacement mechanism. Site directed mutagenesis and X-ray crystallographic studies have also revealed the involvement of other residues such as tyrosine 69, tyrosine 80, and to a somewhat less extent aspartic acid 11 and arginine 112 in catalysis (Wakarchuk, *et al.* 1994a). It is of note that tyrosines 69 and 80, and arginine 112 are entirely conserved among the G family xylanases (Wakarchuk, *et al.* 1994a).

I.6. OBJECTIVES

In the production of paper, during the processing wood, it is necessary to remove lignin, since the latter causes a yellow/brownish colour. This is normally accomplished by the use of chlorine or chlorine containing chemicals leading to the formation of dioxin and other chlorinated organic compounds known to be harmful to the environment. As mentioned earlier, bleaching craft pulp is usually carried out at high temperatures and under alkaline conditions. In order to replace chlorine and chlorine dioxide with xylanase it is critical to identify a thermostable enzyme from a natural source, or to stabilize presently existing xylanases. The small size of *B. circulans* xylanase facilitates hydrolysis of the substrate, since the enzyme has a high diffusion rate. Furthermore, it is unable of degrading cellulose and can be expressed at high levels 100 mg/L. These facts taken with the available X-ray structure, and availability of a number of mutant proteins provide an excellent opportunity to undertake biophysical studies aimed at production of highly stable mutants. The strategy adopted to achieve this goal is based on the introduction of the disulphide bonds into different regions of the protein. Furthermore, various biophysical experiments are designed to understand the mechanism by which increases in stability are gained.

It is understood that two glutamic acids are conserved among G family xylanases and that they play a major role in the hydrolysis of the substrate. A

structure of the enzyme and substrate co-crystallized suggests that one of the acidic residues acts as an acid catalyst and the other as a nucleophile (Campbell, *et al.*, 1993; Wakarchuk, *et al.* 1994a). Regarding the role of the glutamic acids, the questions to be addressed in this thesis are as follows. Firstly, which of the glutamic acids acts as an acid catalyst? To act as an acid catalyst requires the side chain to be protonated at neutral pH, in other words the glutamic acid in question should have an elevated pK_a. This leads to the second question; what are the physical forces that enable an acidic residue to remain protonated at neutral pH? Finally, in terms of stability, what are the costs of such an arrangement?

CHAPTER II

THE EFFECT OF A DISULPHIDE BOND ON THE RATE LIMITING STEP IN THE THERMAL DENATURATION PATHWAY OF *B. circulans* XYLANASE: DIFFERENTIAL SCANNING CALORIMETRIC AND THERMAL INACTIVATION STUDIES

II.1.INTRODUCTION

The introduction of disulphide bonds has proven to be an effective strategy to increase protein stability (Matsumura *et al.*, 1989a,b; Kanaya *et al.*, 1991; Clarke & Fersht, 1993). Therefore, in an attempt to increase stability of the *B. circulans* xylanase a disulphide bond was introduced into the protein. The position of introduction was based on the similarity of its sequence compared

to xylanase A from *Schizophyllum commune*. This bond, between S100C and N148C (to yield the DS1 protein), links the only α-helix of the protein to the nearby β-strand (please see Fig.III.1 in chapter III).

Since, upon denaturation, protein molecules acquire a random coil structure, it was predicted that disulphide bonds decrease conformational entropy of the unfolded state (Flory, 1956). The decrease in entropy is accompanied by an increase in the free energy of the unfolded state, ΔG_U. Any increase in ΔG_U, the difference in the free energy between the unfolded, U, and native state, N, should drive the unfolded state toward the native state, because $\Delta G_U = -RT\ln([U]/[N])$;

$$N \rightleftharpoons U \qquad \text{II.1}$$

This is known as the two-state reversible model. It indicates that denaturation is consistent with a single cooperative transition from the native state to the unfolded state.

There has been considerable interest in studying the mechanism of stabilization of proteins due to incorporation of novel disulphide bonds (Wetzel, 1987; Clarke & Fersht, 1993;). However, most of these studies suffer from incomplete thermodynamic analysis (Betz, 1993). In some studies ΔG_U cannot be determined because denaturation is irreversible. Instead, increased stability

relative to the wild type protein is usually defined as an increase in either the melting point or in the time required for enzymatic activity to decrease 50% at an elevated temperature. Clearly, using this information alone, the mechanism by which a disulphide bond increases the stability of protein cannot be determined. Therefore, a combination of various approaches (see below) was used in order to determine the mechanism of stabilization achieved by the introduction of the disulphide bond.

To assess the extent of stabilization due to introduction of the disulphide bond, differential scanning calorimetry was applied. The detailed thermodynamic analysis of the calorimetric thermograms, however, was hampered by the irreversibility of the thermal unfolding. So far, no general procedure has been offered to interpret differential scanning calorimetry data for the irreversible denaturation of proteins. Nevertheless, Sanchez-Ruiz and his colleagues (1988) have developed a simple model that can be successfully used to obtain the activation energy of unfolding for the two-state irreversible denaturation of proteins. Their strategy is based on the fact that the irreversibility of protein denaturation is accompanied by an increase in the apparent melting point as the rate of heating the sample (scanning rate) is increased. Consequently, we have used a similar strategy to analyze calorimetric data for the wild type xylanase and the DS1 mutant. Since the conditions required for the two-state irreversible denaturation of proteins are not fulfilled, supplementary experiments were

performed in order to understand the mechanism(s) by which the disulphide bond stabilizes the protein.

In the presence of a "subdenaturing" concentration of urea, thermal unfolding for both wild type protein and the mutant turned out to be reversible. Surprisingly, in the case of the wild type xylanase, dependence of the apparent melting point upon scanning rate at the reversible condition appeared to be similar to the irreversible one. This finding seems to be the first experimental evidence that supports the theoretical prediction of Lepock *et al.* (1992). They predicted that the apparent transition temperature for reversible unfolding can also be scan-rate dependent. Moreover, our study indicates that the increased stability of the disulphide bridge containing mutant is a result of the change of the rate-limiting step in the thermal denaturation pathway.

II.2.MATERIALS AND METHODS

Unless otherwise stated, materials used in this study were purchased from the Sigma chemical company. The bacterial strains used in this work have been described in detail elsewhere (Sung *et al.*, 1993; Wakarchuk *et al.*, 1994a). Site-directed mutagenesis was performed by Dr. Warren Wakarchuk at the National Research Council of Canada, Ottawa as already described (Wakarchuk *et al.*, 1994a,b).

II.2.1.Protein expression

E. coli cells containing the plasmid carrying *B. circulans*. xylanase gene were obtained from Dr. Warren Wakarchuk. They were grown in 2YT medium (16 g yeast extract, 10 g bacto-tryptone, 5 g NaCl, 1 L of H_2O). The plasmid contained an ampicillin resistance marker, the *lacI* gene, part of the *lacZ* structural gene, two copies of TAC promoter, and one copy of *lac*UV5 promoter (Wakarchuk *et al.*, 1994a). The antibiotic ampicillin was added at 150 mg/L to all cultures of plasmid-containing strains. Small cultures were used to inoculate fresh medium (1 L) in a shake flask. After about 18 hrs induction by IPTG with the final concentration of 100 μM, cells were harvested by centrifugation.

II.2.2.Protein purification

Protein purification employed a modification of the protocol described by Schleif & Wensink (1981). In an icebath, a mixture of cell paste and alumina was ground for at least 15 min. While being mixed, extraction buffer (10 mM sodium acetate, pH 5.3) and DNase I (with a final concentration of 20 μg/mL) were added. The mixture was centrifuged at 4400 g for 20 min. The supernatant was further centrifuged at 12100 g for 30 min. The purification was continued by exhaustive dialysis of the supernatant against 6 L extraction buffer for 24 hrs using a mco 3500 Spectropor 3 dialysis bag (Canlab, Mississauga, Ontario). After centrifugation for 30 min at 10000 rpm, the supernatant was separated and loaded onto a Poros HS II column (Perseptive Biosystems, Cambridge, MA) pre-equilibrated with 10 mM sodium acetate pH, 5.3. The column was eluted with the same buffer until zero absorbance was achieved. It was further eluted with a gradient of 0-0.3 M NaCl at 5 mL/min flow rate. The enzyme eluted at a salt concentration of about 0.12 M. The fractions containing xylanase were analyzed by gel electrophoresis. Using an Amicon filter, with less than 3000 Da molecular weight cutoff (Amicon, Danvers, MA), the eluent was concentrated to final volume of 5 mL. The sample was applied to Toyopearl resin column (HW 50-s, 1000-90000 MW, Supelco Canada, Mississauga, Ontario) that was already equilibrated with 50 mM ammonium acetate pH 6.0, and was eluted with the same buffer at 0.5

mL/min flow rate. The concentration of xylanase or its mutants was determined from the absorbance of 280 nm, using an extinction coefficient of $A_{280}^{1mg/mL} = 4.07$.

II.2.3.Enzyme activity

Enzyme activity was measured based on the reaction of reducing sugars with hydroxybenzoic acid hydrazide reagent (Lever, 1972). Experimental mixtures contained 7 mg/mL soluble fraction of Birchwood xylan and 4 μg/mL of enzyme in assay buffer (50 mM sodium citrate, pH 5.5). Following 3 minutes incubation at 40 °C, 50 μl of the mixture was mixed with one mL of 10 mM NaOH to stop the hydrolysis. Hydroxybenzoic acid hydrazide reagent with a final concentration of 0.05 M was added to the solution. To develop the colour, samples were immersed in boiling water for 10 minutes. Intensity of the colour resulting from the reaction was measured at 420 nm.

II.2.4.Thermal inactivation kinetics

For thermal inactivation kinetics experiments, solutions of wild type xylanase and disulphide bridge mutant (0.125-1 mg/mL) were immersed in a water bath at different temperatures and their activities were measured after periodic withdrawal of an aliquot. Since the plot of $\ln([E]/[E_0])$ ($[E_0]$ and [E] are the concentrations of the active enzyme at the time zero and t, respectively) *vs.*

time at a given temperature results in a straight line, the thermal denaturation of the wild type enzyme follows a first-order rate law. On the other hand, the plot of 1/[E] vs. time provides a straight line for the disulphide mutant indicating that thermal denaturation kinetics of the mutant obeys a second-order rate law. In both cases the slope of the plots provides apparent kinetic rate constants (K_{app}) for the irreversible denaturation of the wild type and disulphide bridge xylanases.

II.2.5.Differential scanning calorimetry

Calorimetric thermograms were obtained using a MC-2 Microcal differential scanning calorimeter. Protein solutions were prepared in ammonium acetate buffer, pH 6.0, at a concentration of 0.5-1 mg/mL. All solutions were degassed under vacuum. The reversibility of the thermally induced transitions was always checked by reheating the solution in the calorimeter cell immediately after cooling, following the first run. Baselines obtained by filling both cells with the corresponding buffer for each particular condition were subtracted from the sample experimental trace, thus giving the apparent heat capacity profile. The transitions were corrected for the minor difference in heat capacity between the initial and the final states, using the Progress baseline procedure. The resulting curve, after normalization to the concentration of protein, is called the excess heat capacity profile. Data treatment was performed

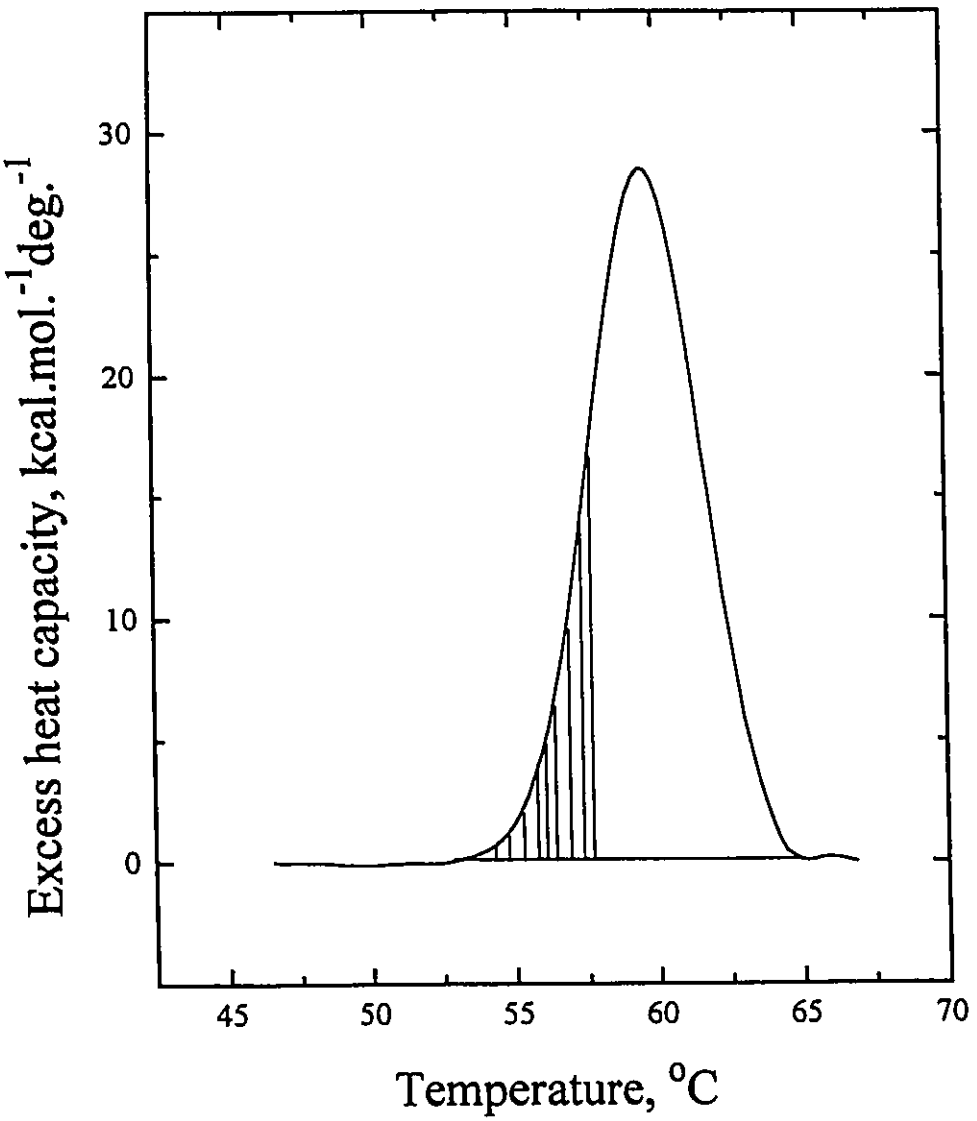

Fig.II.1. A typical excess heat capacity curve versus temperature for the wild type xylanase in ammonium acetate buffer obtained by a MC-2 differential scanning calorimeter. The hatched area is proportional to the heat evolved at a given temperature, Q.

using the Origin software provided by the manufacturer of the calorimeter (Microcal Inc.). The enthalpy of denaturation was determined by integration of the heat capacity function (Fig.II.1). Total enthalpy of denaturation (Q_t) corresponds to the full area under the curve. Whereas, enthalpy of partial denaturation of protein (Q) can be obtained from integration of the heat capacity function taken from the temperature where the enzyme is in its native form to the desired temperature.

Due to the slow instrumental response of differential scanning calorimeters in some cases, the shape of calorimetric thermograms is distorted (Mayorga & Freire, 1987). Fig.II.2 shows the shape of the output, and corrected signals at various scanning rates. Ideally, the output signal should be a rectangle. As is clear from the Fig.II.2 the shape of the output signal is increasingly distorted as scanning rate increases. Mayorga & Freire (1987) have developed a mathematical procedure by which such distortions can be corrected. These distortions are more evident for sharp transitions. As already reported (Galisteo *et al.*, 1991), in the case of proteins due to their broad calorimetric transitions, the instrumental distortions of the shape of the heat capacity function can be ignored (Fig.II.3). This figure shows the calorimetric thermograms of ribonuclease before and after a correction based on the dynamic deconvolution procedure. A small dependence of melting point upon scanning rate can be observed which is in agreement with previous reports

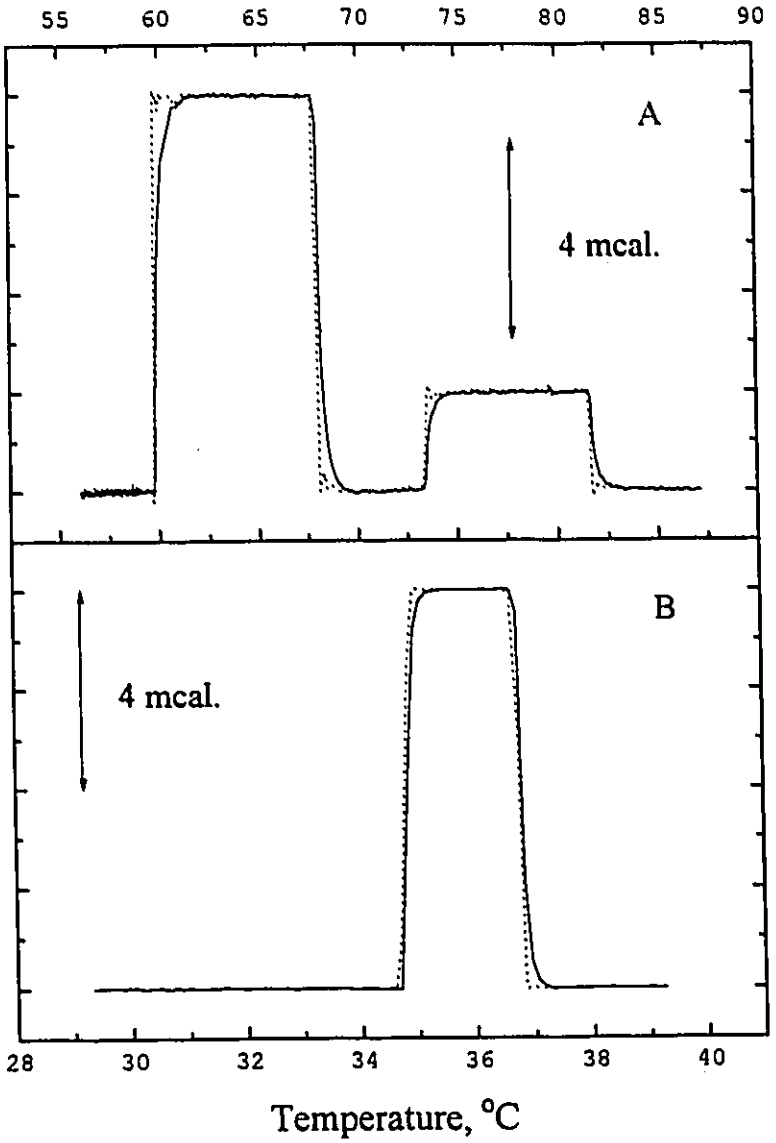

Fig.II.2. A typical instrumental response (output signal, solid line) to a rectangular calibration pulse (input signal). Dashed line is the corrected signal based on a dynamic deconvolution procedure. A, two input signals with intensities of 8 and 2 mcal at the scanning rate of 84 deg./hr. B, An input signal with the intensity of 8 mcal at the scanning rate of 20 deg./hr.

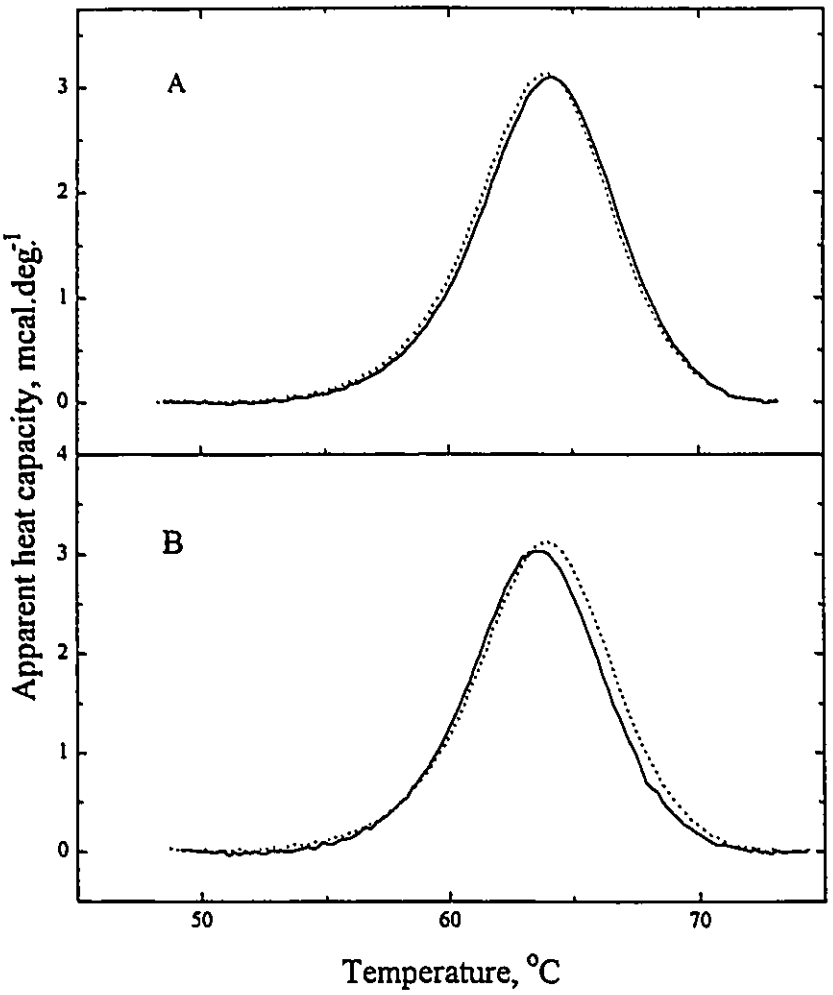

Fig.II.3. A, Differential scanning calorimetric thermograms of ribonuclease before, solid line, and after, dashed line, instrumental response correction at the scanning rate of 84 deg./hr. B, The comparison of the DSC data for ribonuclease at the scanning rate of 20 deg./hr, solid line, and 84 deg./hr, dashed line, after removing instrumental distortions.

(Mayorga & Freire, 1987). Ribonuclease has been chosen as a control to make sure that scan-rate dependence observed for the xylanases is not an artifact from the calorimeter used throughout this study.

II.2.6.Circular dichroism spectroscopy

The CD spectra of xylanase proteins were obtained using a JASCO J-600 spectropolarimeter. The instrument was calibrated with ammonium-*d*-camphoresulphonate. Spectra in the near UV region were measured in a 1 cm pathlength cylindrical quartz cell with a protein concentration of about 0.3-0.5 mg/mL in either 50 mM ammonium acetate or 20 mM phosphate buffer. Spectra in the far UV region were measured in a 0.02 cm pathlength cylindrical quartz cell with a similar protein concentration in 20 mM phosphate buffer. The normalization of spectra was performed using the software provided by the instrument manufacturer. The molecular weight of the wild type protein was considered to be 20,397 Da. Except for the case of cXI and cDS1 mutants, small variations in the molecular weight due to mutations were ignored during the normalization of the mutants' spectra.

II.3. DIFFERENTIAL SCANNING CALORIMETRY OF THE WILD TYPE XYLANASE AND DISULPHIDE BRIDGE VARIANT (DS1) UNDER IRREVERSIBLE CONDITIONS

Information obtained by differential scanning calorimetry (DSC) can be treated based upon reversible thermodynamics if reversibility of the thermal denaturation is maintained throughout the transition zone. This reversibility can be verified by reproducibility of a thermogram upon a second heating of a cooled sample (Freire *et al.*, 1990). Fig.II.4 shows the original DSC data for the wild type xylanase and DS1 variant in ammonium acetate buffer. As is clear from the figure, the thermal denaturation process occurs irreversibly as indicated by the lack of any transition in the second run. Furthermore, calorimetric profiles show a clear scan-rate dependence (Fig.II.5, Fig.II.6) even after correction for instrumental response.

Scan-rate dependence of calorimetric thermograms has been assumed to arise from the presence of an irreversible step in the thermal denaturation pathway (Sanchez-Ruiz *et al.*, 1988; Freire *et al.*, 1990; Sanchez-Ruiz, 1992). In other words, the protein denaturation process is controlled by kinetic rather than thermodynamic factors. In such a case, the extent of denaturation of the protein depends on the temperature and the length of time that the protein spends at that temperature. Therefore, at lower scanning rates, the melting point of the protein will be less than that of higher scanning rates, because there is more time for irreversible denaturation to occur during the run.

The presence of an irreversible step in the denaturation pathway complicates the obtention of valuable information that can be obtained if reversible thermodynamics applies. The first major attempt to overcome this obstacle was made by a Spanish group (Sanchez-Ruiz *et al.*, 1988). They successfully demonstrated that when denaturation of a protein occurs between only the native state "N" and an irreversibly denatured state "I" ($N \rightarrow I$, the so called two-state irreversible model) the activation energy of denaturation can be determined from the slope of lnK, and $\ln(\ln(Q_t/(Q_t-Q)))$ versus $1/T$, or from the slope of $\ln(v/T_m^2)$ versus $1/T_m$. based on following equations:

$$K=\frac{vC_P}{Q_t-Q} \qquad \text{II.1}$$

$$\frac{v}{T_m^2} = \frac{AE}{R} \exp(-\frac{E}{RT_m}) \qquad \text{II.2}$$

$$\ln[\ln\frac{Q_t}{Q_t-Q}]=\frac{E}{R}[\frac{1}{T_m}-\frac{1}{T}] \qquad \text{II.3}$$

where K is the rate constant, v the scanning rate, Q_t the total heat of the calorimetric transition, Q the heat evolved at a given temperature, C_P the excess heat capacity at that temperature, E the activation energy, A the frequency factor in the Arrhenius equation, and T_m the apparent melting point in degrees

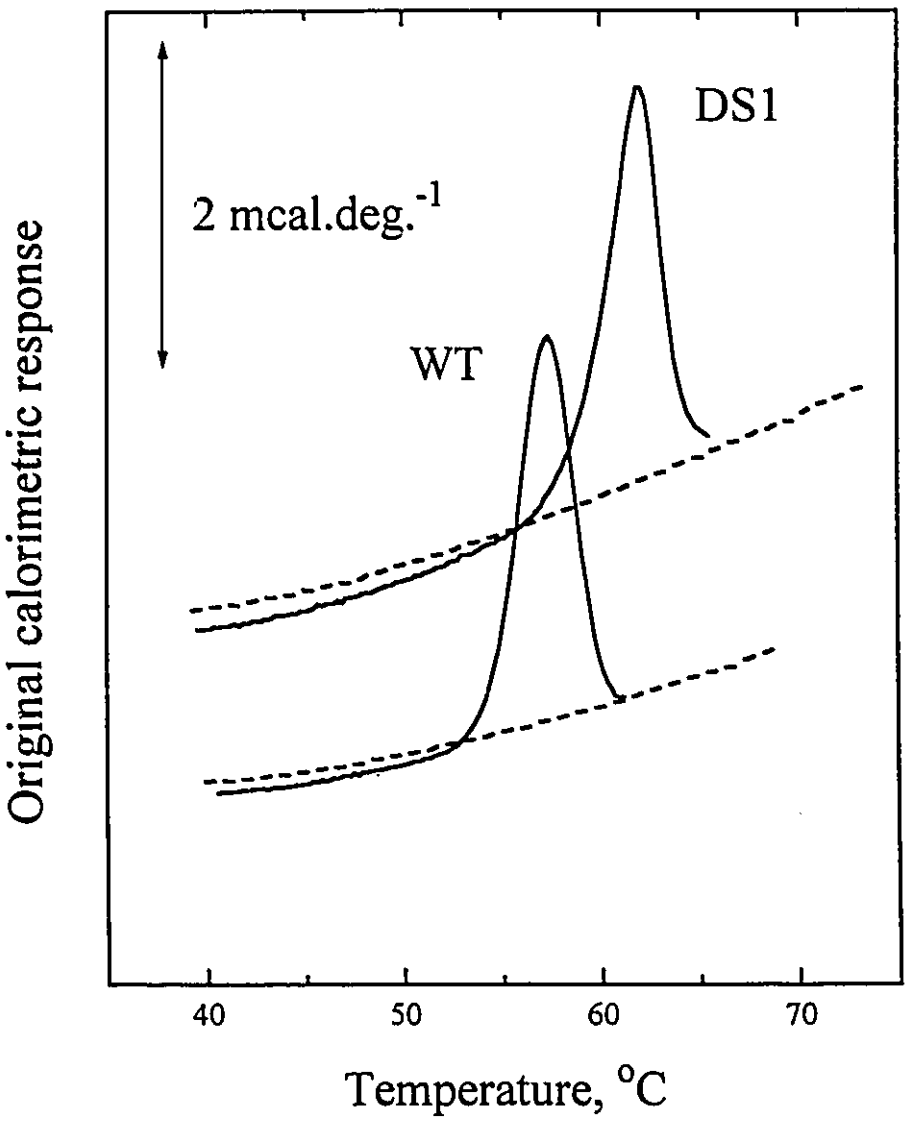

Fig.II.4. Original calorimetric recordings for the wild type xylanase (WT) and DS1 mutant at a scanning rate of 13 °C/hr in 50 mM ammonium acetate, pH 6.0, with the protein concentration of approximately 1 mg/mL. The dashed lines are the second heating runs after cooling down the samples.

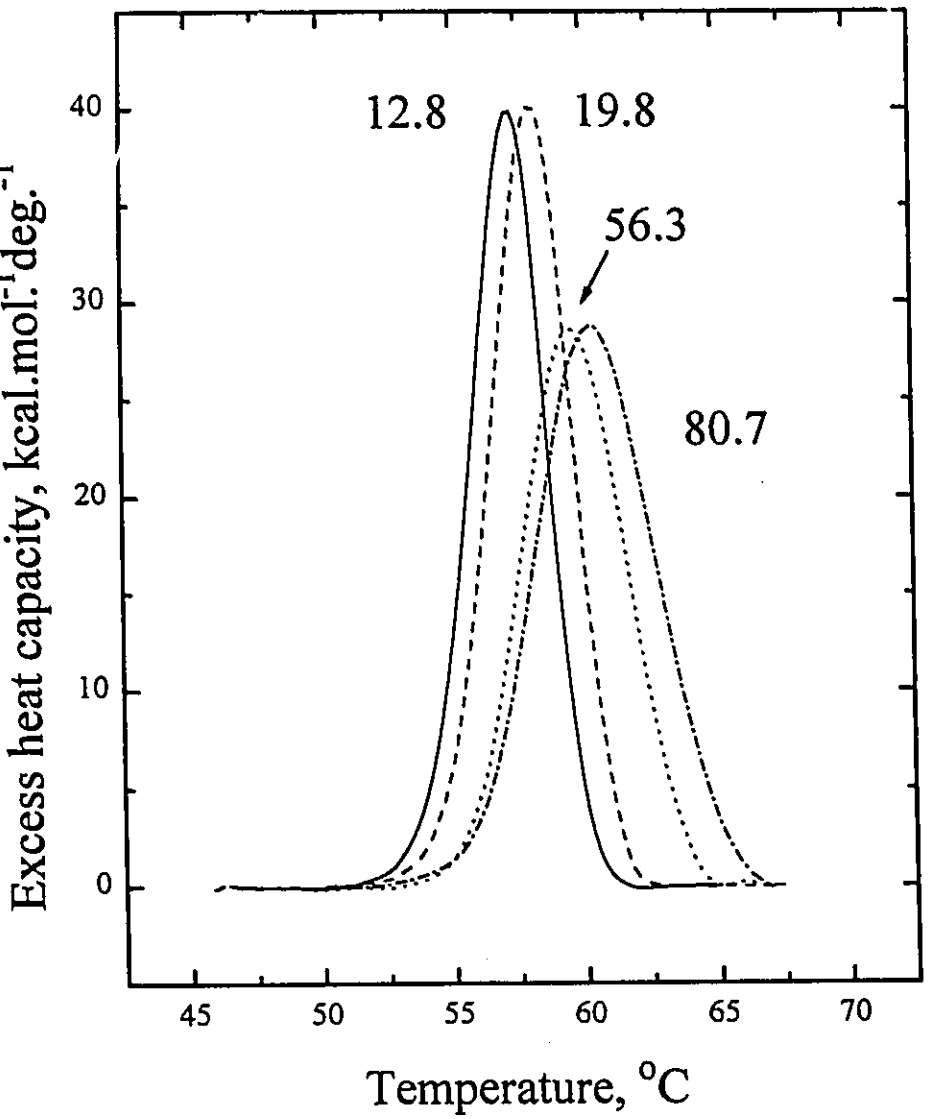

Fig.II.5. Differential scanning calorimetric transitions for wild type xylanase at different scanning rates. The numbers represent the scanning rate in degs./hr.

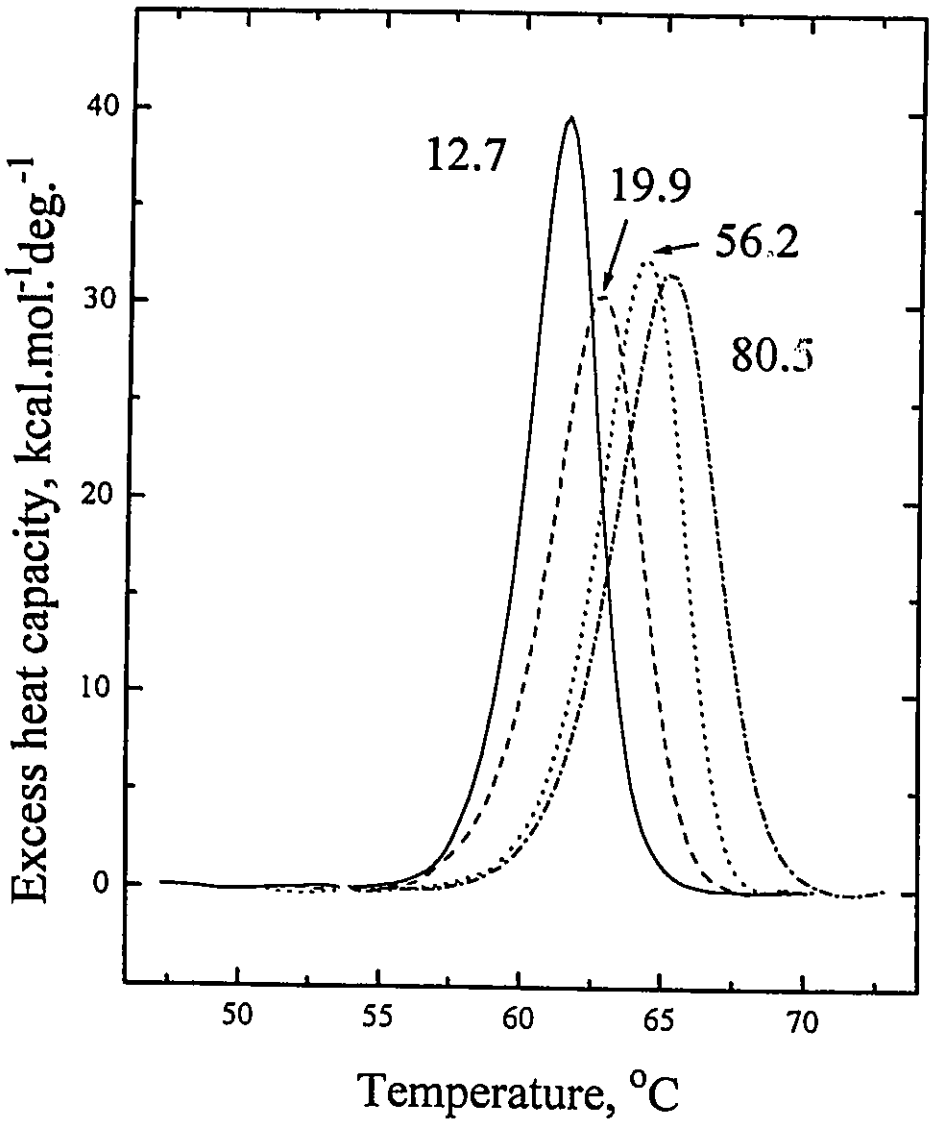

Fig.II.6. Differential scanning calorimetric transitions for the DS1 xylanase at different scanning rates. The numbers represent the scanning rate in degs./hr.

Kelvin. The two-state irreversible model is an approximation of a more general and realistic model with $k_1 < k_3$ and $k_3 >> k_2$ that can be expressed as (Lumry & Eyring, 1954):

$$N \underset{k_2}{\overset{k_1}{\rightleftharpoons}} U \xrightarrow{k_3} I \qquad \text{II.4}$$

In order to determine whether or not the denaturation mechanism obeys a two-state irreversible model, calorimetric data were analyzed based on Equations II.1-II.3. It has been shown that if lnK and $\ln[\ln(Q_t/(Q_t-Q))]$ versus 1/T and $\ln(v/T_m^2)$ against $1/T_m$ remain linear, the denaturation process obeys a two-state irreversible model. In such a case the activation energy can be easily obtained form the slope of the plots. Denaturation of the wild type and DS1 xylanase cannot be approximated by a two-state irreversible model as indicated by the nonlinear curves obtained for both lnK and $\ln[\ln(Q_t/(Q_t-Q))]$ versus 1/T (Fig.II.7.B and C, Fig.II.8.B and C), although the plot of $\ln(v/T_m^2)$ against $1/T_m$ is linear for both of the proteins (Fig.II.7.A and Fig.II.8.A). Arriaga *et al.* (1992), based on studying irreversible denaturation of β-lactamase I from *Bacillus cereus*, have concluded that the linear behaviour of $\ln(v/T_m^2)$ against $1/T_m$ (Equation II.2) is the most rigorous test for applicability of the two-state

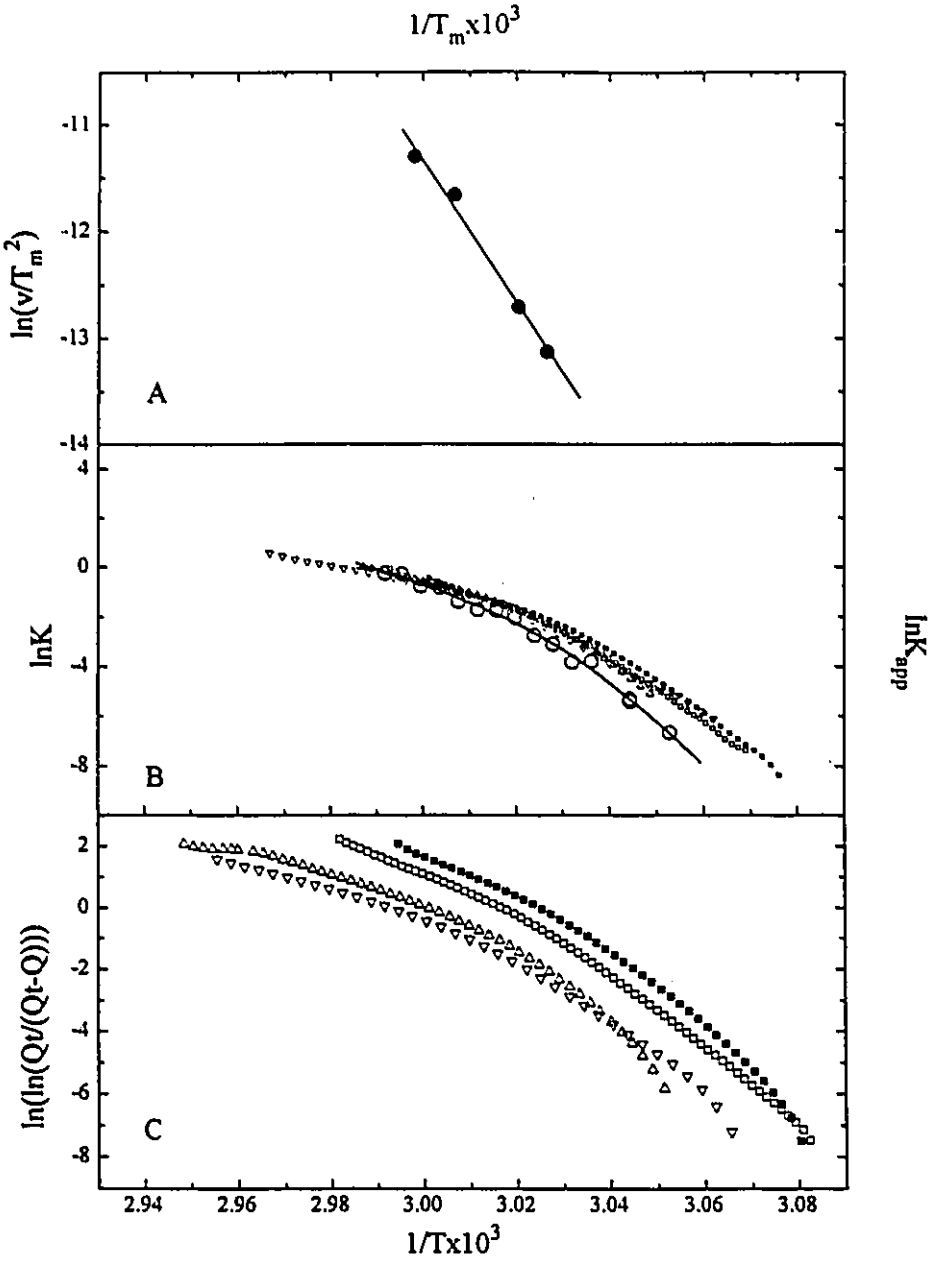

Fig.II.7. Plots corresponding to equations (II.1-II.3) in the text for the wild type xylanase. (A) Plot of $\ln(v/T_m^2)$ versus $1/T_m$. (B) Arrhenius plots obtained from the calorimetric transitions with varying scanning rates of 12.8 (■), 19.8 (□), 56.3 (△), and 80.7 deg./hour (▽) and from thermal inactivation kinetics (O). (C) $\ln(\ln(Q_t/(Q_t-Q)))$ versus $1/T$ at the scanning rates of 12.8 (■), 19.8 (□), 56.3 (△), and 80.7 deg./hour (▽).

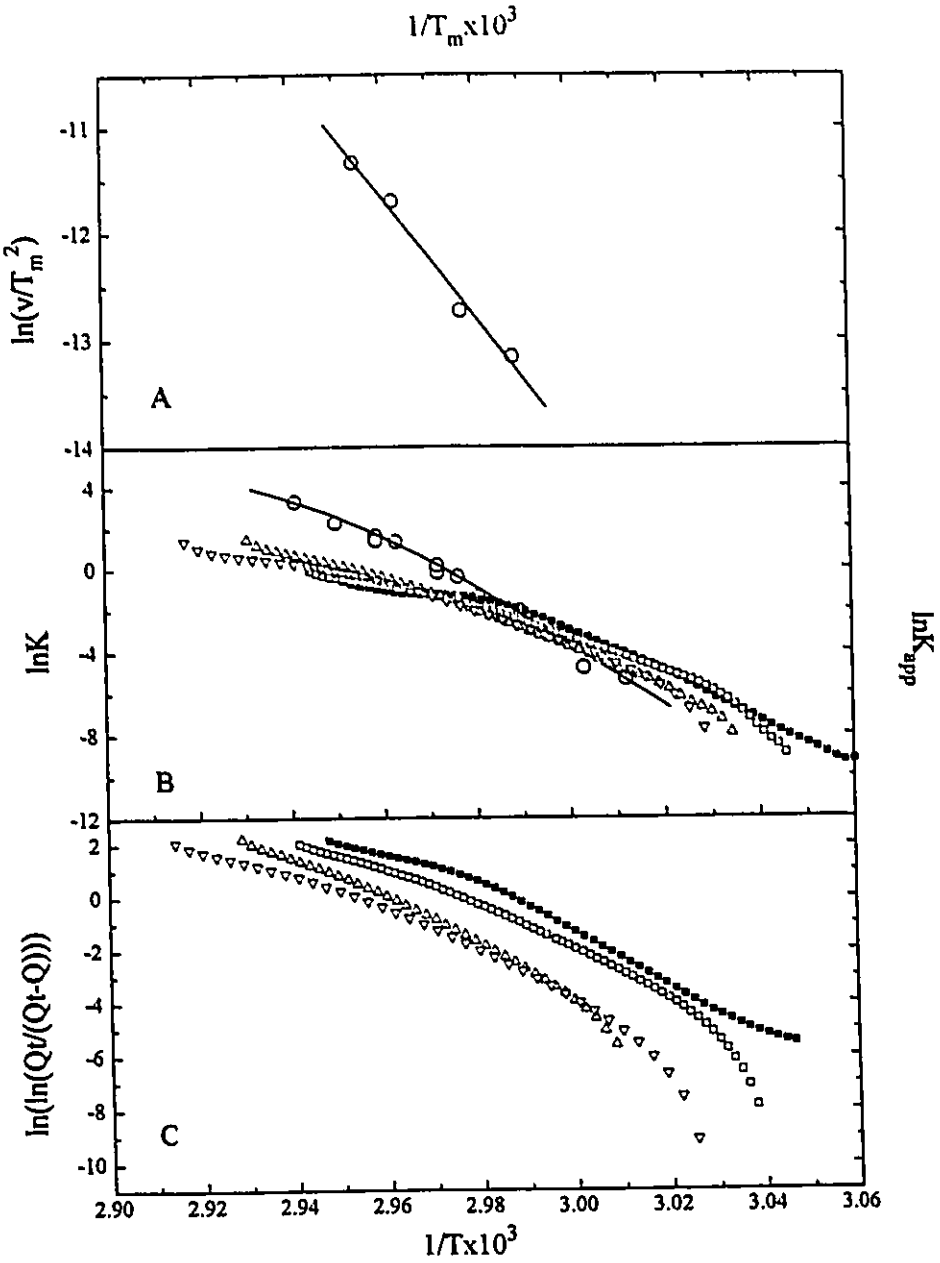

Fig.II.8. Plots corresponding to equations (II.1-II.3) in the text for the DS1 xylanase. (A) Plot of $\ln(v/T_m^2)$ versus $1/T_m$. (B) Arrhenius plots obtained from the calorimetric transitions with varying scanning rates of 12.8 (■), 19.8 (□), 56.3 (Δ), and 80.7 deg./hour (∇), and from thermal inactivation kinetics (O). (C) $\ln(\ln(Q_t/(Q_t-Q)))$ versus 1/T at the scanning rates of 12.8 (■), 19.8 (□), 56.3 (Δ), and 80.7 deg./hour (∇).

irreversible model. However, our results indicate that this criterion is not necessarily of general validity. Clearly in the case of xylanase to be able to apply the two-state irreversible model each Equation, II.1, II.2, and II.3, should be valid.

II.4.REVERSIBLE UNFOLDING OF THE WILD TYPE XYLANASE AND THE DS1 MUTANT

The irreversibility of calorimetric scans of xylanase and its mutant may be due to the aggregation of the unfolded (or partially unfolded) protein. Since in some cases aggregation occurring during thermal denaturation can be prevented by agents such as guanidinium chloride or urea (Freire *et al.*, 1992), the DSC scan of xylanase and the mutant was studied in the presence of 2.5 M urea. At the scanning rate of 58 degs./hr and in the presence of urea, calorimetric scans are accompanied by 5.6 and 5.0 degs. decrease in the melting point of wild type xylanase and DS1 mutant, respectively. The presence of urea is not accompanied by any detectable change in the structure of either the wild type xylanase (see Fig.III.10 in Chapter.III) or the DS1 mutant (Fig.II.9) as verified by circular dichroism spectroscopy. At this concentration of denaturant, reversible unfolding of both wild type and the DS1 xylanase was observed (Fig.II.10). Therefore, the irreversibility seems to be mainly a result of aggregation. Due to the perturbed shape of the transition, at the scanning rate

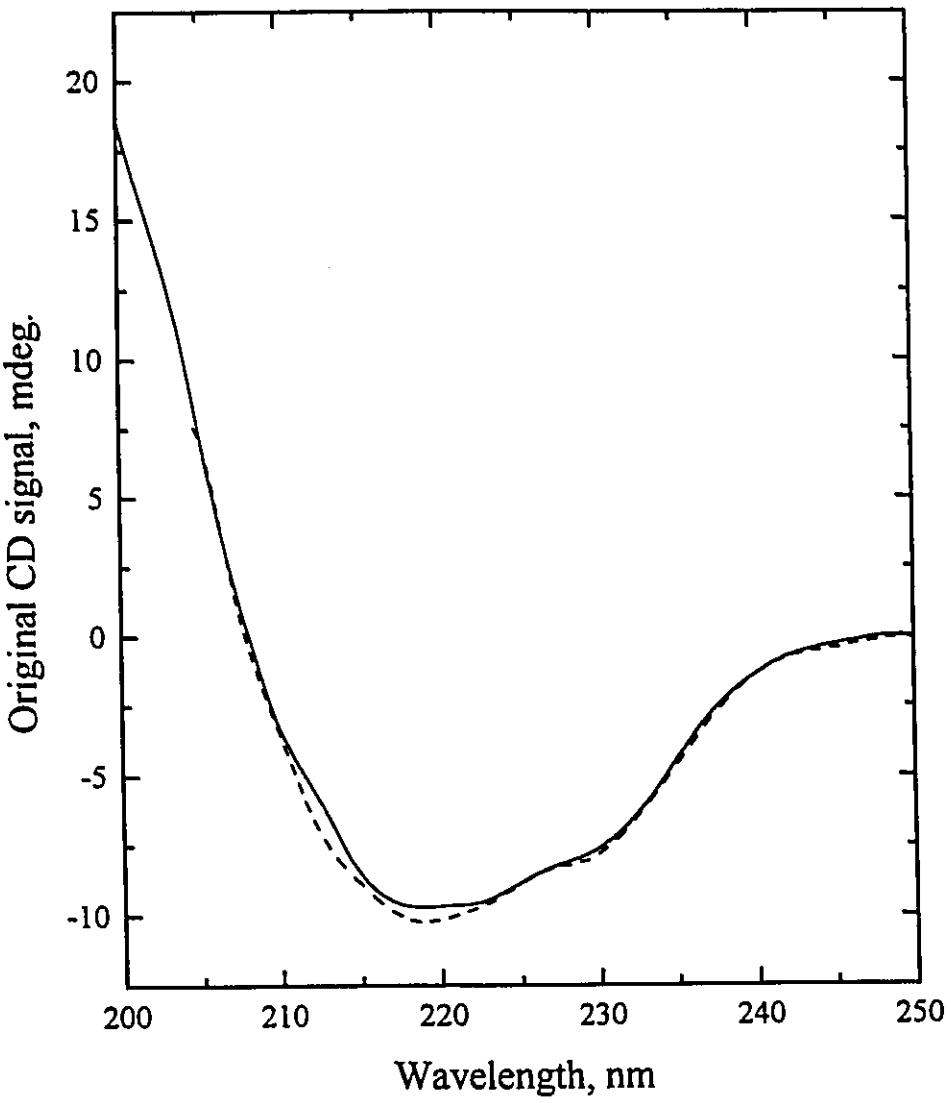

Fig.II.9. Far-UV CD spectrum of the DS1 mutant with the protein concentration of 0.45 mg/mL in the absence, solid line, and the presence, dashed line, of 2.5 M urea in 20 mM phosphate buffer at pH 6.0.

of 58 degs/hr, an attempt to fit the data to the two-state reversible model failed (Fig.II.11). Since *B. circulans.* xylanase is a small single-domain globular protein with molecular weight of 20 kDa (Campbell *et al.*, 1993) and there is no evidence for dimerization, the perturbed shape of the thermograms are likely due to high scanning rates. This is supported by the fact that lowering the scanning rate is accompanied by diminution of the distortion of the shape of the thermograms (Fig.II.11). At the lowest scanning rate, 13 degs./hr, the calorimetric data can be fitted to the two-state reversible model. In the presence of urea, 133 and 138 kcal/mol are obtained for the calorimetric enthalpy of the wild type xylanase and disulphide bridge mutant, respectively. Moreover, based on the following equation, the change in free energy of stabilization due to the introduction of disulphide bond in the presence of 2.5 M urea was found to be 3.1 kcal/mol;

$$\Delta(\Delta G)=\Delta G(mutant)-\Delta G(Wild\ type) \qquad \text{II.5}$$

ΔG(Wild type) is zero at t_m, while the ΔG(mutant) can be obtained by the Gibbs-Helmholtz equation (Equation III.6 in Chapter III). Since no consistent change is observed for the C_p upon denaturation, the ΔC_p value was considered to be zero. It is of note that, in spite of the considerable increase in the stability of the DS1 mutant, the engineered disulphide bond does not alter the secondary

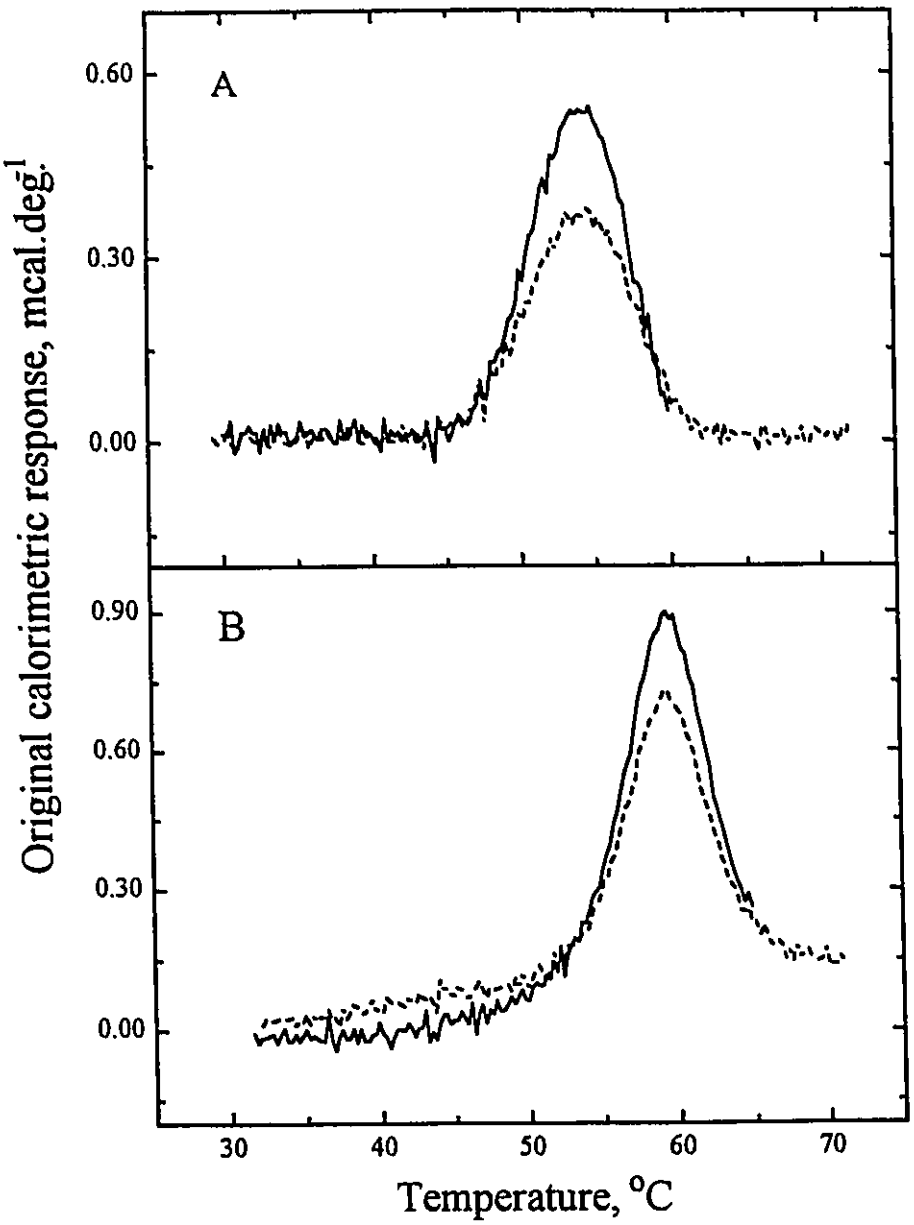

Fig.II.10. Original calorimetric recordings for the wild type xylanase, A, and disulphide-bridge mutant, B, at the scanning rate of 58.0 °C/hr in 2.5 M urea at pH 6.0 with protein concentration at about 0.5 and 0.6 mg/mL, respectively. The dashed lines are the second heating run after cooling down the sample.

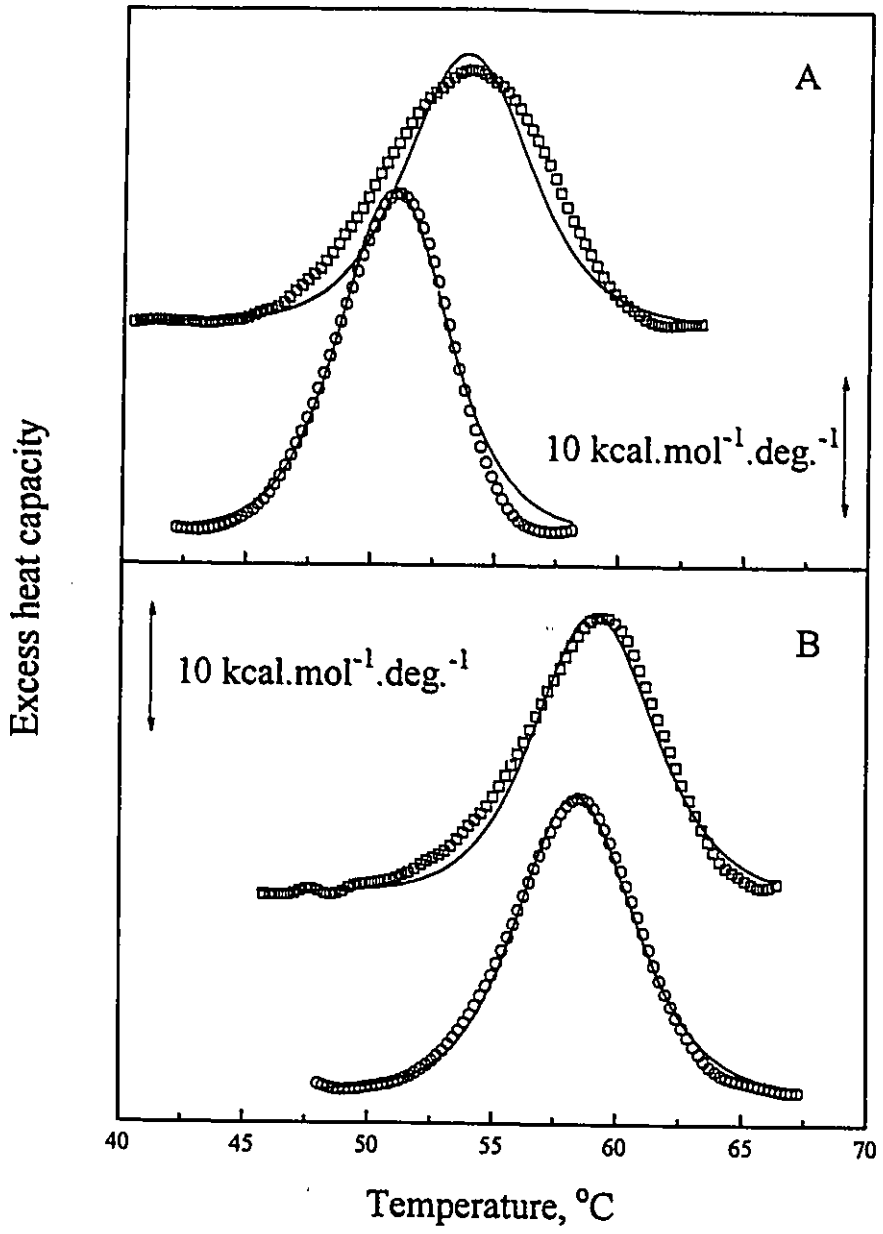

Fig.II.11. Differential scanning calorimetric thermograms and the best fit of the two-state reversible model for the reversible denaturation of the, A, wild type at two different scanning rates of 13.3 (O), and 58.7 (□) °C/hr and, B, disulphide-bridge xylanase at the scanning rates of 13.2 (O) and 58.3 (□) °C/hr in the presence of 2.5 M urea.

and tertiary structure of the protein, as evidenced by circular dichroism spectroscopy (see Fig.III.4 and Fig.III.5 in Chapter III) and also by X-ray crystallography (Wakarchuk, *et al.*, 1994b). Moreover, introduction of the disulphide bond did not lead to any reduction in the enzymatic activity. Thus, the locus chosen as the site of disulphide bond seems to be suitable as it enhances protein stability with no change in enzymatic activity.

Surprisingly, in addition to the distortion of the shapes of the endotherms (Fig.II.11), dependence of the apparent melting point upon scanning rate was observed for both wild type and DS1 xylanase in the presence of urea (Fig.II.12 and Fig.II.13). The comparison of Fig.II.12 with Fig.II.5 clearly indicates that for wild type xylanase, presence or absence of an irreversible step has almost no effect on scan-rate dependence of calorimetric thermograms. Therefore, the overall thermal denaturation rate is controlled by the rate of reversible unfolding, i.e. $k_1 \leq k_3$, Equation II.4. This condition is normally seen when protein denaturation follows a two state irreversible model (Sanchez-Ruiz *et al.*, 1988). Additionally, the two state irreversible denaturation of proteins can be described as the rate of refolding of unfolded state (U) to the native state (N) being much slower than its conversion to the irreversible state (I). It seems that the latter criterion is not fulfilled by wild type xylanase, thus deviation from the two state irreversible model is observed.

For the DS1 mutant, however, the scan-rate dependence of the apparent

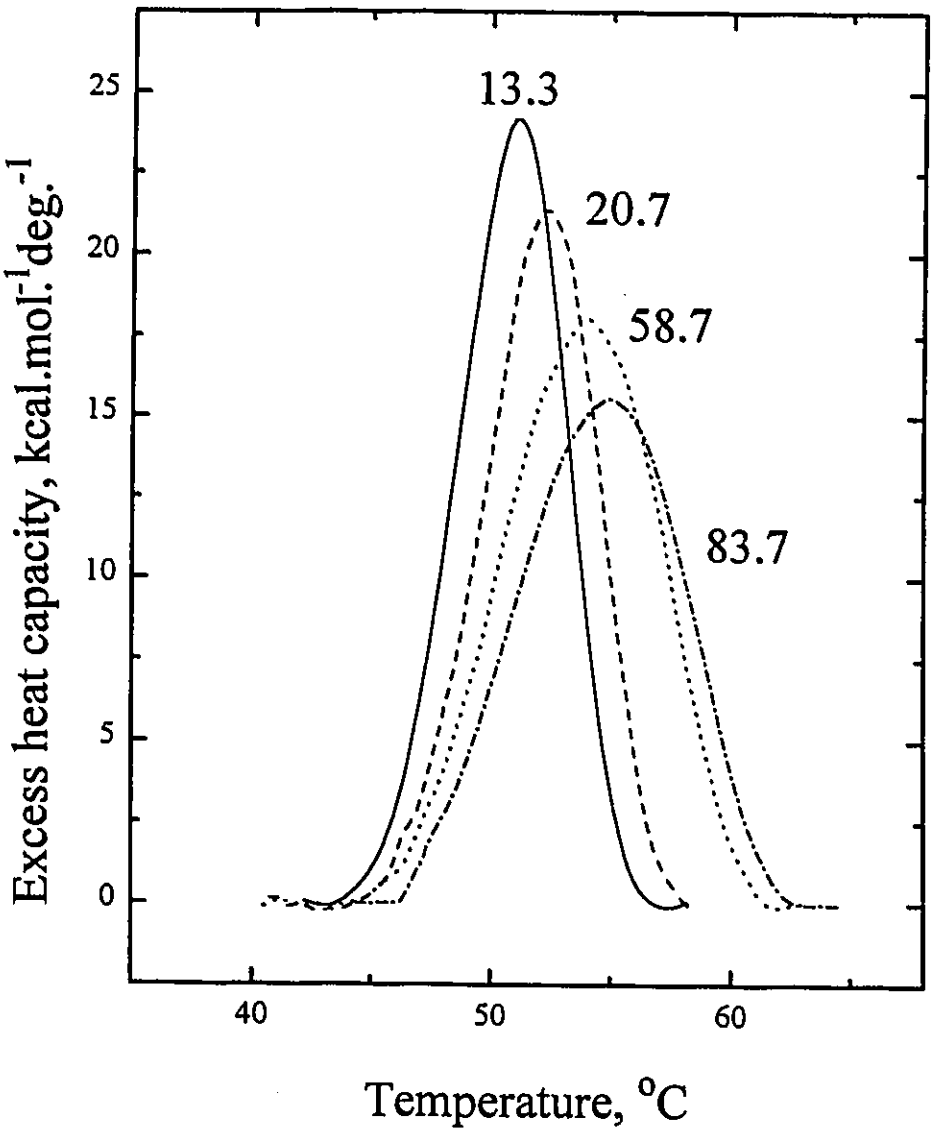

Fig.II.12. Differential scanning calorimetric transitions for the wild type xylanase at different scanning rates in 2.5 M urea. The numbers represent the scanning rates in deg./hr.

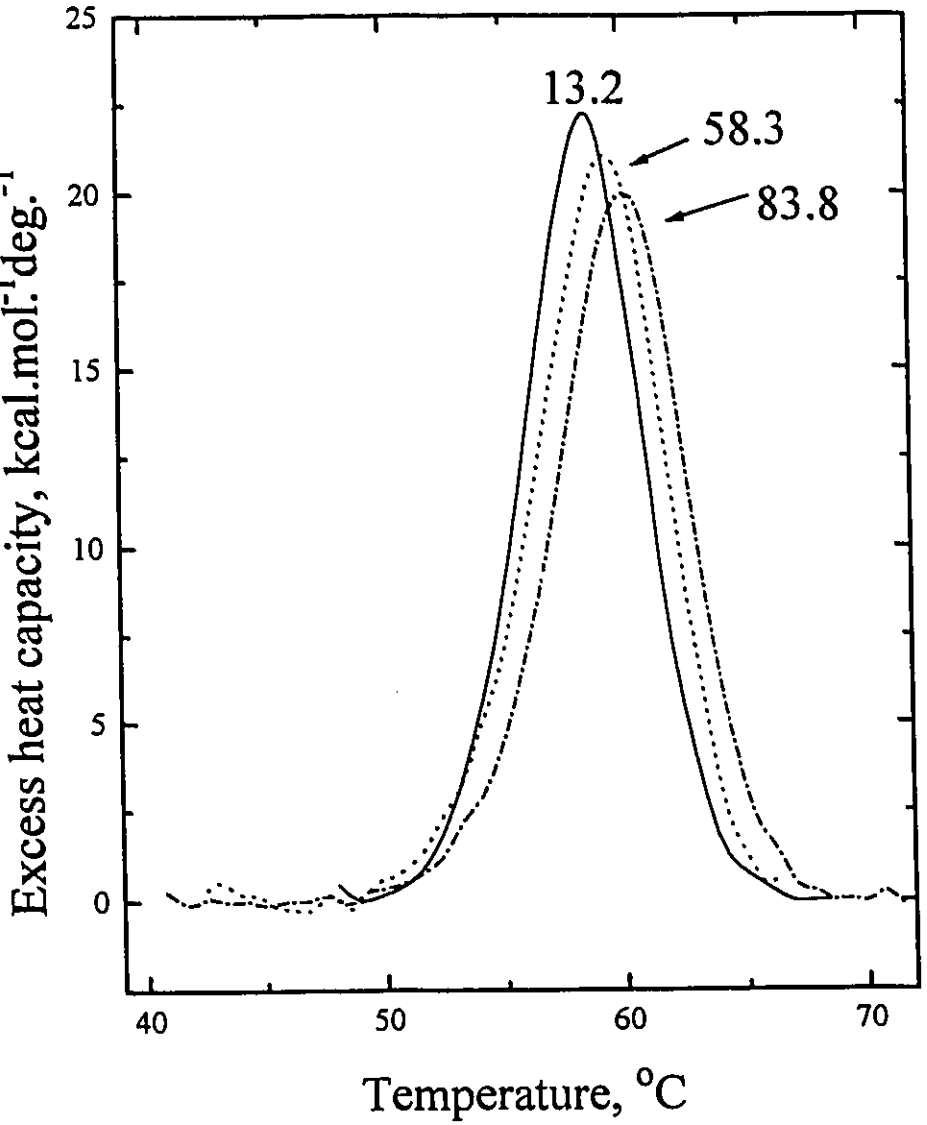

Fig.II.13. Differential scanning calorimetric transitions for the DS1 mutant at different scanning rates in 2.5 M urea. The numbers represent the scanning rates in deg./hr.

melting point is less in the presence of urea (Fig.II.13) than in its absence (Fig.II.6). These data suggest that although the rate of reversible unfolding of the disulphide mutant (DS1) is low, it does not control the overall rate of protein denaturation. In this case it seems that irreversible denaturation is the rate determining step of the thermal denaturation pathway. This conclusion is further supported by the thermal inactivation kinetics experiments described below. Lepock and his coworkers (1992), by simulating differential scanning profiles for reversible and irreversible protein denaturation, have predicted that the apparent transition temperature for completely reversible unfolding can have a scan-rate dependence when the scan rate exceeds the rate of unfolding. Apparently the work described in this chapter provides the first experimental evidence that argues for the validity of Lepock's prediction. Furthermore, it is shown that the shape of the thermograms are increasingly distorted as scanning rate increases (Fig.II.11). Therefore, in order to avoid misleading analysis of the perturbed thermogram shapes, due to unsuitable scanning rates, calorimetric runs should be performed at different scanning rates to make sure that there is no perturbation in the shape of the DSC thermograms. In other words, experiments should be carried out at a scanning rate where complete equilibrium is established between the folded and unfolded form(s) of a protein.

It is interesting to note that there are no detailed reports regarding a high scan-rate dependence for the reversible denaturation of a protein. This is

probably due to the fact that there has been no reason to check scan-rate dependence of calorimetric endotherms when the process is reversible. Possibly the only reported study dealing with scan-rate dependence of the reversible denaturation of a protein was performed by Mayorga & Freire (1987). They observed a 10 seconds relaxation time for the reversible unfolding of ribonuclease at a temperature close to its melting point. This corresponds to less than 0.3 degs. increase in the melting point of the ribonuclease due to the change of scanning rate from 10 to 90 deg./hr. This is in no way comparable to *B. circulans* xylanase for which an approximately 4 degs. increase of the apparent melting point was observed for a similar change in the scanning rate.

II.5.THERMAL INACTIVATION KINETICS

As shown previously (Arriaga *et al.*, 1992; Galisteo *et al.*, 1991; Freire *et al.*, 1990) interpretation of DSC data can be aided greatly by studying the thermal inactivation kinetics of enzymes. This approach, accompanied by the results from differential scanning calorimetry, allows us to characterize the mechanism of the thermal denaturation of both the wild type xylanase and disulphide-bridge mutant. Since, the plot of $\ln([E]/[E_0])$ versus time results in a straight line (Fig.II.14), thermal denaturation of the wild type xylanase obeys a first-order rate law. The slope of this line provides the apparent reaction rate constant (K_{app}). As the protein concentration was increased no change in the

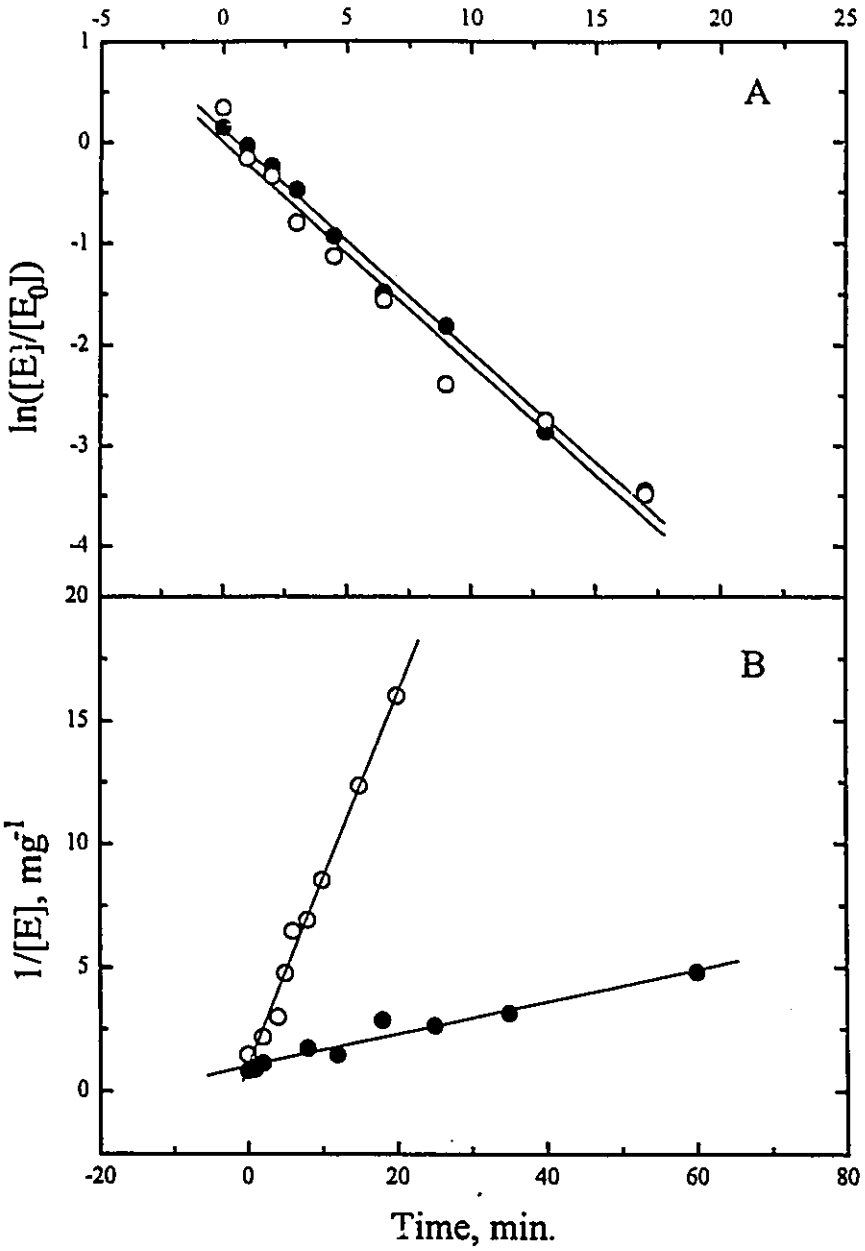

Fig.II.14. Thermal inactivation kinetics of the wild type and disulphide bridge xylanase, DS1, at 58.5 and 63.5 °C, respectively. (A) Plot of the ln ($[E]/[E_0]$) versus time at two different concentrations of the wild type enzyme, (●) 0.125 mg/mL, and (O) 1 mg/mL. (B) Plot of 1/[E] versus time at two different concentrations of the disulphide-bridge mutant, (●) 0.125 mg/mL, and (O) 1 mg/mL. $[E_0]$ and [E] are the concentrations of the enzyme at the time zero and t, respectively.

values of K_{app} was observed (Fig.II.14). In other words, K_{app} for the thermal denaturation of the wild type xylanase is concentration independent. Thus, the rate limiting step in the denaturation of this protein cannot be ascribed to an aggregation process, i.e. $k_3 \geq k_1$. This is further supported by the fact that the apparent melting point for the reversible denaturation of the wild type xylanase (Fig.II.12) shows as much scan-rate dependence as the irreversible denaturation (Fig.II.5).

The results from calorimetry taken with the results from thermal inactivation kinetics experiments indicate that, for the wild type xylanase, the scan-rate dependence of the calorimetric thermograms is a result of a slow step during the reversible unfolding of the protein rather than the presence of an irreversible step. In the case of the DS1 mutant, however, the plot of 1/[E] versus time results in a straight line (Fig.II.14). Consequently, kinetics of the thermal denaturation of this mutant complies with the second-order rate law. The apparent kinetic rate-constant (K_{app}) can be obtained from the slope of the plot. Unlike wild type xylanase, K_{app} for the DS1 mutant increases as the concentration of the protein is being raised (Fig.II.14). The second-order rate reaction behaviour taken with the dependence of the denaturation kinetics upon concentration suggest that, for the DS1 mutant, aggregation is the rate limiting step in the denaturation pathway, i.e. $k_3 < k_1$, Equation II.4. This observation completely supports the finding from DSC that the irreversible step in the

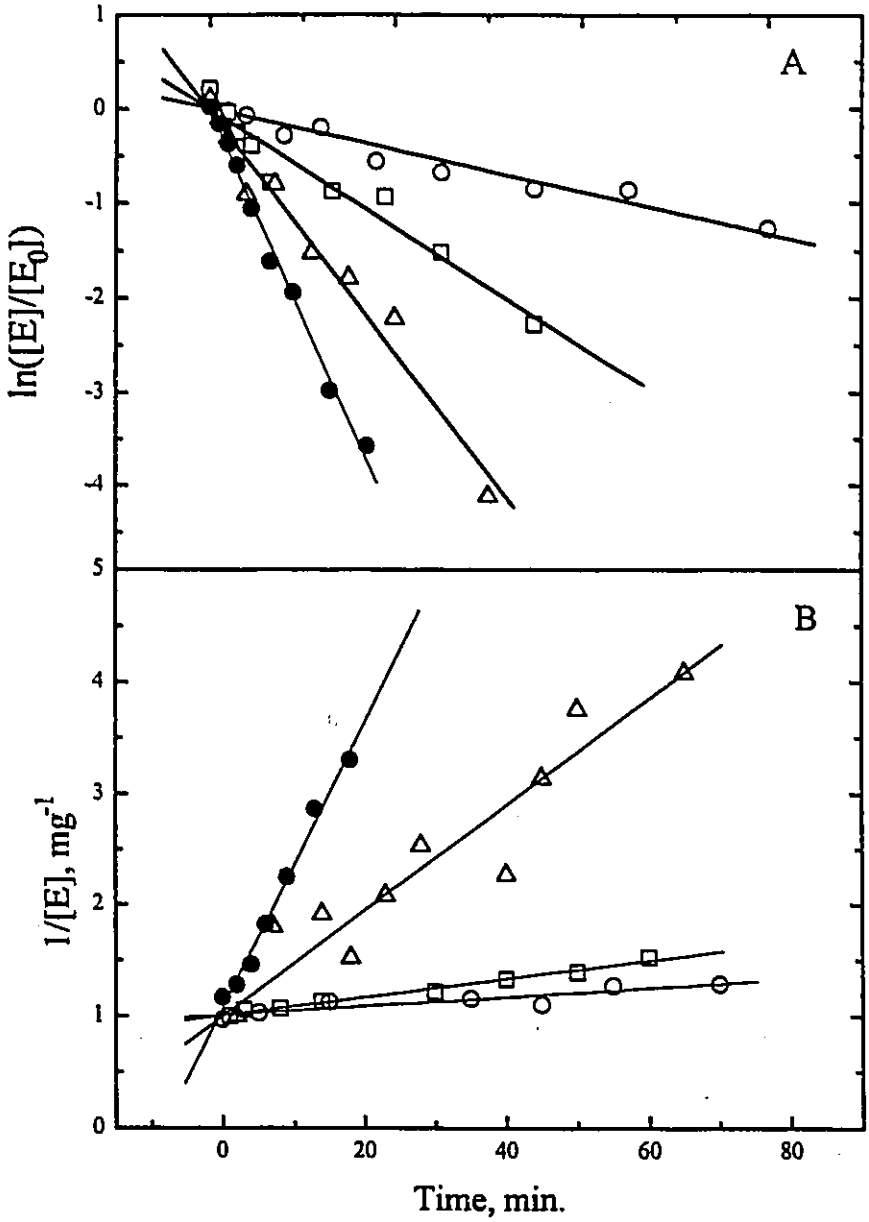

Fig.II.15. Thermal inactivation kinetics of the wild type and disulphide mutant xylanase at 0.125 and 1 mg/mL, respectively at different temperatures. (A) wild type protein at (O) 57, (□) 57.5, (△) 58, and (●) 58.5 °C. (B) Disulphide-bridge mutant at (O) 59, (□) 60, (△) 61, and (●) 61.5 °C.

denaturation pathway of the DS1 mutant controls the rate of protein denaturation.

In order to construct an Arrhenius plot, the kinetic constants for the denaturation of the wild type and DS1 xylanase (K_{app}) were obtained at different temperatures (Fig.II.15). The Arrhenius plots for the wild type protein and the mutant either obtained from thermal inactivation kinetics or from DSC data (Fig.II.7 and Fig.II.8) appear to be non-linear. This indicates that the rate constants for the thermal denaturation of both wild type and the DS1 xylanases consist of the rate constants of the different steps on the denaturation pathway (i.e. K_{app} is a function of k_1, k_2, and k_3). In other words, the kinetic rate constant values of individual steps on the denaturation pathway contribute to determine the overall denaturation rate. The lack of complete superimposability of curves in Fig.II.7.B and Fig.II.8.B can be explained as follows. The design of the thermal inactivation kinetics experiments requires that the heat treated samples are cooled down in order to determine the proportion of the native (N) and irreversibly denatured (I) forms of the protein. During the cooling process, the reversibly unfolded form (U) is being distributed between the native state (N) and irreversibly denatured state (I). Therefore the amount of both native (N) and irreversibly denatured (I) forms are overestimated. The extent of overestimation of either of these species depends on the relative values of k_2 and k_3, and also population of the unfolded state. Obviously, in the case of wild type xylanase,

this deviation is negligible (Fig.II.7) indicating that, due to slow reversible unfolding rate, the unfolded state (U) is not populated. However for the DS1 mutant, since $k_3 < k_1$, the unfolded state probably is more populated. Upon cooling, its refolding to the native state leads to a greater error in estimating the concentration of the native state at various temperatures. Furthermore, the two-state irreversible model is based on the assumption that the thermal denaturation process follows a first-order rate law, that is certainly not the case for the DS1 mutant.

For the wild type xylanase, the apparent rate constants (K_{app}) obtained from thermal inactivation kinetics are similar to those obtained from DSC (Fig.II.7). As shown in the Appendix, K_{app} values from thermal inactivation kinetics can be used to predict the molar fraction of the native form as a function of temperature. Moreover, since heat capacity at constant pressure (C_P) is proportional to dX_N/dT, C_P/Q_t (or $1/Q_t dQ/dT$) can be predicted and compared to experimental values obtained from DSC (Fig.II.16). Two assumptions were made to establish a relationship between the thermal inactivation kinetics and DSC. Firstly, the enthalpy of conversion of the unfolded state (U) to the irreversibly denatured state (I) can be ignored in comparison to the enthalpy of the reversible unfolding. Secondly, the concentration of the unfolded state (U) is almost negligible at any temperature. In other words, in the thermal inactivation kinetic experiments, any overestimation

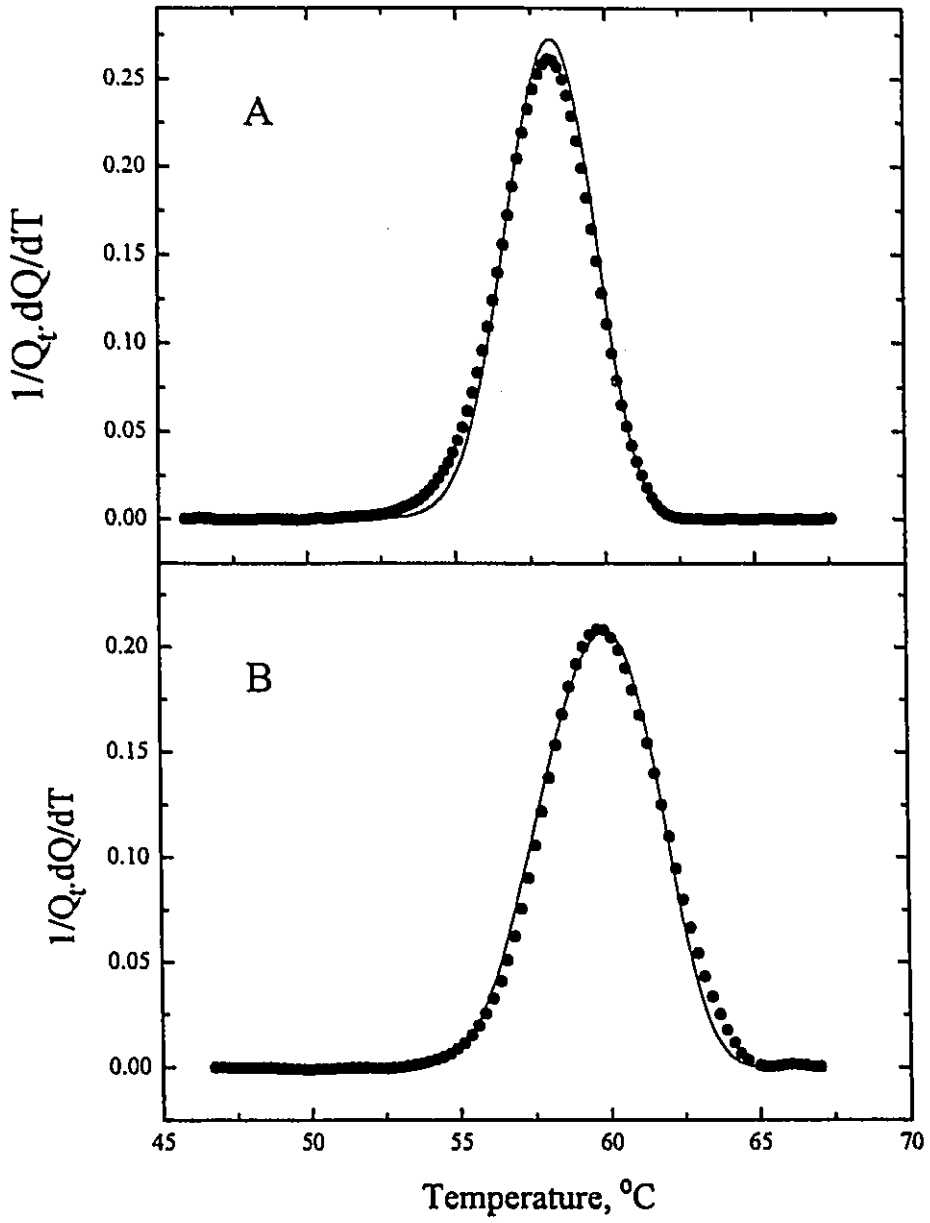

Fig.II.16. The comparison of experimental, dots, and predicted calorimetric thermograms, solid line, for the wild type xylanase normalized to total enthalpy of denaturation ($1/Q_t.dQ/dT$) at two scanning rates of 20 deg./hr, panel A, and 56 deg./hr., panel B.

made in determination of the concentration of the native state (N) due to refolding of the unfolded state can be ignored. Fig.II.16 shows the comparison of $1/Q_t dQ/dT$ values obtained from DSC with those predicted from thermal inactivation kinetics based on equation A-9 (see Appendix). Excellent agreement is seen between the experimental and predicted values, indicating that the assumptions made to develop the equations for the wild type protein hold true. The negligible concentration of the unfolded state indicates that equilibrium is not established between the folded and unfolded state. Thus, application of the two state reversible model to extract thermodynamic parameters is not permissable.

II.6.MECHANISM OF THE THERMAL DENATURATION

As mentioned earlier, in the presence of urea and at lower scanning rates, calorimetric endotherms of the wild type xylanase and its disulphide bond mutant, DS1, can be fitted to a two state reversible model, although a small deviation can be seen for the wild type protein at the very end part of the transition. Applicability of two state reversible model and the small size of the protein implies that the reversible unfolding probably consists of just one populated unfolded form (U). The unfolding probably leads to the exposure of an hydrophobic surface which, in the absence of urea, results in aggregation. Therefore, the unfolded form (U) can either refold to the native form (N) or can

be irreversibly denatured to the aggregated form (I) according to the Lumry & Eyring model (1954):

$$N \underset{k_2}{\overset{k_1}{\rightleftharpoons}} U \xrightarrow{k_3} I \qquad \text{II.6}$$

where k_1, k_2, and k_3 are the kinetic rate constants for unfolding, folding and for irreversible denaturation of the protein, and N, U, and I, are the native, unfolded and irreversibly denatured states of the protein, respectively. This mechanism of denaturation applies for both wild type xylanase and its disulphide mutant. The difference is in the rate limiting step, which is k_1 for the former and k_3 for the latter. Thus, introducing the disulphide bond stabilizes the xylanase by changing the rate limiting step of the denaturation pathway. The mechanism by which the disulphide bond changes the rate limiting step in the thermal denaturation of xylanase is unclear. It has been suggested (Cleland & Wang, 1990) that the exposure of an hydrophobic surface due to unfolding enhances hydrophobic interactions, which leads to aggregation. Furthermore, a study of bovine growth hormone has shown that association of the unfolded forms in order to form aggregates involves distinct structural elements (Brems, 1988). If aggregation proceeds according to a mechanism which involves specific interaction of structural elements, then certain positions in the polypeptide chain will carry information relevant to the process (Mitraki *et al.* 1991). Perhaps, in

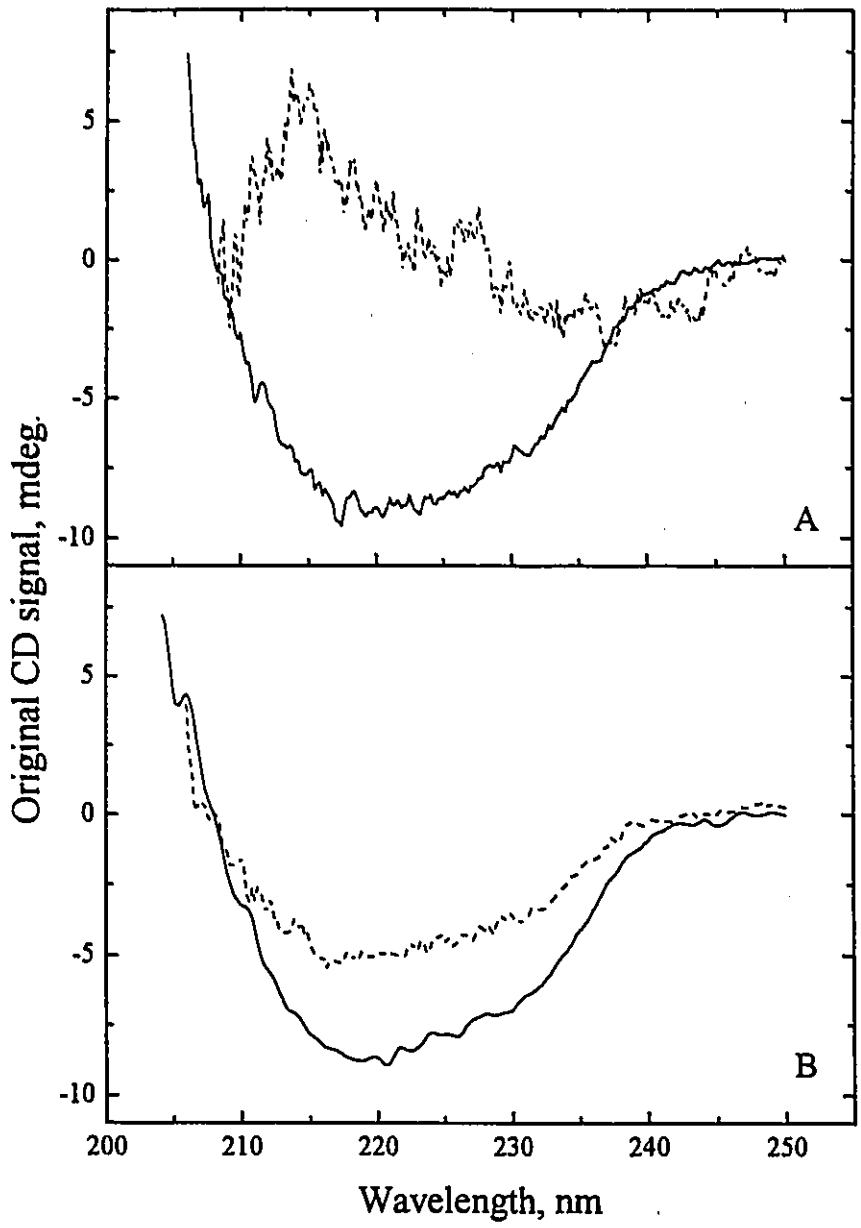

Fig.II.17. CD spectrum of the wild type xylanase, panel A, and DS1 mutant, panel B, before, solid line, and after, dashed line, two consecutive DSC scans with the scanning rate of 56 deg./hr. The final temperature of the samples after each run was 80 °C.

the case of xylanase, the presence of the disulphide bond restricts the exposure of the hydrophobic surface and putative elements that are required for the initiation of aggregation. In order to asses the ability of the S100C/N148C disulphide bond to prevent aggregation, the secondary structure of the wild type protein was compared to the DS1 mutant after two consecutive scans in the presence of 2.5 M urea with scanning rate of 56 °C/hr (Fig.II.17). This figure shows that, after the second calorimetric scan, the original secondary structure of the wild type protein was lost. Furthermore, long exposure of the protein to high temperatures results in aggregation as indicated by the noisier spectrum and also by visual inspection. However, the presence of the disulphide bond in the DS1 mutant protects the protein from complete aggregation and denaturation after a similar treatment. This experiment suggests that the introduction of disulphide bonds can be used as a tool to prevent aggregation by restricting the exposure of hydrophobic surfaces (and possibly the putative elements that are required for aggregation). A similar argument has been employed to explain the enhanced stability of the T4 lysozyme (Wetzel *et al.*, 1988). They have suggested that a 3-97 disulphide bond may stabilize T4 lysozyme by restricting the exposure of hydrophobic surfaces.

The differential scanning calorimetric thermograms for the irreversible denaturation of proteins have two important characteristics. Firstly, the thermograms are highly scan-rate dependent, and secondly, their shapes are

distorted (Sanchez-Ruiz *et al.*, 1988; Freire *et al.*, 1990; Lepock *et al.*, 1992; Sanchez-Ruiz, 1992). The present research provides convincing evidence that these characteristics are not restricted to irreversible denaturation of proteins. They should be considered in analyzing DSC data of the reversible denaturation of proteins. An additional point is that the introduction of the disulphide bond in DS1 mutant enhances the stability of the xylanase by changing the rate limiting step in the denaturation pathway probably by restricting the exposure of the hydrophobic surface.

II.7.SUMMARY AND CONCLUSION

The thermal denaturation of *B. circulans* xylanase and its disulphide bridge containing mutant, DS1, (S100C/N148C) was investigated by differential scanning calorimetry (DSC) and thermal inactivation kinetics. The thermal denaturation of both proteins was found to be irreversible due to aggregation. Furthermore their apparent transition temperatures showed a considerable dependence upon scanning rate, even after correction for instrumental response. In the presence of a "subdenaturing" concentration of urea, a transition was observed in the second run indicating the reversibility of denaturation at that condition. Interestingly, the same extent of scan-rate dependence was observed for the apparent melting point of the reversible and irreversible denaturation of the wild type protein. Calorimetric thermograms of the DS1 mutant, on the other hand, showed a smaller degree of scan-rate dependence in the presence of urea than its absence. Consequently, as for irreversible denaturation, the apparent transition temperature for the reversible denaturation of proteins can also be scan-rate dependent. This dependence leads to a distortion and asymmetry of the endotherms at higher scanning rates which can be misleading. Therefore it is suggested that, in the case of reversible denaturation when asymmetric curves are observed, scan-rate dependence should be checked prior to any data analysis. It was also found that introducing a disulphide bond, in the DS1 mutant, stabilizes the protein by

changing the rate limiting step on the thermal denaturation pathway.

CHAPTER III

COOPERATIVE STABILIZATION EFFECT UPON THE INTRODUCTION OF DISULPHIDE BONDS IN *Bacillus circulans* XYLANASE

III.1. INTRODUCTION

Site directed mutagenesis, as an important strategy to modify proteins, provides a powerful tool to improve protein stability by introducing additional interactions within a protein. It has been shown that introducing disulphide bonds can substantially enhance protein stability (Wetzel, *et al.* 1988, Matsumura, *et al.* 1989; Clarke & Fersht, 1993). The stabilizing effect of a

covalent cross-link is usually assumed to arise from its destabilizing effect on the unfolded state, by decreasing its conformational entropy (Creighton, 1988). This is due to the fact that the presence of a covalent cross-link limits the motional freedom of the protein backbone in the unfolded state, thereby decreasing the entropy. In contrast to other interactions, for instance hydrogen bonds and electrostatic interactions, formation of a disulphide bridge as a covalent bond requires strict stereochemical conditions regarding the relative positions and orientations of the two participating cysteine residues (Creighton, 1988). The difficulties in designing new disulphide bonds inside proteins can be overcome by comparing homologous proteins. A comparison of the low molecular weight xylanase A sequence from *Schizophyllum commune* with the xylanase from *Bacillus circulans* revealed the presence of a disulphide bridge between positions 111 and 160 in the former, which corresponds to positions 100 and 148 in the latter. (Oku, *et al.* 1993). Therefore, a disulphide bond was introduced at this position (Fig.III.1). With the additional idea that a cross-link in the centre of the α-helix (instead of a S-S bond located at the edge of the α-helix as in the DS1 mutant, see Fig.III.1) may be more effective in enhancing xylanase stability, another disulphide bridge was established between residues 98 and 152 (DS2).

It has been suggested that the increase in stability of a protein due to the introduction of a disulphide bond is proportional to the number of residues

linked by the S-S bond (Pace, *et al.*, 1988). Verification of this notion requires introducing a disulphide bond into two positions in a way that the number of residues looped by the cross-links is different. Since, in *B. circulans* xylanase, the N-terminus is located in proximity to the C-terminus, it is possible to join them by introducing a disulphide bond. The resulting protein is called circular xylanase (cXI, Fig.III.2). The comparison of the $\Delta\Delta G$ of stabilization of this mutant with that of the DS1 mutant provided the opportunity to evaluate stability predictions based on number of residues encompassed by a cross-link. Furthermore, the stabilization effect of the simultaneous introduction of two disulphide bonds, DS1 and cXI, was investigated by differential scanning calorimetry and chemical denaturation. Table III.1. summarizes the position of the mutations and relative activity of different variants.

Fig.III.1. The fold of the DS1 mutant showing the position of the disulphide bond.

Fig.III.2. The position of disulphide bond in the cXI mutant.

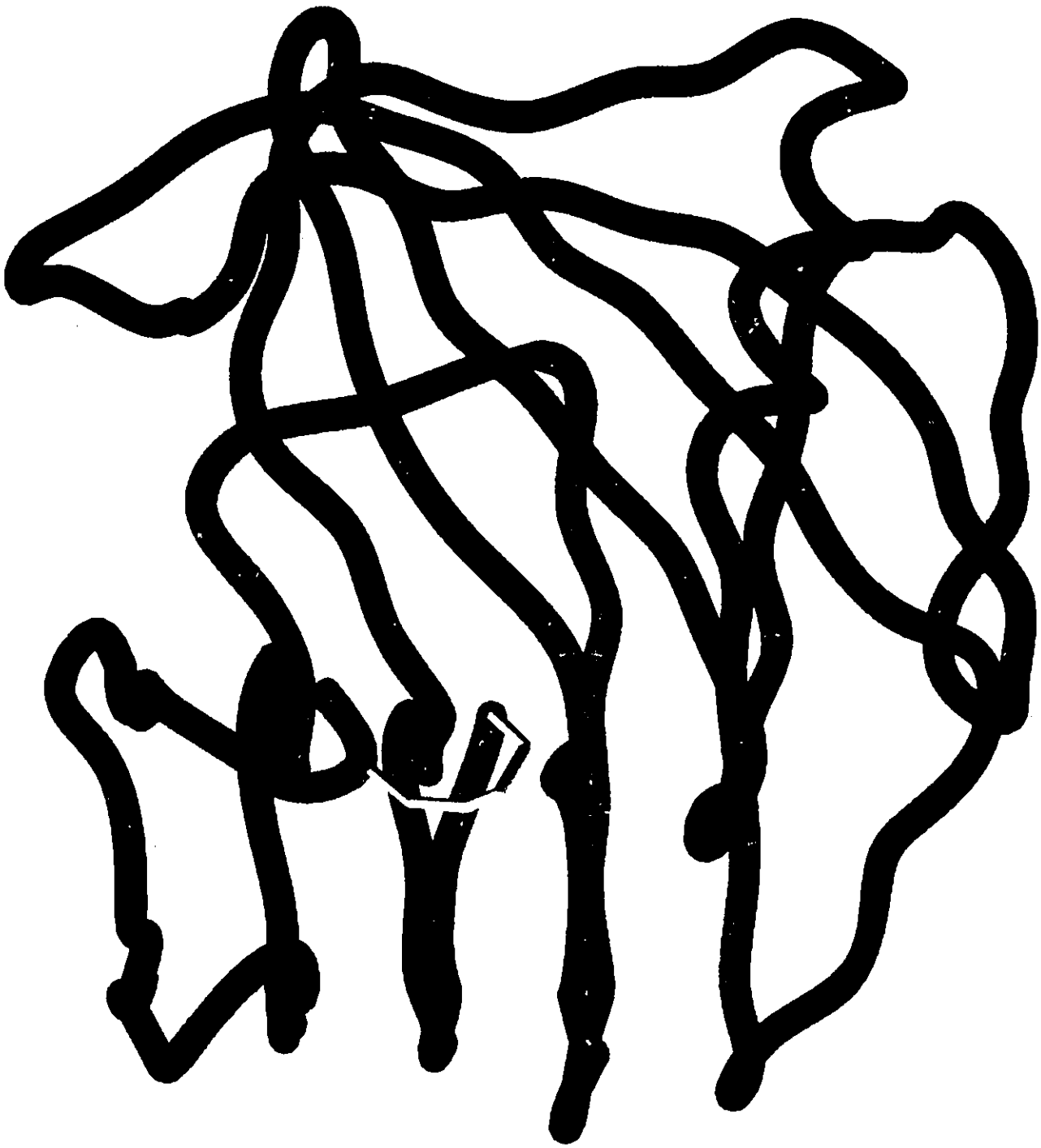

Table.III.1. The position of disulphide bonds introduced into *B. circulans* xylanase and their relative activities.

Protein	Amino acid changes	Description	Relative activity%
Wild type	-	no disulphide bond is present in the structure	100
DS1	S100C, N148C	Single disulphide bond mutant	110
DS2	V98C, A152C	Single disulphide bond mutant	95
cXI	A1GC[a], G187[b], C188	C-terminal is joined to N-terminal	96
cDS1	S100C, N148C, A1GC, G187, C188	Combination of DS1 and cXI mutations	68

[a]The N-terminus was changed by the deletion of alanine1 and the addition of glycine and cysteine.

[b]The residues 187 and 188 were additions to the C-terminus with the numbering based on the N-terminal glycine being residue 1 (Wakarchuk, *et al.* 1994b).

III.2.MATERIALS AND METHODS

Differential scanning calorimetry, circular dichroism spectroscopy, and enzymatic activity measurements were performed as described in Chapter II.

III.2.1.Chemical denaturation experiments

Guanidinium chloride or urea promoted unfolding was monitored by circular dichroism spectroscopy at 228 and 227 nm, respectively. A stock solution of urea with a concentration of 7.8 M was prepared and stored at -20 °C to minimize formation of ammonium cyanate on storage. Similarly, a 5 M stock solution of guanidinium chloride (GdmHCl) was prepared in 20 mM phosphate buffer and stored in -4 °C. For each point on the denaturation profile, 20 μl solution of the enzyme was diluted in a 180 μl mixture of the appropriate amount of denaturant and buffer and incubated for about 15 hrs at 24 °C. Unfolding was found to be completely reversible as shown in Fig.III.14.

III.2.2.Analysis of guanidinium chloride denaturation

The equilibrium constant for unfolding, K, is calculated from the following equation:

$$K=\frac{[U]}{[F]}=\frac{\Theta_{228}-\Theta_F}{\Theta_U-\Theta_{228}} \qquad \text{III.1}$$

where θ_{228} is the observed CD signal and θ_F and θ_U are the values of the CD signal of the folded and unfolded forms of the protein. It has been experimentally demonstrated that the free energy of the unfolded protein, ΔG_U, is linearly related to the concentration of denaturant (Greene & Pace, 1974):

$$\Delta G_U = \Delta G_d(H_2O) - m[denaturant] \qquad \text{III.2}$$

m is a parameter showing the dependence of ΔG_U on the concentration of denaturant and $\Delta G_d(H_2O)$ the free energy of unfolding in the absence of denaturant. Since, $\Delta G_U = -RTlnK$, then:

$$\Delta G_d(H_2O) - m[denaturant] = -RTlnK \qquad \text{III.3}$$

incorporation of the K value from equation III.1 into equation III.3 and its rearrangement leads to equation III.4:

$$\theta_{228} = \frac{\theta_F + \theta_U \exp\{\frac{m[D] - \Delta G_d(H2O)}{RT}\}}{1 + \exp\{\frac{m[D] - \Delta G_d(H2O)}{RT}\}} \qquad \text{III.4}$$

where [D] is the concentration of denaturant. Using Origin software,

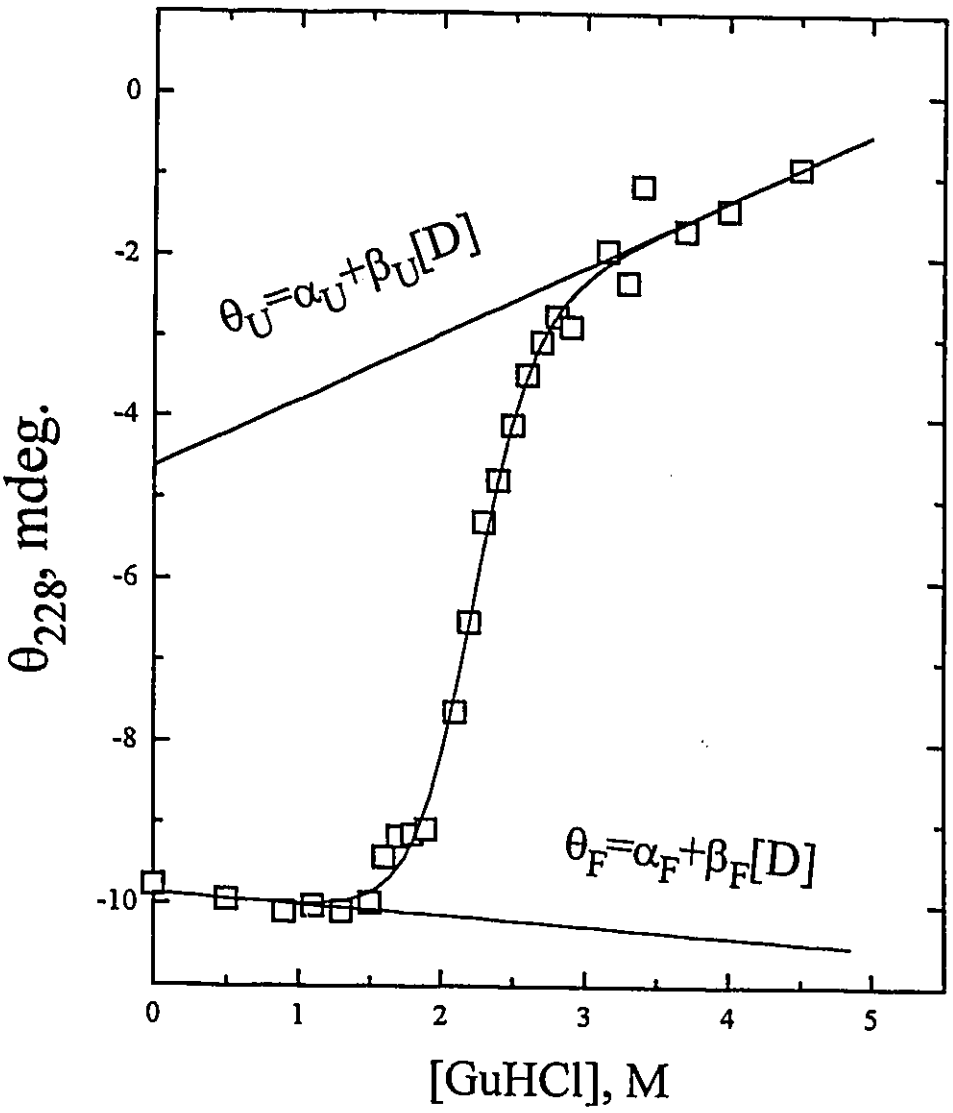

Fig.III.3. Guanidinium chloride denaturation curve of the cXI mutant showing the extrapolation of the plateau region in order to estimate θ_F and θ_U values.

experimental data were directly fitted to equation III.4 in order to obtain the values of m and $\Delta G_d(H_2O)$. The values of θ_F and θ_U at any concentration of denaturant can be obtained by linear extrapolation of the two plateau regions (Fig.III.3). Incorporation of this point in equation III.4 yields the final form of the equation (please refer to Equation III.7 in Section III.6).

III.3. CHARACTERIZATION OF THE MUTANTS

Prior to any assessment of the stability achieved by site directed mutagenesis, it is essential to determine whether or not different variants of the xylanase are properly folded. Therefore, the secondary and tertiary structures of wild type xylanase and its variants were compared using far and near-UV circular dichroism spectroscopy (Fig.III.4, Fig.III.5). The secondary structure of all of the mutants remains essentially unchanged, since no major differences can be seen in the far-UV circular dichroism spectra of the mutants compared to wild type (Fig.III.4). Furthermore, except for the DS2 mutant, the near-UV CD spectra of the wild type and mutants appear to be identical. The near-UV CD spectrum results from the near-UV electronic transitions of aromatic side chains, and their coupling with electronic transitions arising from aromatic residues, peptide bonds, and charged groups in an asymmetric environment (Strickland, 1974; Sears & Beychok, 1973). Therefore, any change in the environment of these residues, due to change in tertiary structure, would affect these electronic transitions leading to a different spectrum. Accordingly, identical near-UV CD spectra indicate that the tertiary structure of the mutants remained intact. Only in the case of the DS2 variant, elipticity was increased with respect to the wild type indicating a somewhat altered tertiary structure (Fig.III.5). Overall, the circular dichroism data indicate that these mutations do not hamper proper folding of the proteins.

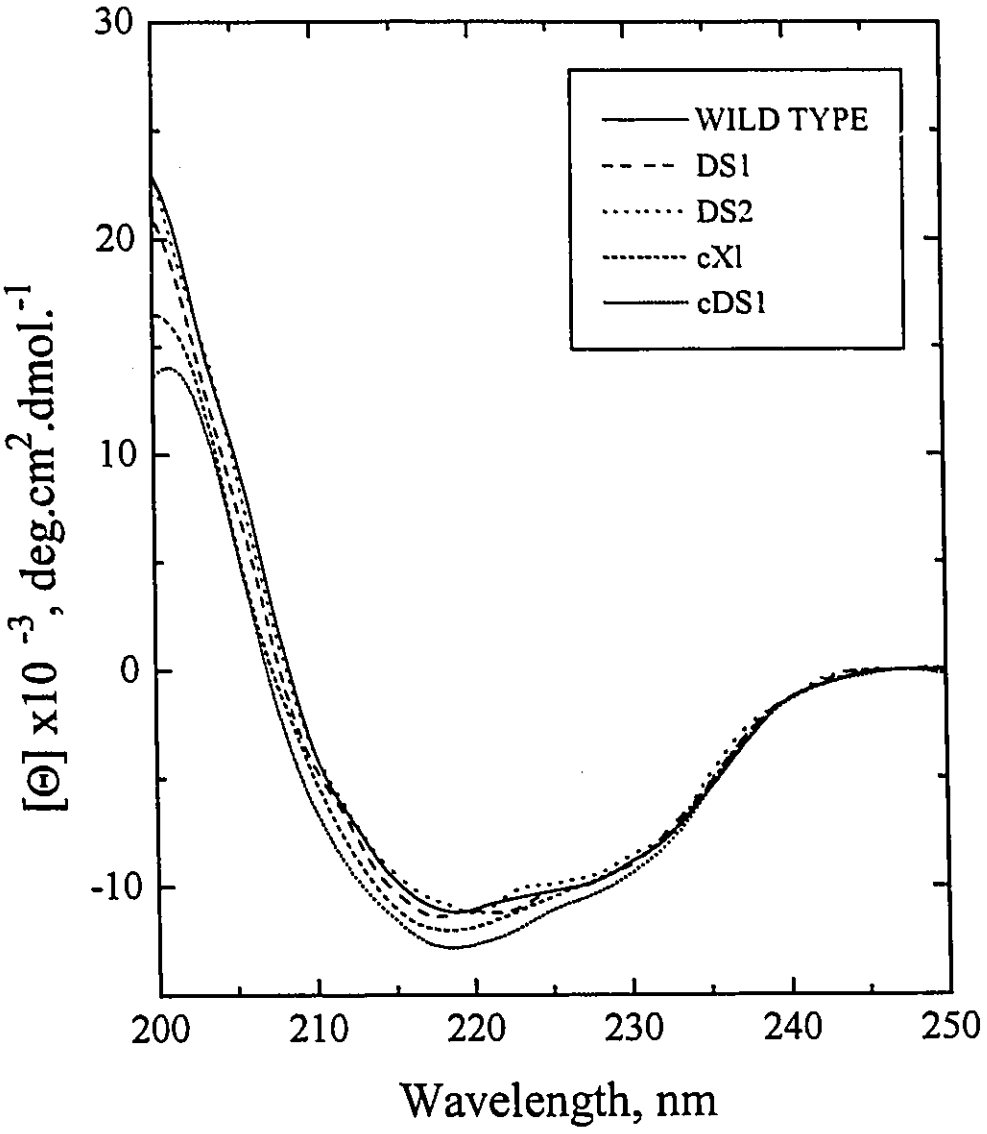

Fig.III.4. Far-UV circular dichroism spectra of the wild type xylanase and its disulphide bond mutants in 20 mM phosphate buffer at pH 6.0.

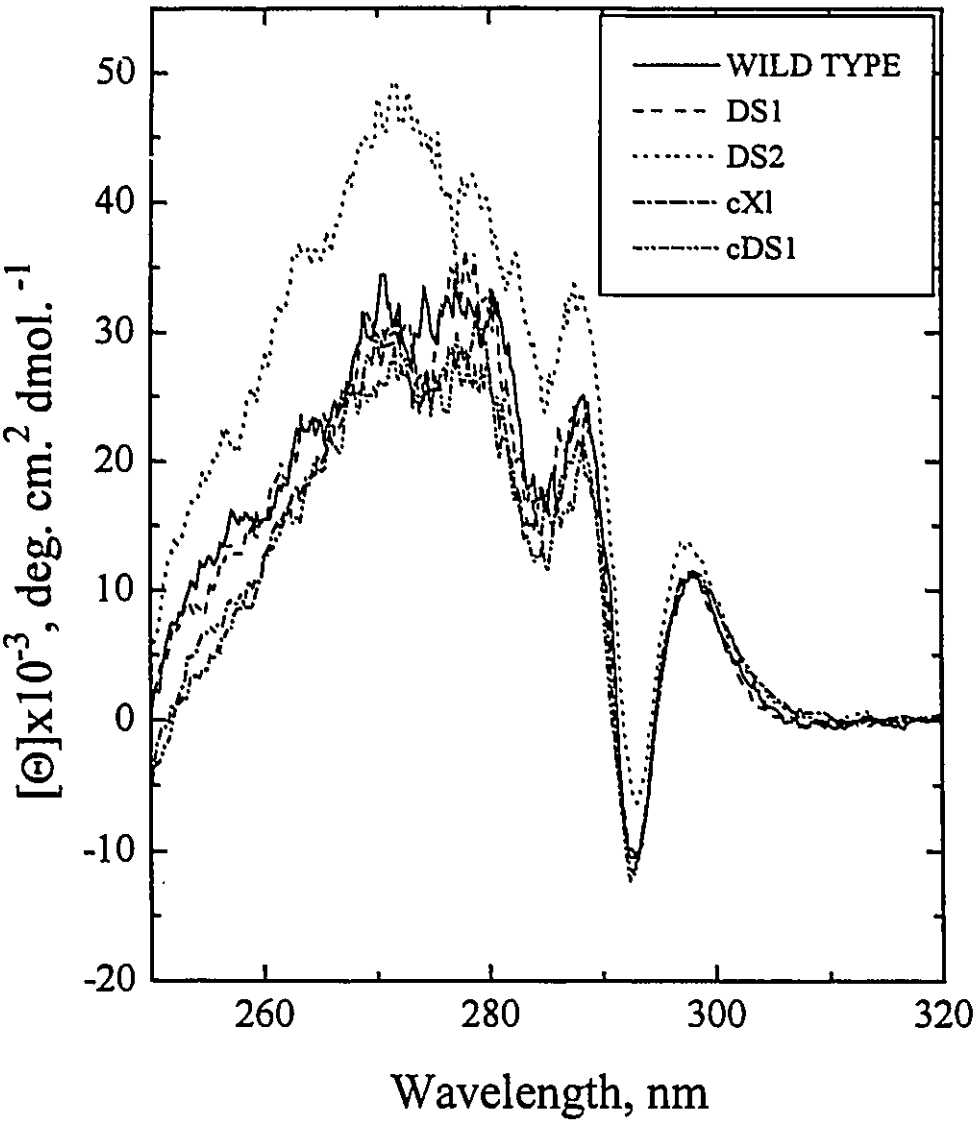

Fig.III.5. Near-UV circular dichroism spectra of the wild type xylanase and its disulphide bond mutants in 50 mM ammonium acetate buffer at pH 6.0.

All of the mutants maintained high enzymatic activity (Table.III.1) with the exception of cDS1 variant. This mutant contains two disulphide bonds with identical positions to those in DS1 and cXI. When the disulphide bonds are introduced singly, as the DS1 or cXI variants, enzymatic activity remained intact. However, simultaneous introduction of the two is accompanied by 32% decrease in activity. Considering the fact that the simultaneous introduction of two disulphide bonds did not alter the secondary or tertiary structure (Fig.III.4, Fig.III.5), activity decrease may be a consequence of an increase in rigidity of structure or some minor local changes that cannot be detected by CD.

III.4. DSC STUDIES OF THE WILD TYPE XYLANASE AND ITS VARIANTS UNDER IRREVERSIBLE DENATURATION CONDITIONS

To compare the effects of different substitutions on thermal stability, differential scanning calorimetry was applied. This technique can be used to determine the thermodynamic parameters of the thermal unfolding, when the process is reversible. The thermal denaturation of the wild type xylanase and its variants in buffer was found to be irreversible, as no transition was observed in the second run (Fig.III.6). Consequently, thermodynamic parameters cannot be determined under such conditions. Moreover, the melting temperature (t_m) of the wild type protein and its variants showed a dependence upon the rate of temperature increase (scanning rate). These facts indicate that the thermal

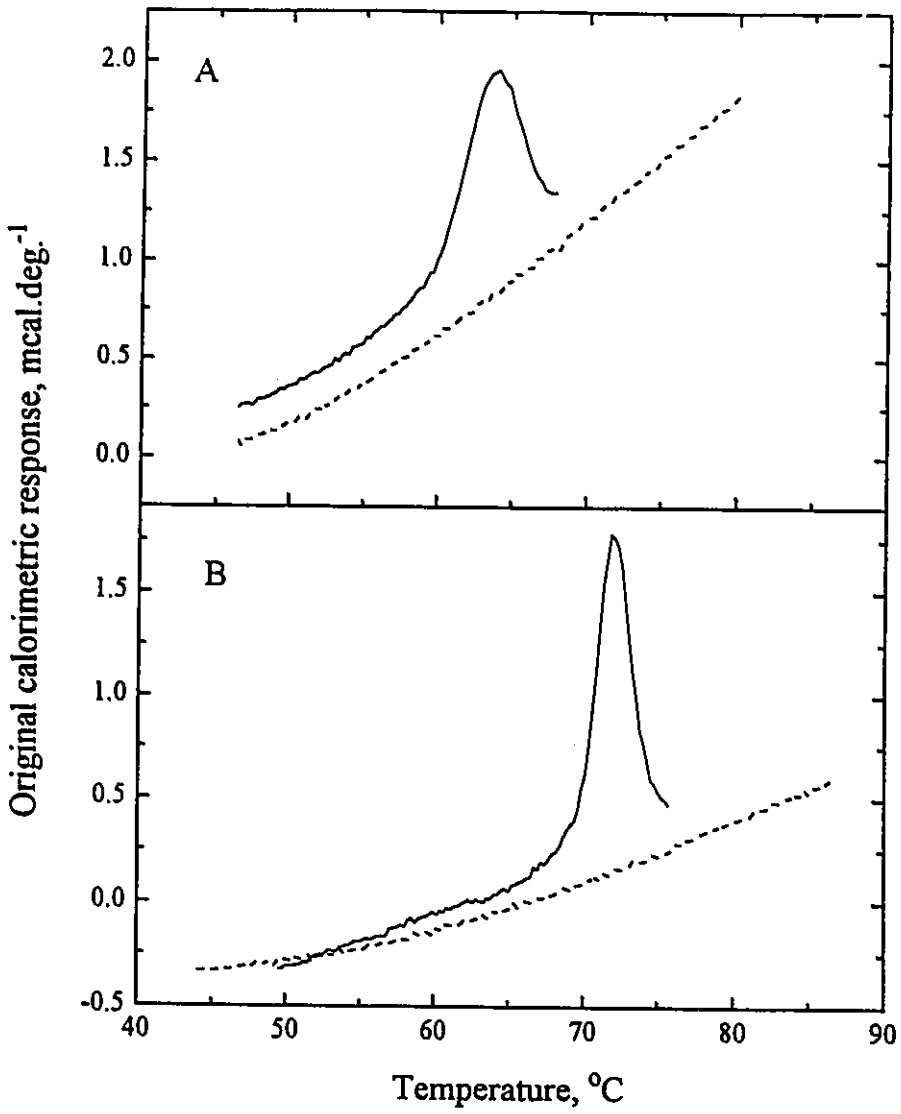

Fig.III.6. Original calorimetric recordings for the cXI, A, and cDS1, B, mutants of *B. circulans* xylanase at the scanning rate of about 58 °C/hr in 50 mM ammonium acetate, pH 6.0, with protein concentrations of approximately 0.54 and 0.59 mg/mL, respectively. The dashed lines are the second heating run after cooling down the samples.

denaturation is controlled by kinetic rather than thermodynamic factors. Nevertheless, for the sake of comparison of the stability achieved by mutations, the melting point (t_m) of the mutants was compared to wild type xylanase under conditions of identical scan-rates. All of the mutants achieved considerable enhanced stability with respect to the wild type (Fig.III.7, Table.III.2). The cDS1 variant with a 12 degrees increase in the melting point showed the maximum increased stability. A comparison of the melting temperature for the cDS1, DS1 and cXI mutants revealed that the enhanced stability of the cDS1 variant due to the introduction of two disulphide bonds (S100C, N148C and A1GC, G187, C188, bonds) seems to be a cooperative effect in stabilization rather than additive. This conclusion was further supported by the chemical denaturation as well as thermal denaturation in the presence of urea (see Tables III.2, III.3, and III.4).

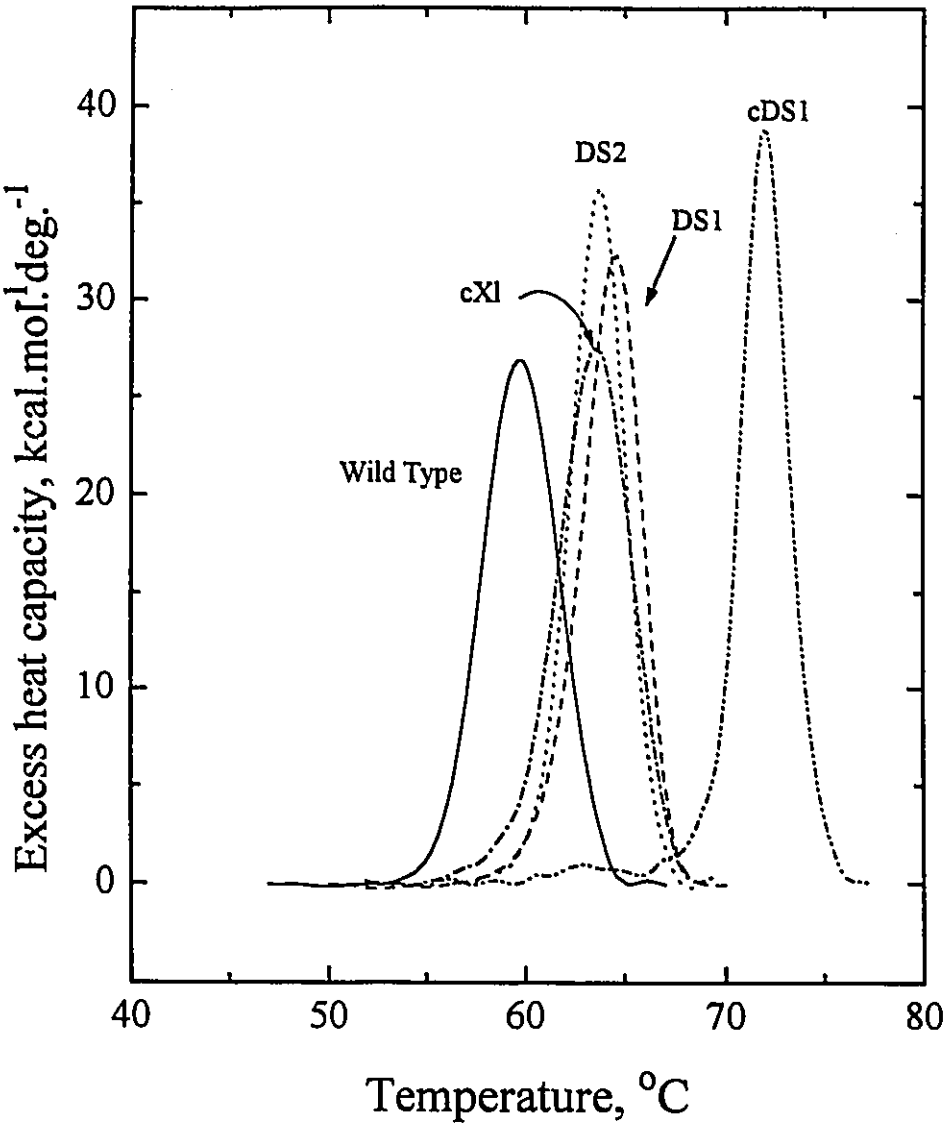

Fig.III.7. Differential scanning calorimetric transitions for the wild type xylanase and its disulphide bond variants with the scanning rate of about 57 °C/hr at pH 6.0 in ammonium acetate buffer.

Table III.2. Melting points of the wild type *B. circulans* xylanase and its variants in 50 mM ammonium acetate obtained by differential scanning calorimetry with a scanning rate of about 57 °C/hr.

Protein	Wild type	DS1	DS2	cXI	cDS1
t_m(°C)	59.7	64.7	63.8	63.5	72.0
*Δt_m	0.0	5.0	4.1	3.8	12.3

* Δt_m is equal to the difference between the melting point of the mutant and wild type.

III.5. DSC STUDIES OF THE WILD TYPE XYLANASE AND ITS VARIANTS UNDER REVERSIBLE DENATURATION CONDITIONS

As mentioned earlier thermal denaturation of the wild type xylanase and its variants appeared to be irreversible due to aggregation. It has been shown that the aggregation of proteins can be prevented by denaturating agents like urea, or guanidinium chloride (Freire, *et al.*, 1992). Hence, thermal denaturation of wild type and mutant xylanases was investigated in the presence of these agents. The presence of guanidinium chloride did not lead to reversible thermal unfolding, as no transition was observed in the second heating run. The presence of urea, however, prevented aggregation of all of the mutants leading to their reversible denaturation (Fig.III.8, and Fig.III.9). The extent of reversibility was found to be dependent upon concentration of urea. Since the reversibility of the thermal denaturation was improved up to 2.5 M urea concentration, this concentration of urea was chosen to study reversible thermal denaturation of the wild type protein and its variants. In order to make sure that the presence of urea did not result in a major change in xylanase structure, circular dichroism spectra of the protein were measured at various urea concentrations. Fig.III.10 shows that the CD spectrum of the protein remains essentially unchanged between zero and 5.5 molar urea concentration. As the urea concentration was increased further, an abrupt change of the protein structure occurred (Fig.III.10, Fig.III.11). Therefore, conducting thermal

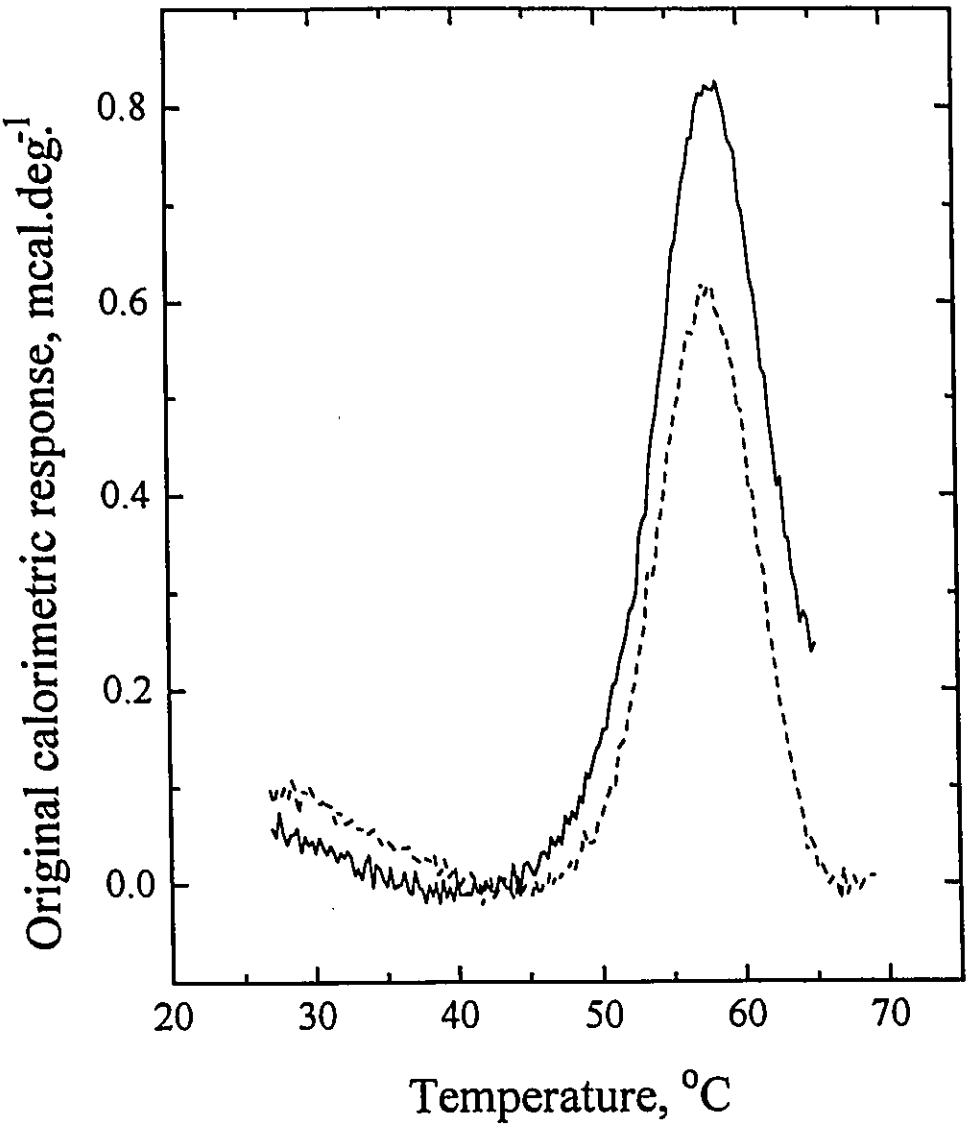

Fig.III.8. Original calorimetric recording for the cXI mutant with the protein concentration of about 0.5 mg/mL in 2.5 M urea concentration at pH 6.0. The solid line shows the first heating run with the scanning rate of 58.0 °C/hr. The dotted line is the second run after immediate cooling the sample.

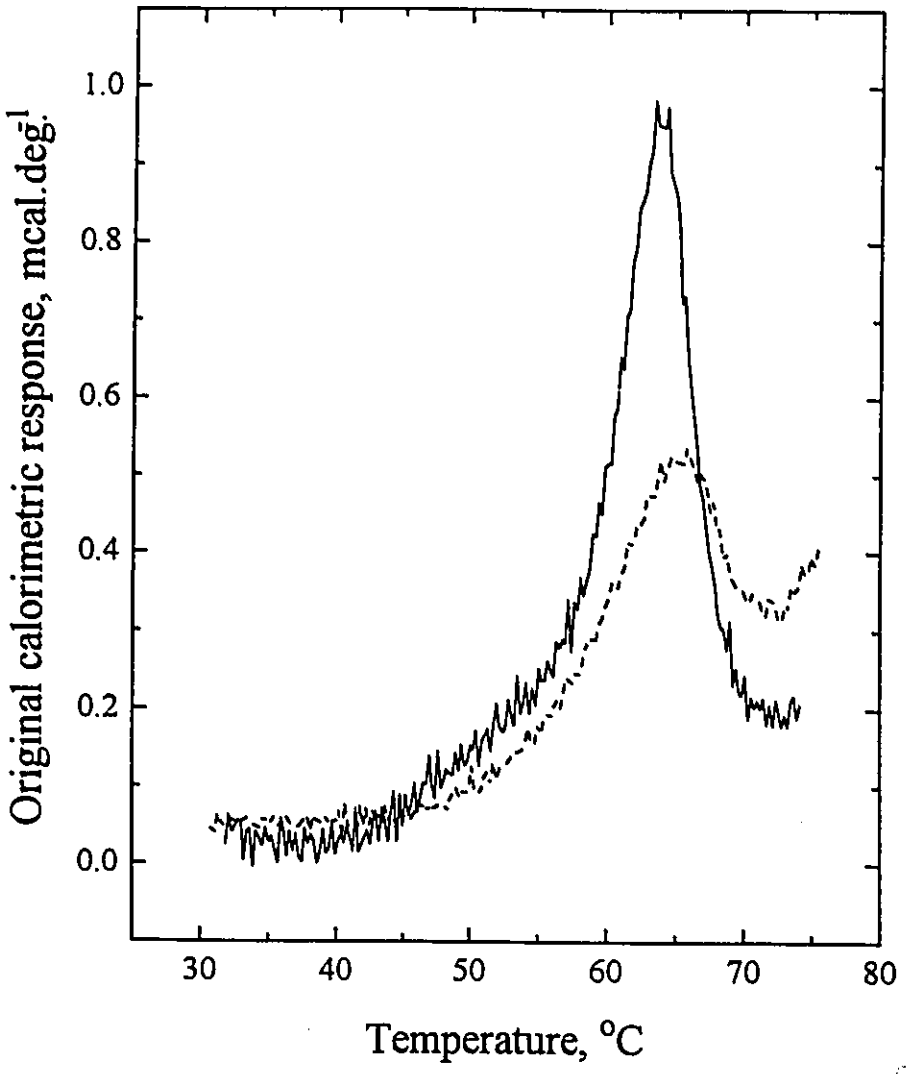

Fig.III.9. Original calorimetric recording for the cDS1 mutant with the protein concentration of about 0.5 mg/mL in 2.5 M urea concentration at pH 6.0. The solid line shows the first heating run with the scanning rate of 13.0 °C/hr. The dotted line is the second run with the scanning rate of about 58.0 °C/hr after immediate cooling the sample.

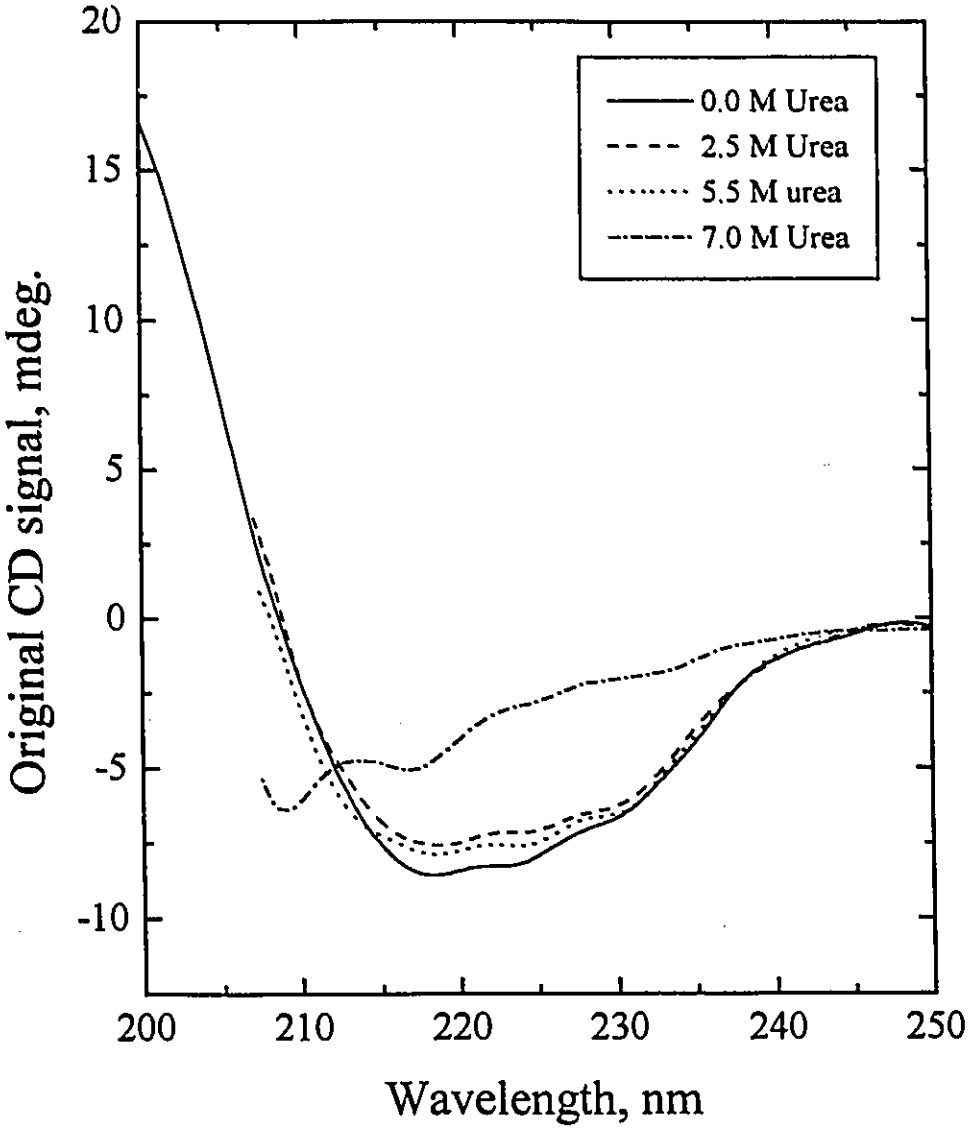

Fig.III.10. Far-UV circular dichroism spectra of the wild type xylanase with a protein concentration of about 0.4 mg/mL in various concentrations of urea.

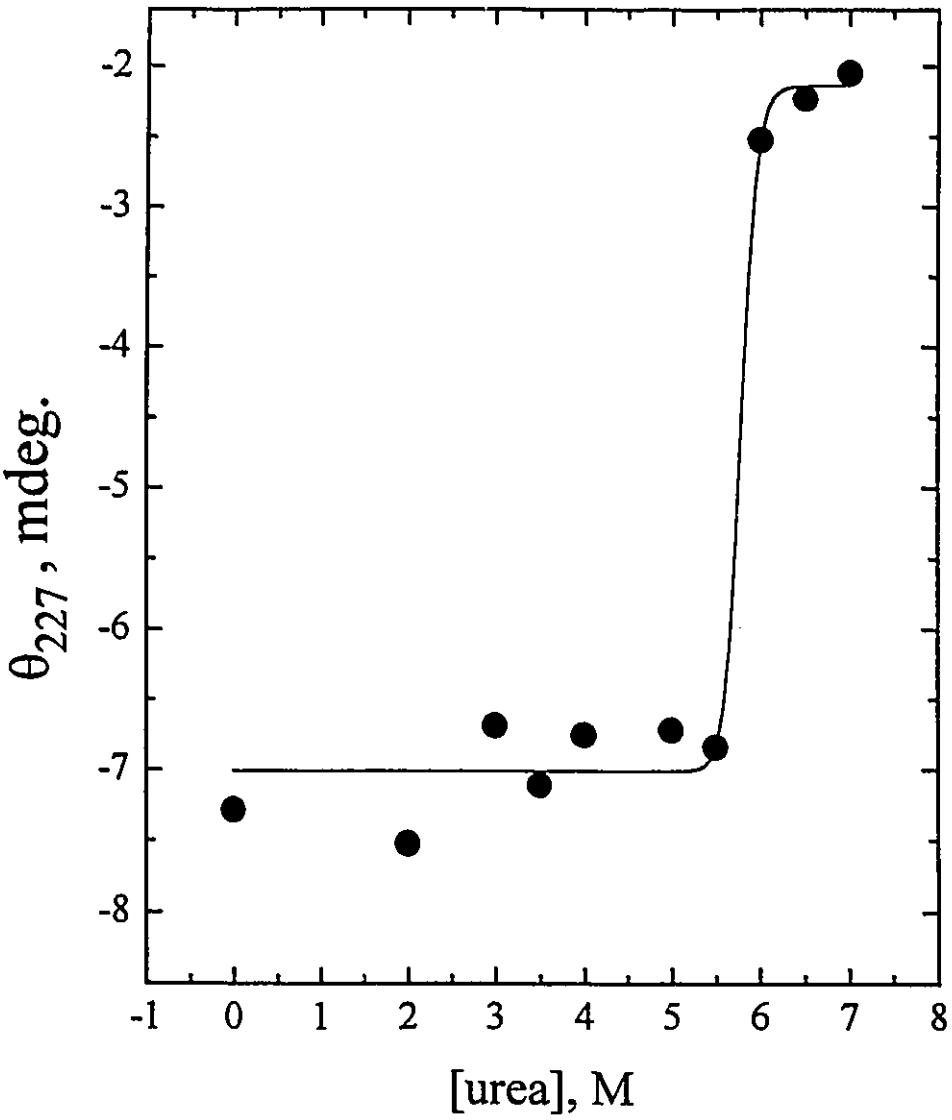

Fig.III.11. Urea denaturation curve of the wild type xylanase. The decline of secondary structure was monitored at 227 nm by circular dichroism spectroscopy.

denaturation in 2.5 M urea is justifiable, since under such conditions the proteins are far from the point where chemical denaturation takes place.

Under reversible conditions, thermodynamic parameters for the wild type xylanase and mutants can be obtained by differential scanning calorimetry. The area under each thermogram is equal to the calorimetric enthalpy (ΔH) of thermal denaturation (Fig.III.12). Using equation III.5, from the shift in T_m, the changes in the apparent stability of mutants relative to the wild type, Δ(ΔG) can be evaluated at the T_m of the wild type protein:

$$\Delta(\Delta G)=\Delta G(Mutant)-\Delta G(Wild\ Type) \qquad \text{III.5}$$

ΔG(Wild Type) is zero at T_m, while the ΔG(Mutant) can be obtain by the following form of the Gibbs-Helmholtz equation:

$$\Delta G(Mutant)=\Delta H[1-\frac{T_m}{T_m'}]-\Delta C_P[T_m'-T_m+T_m.\ln\frac{T_m}{T_m'}] \qquad \text{III.6}$$

where T_m and T_m' are the melting temperature for wild type and mutant xylanase, respectively. ΔH is the calorimetric enthalpy of the mutant at T_m', and ΔC_p is the heat capacity change for the mutant. Since, for the wild type xylanase

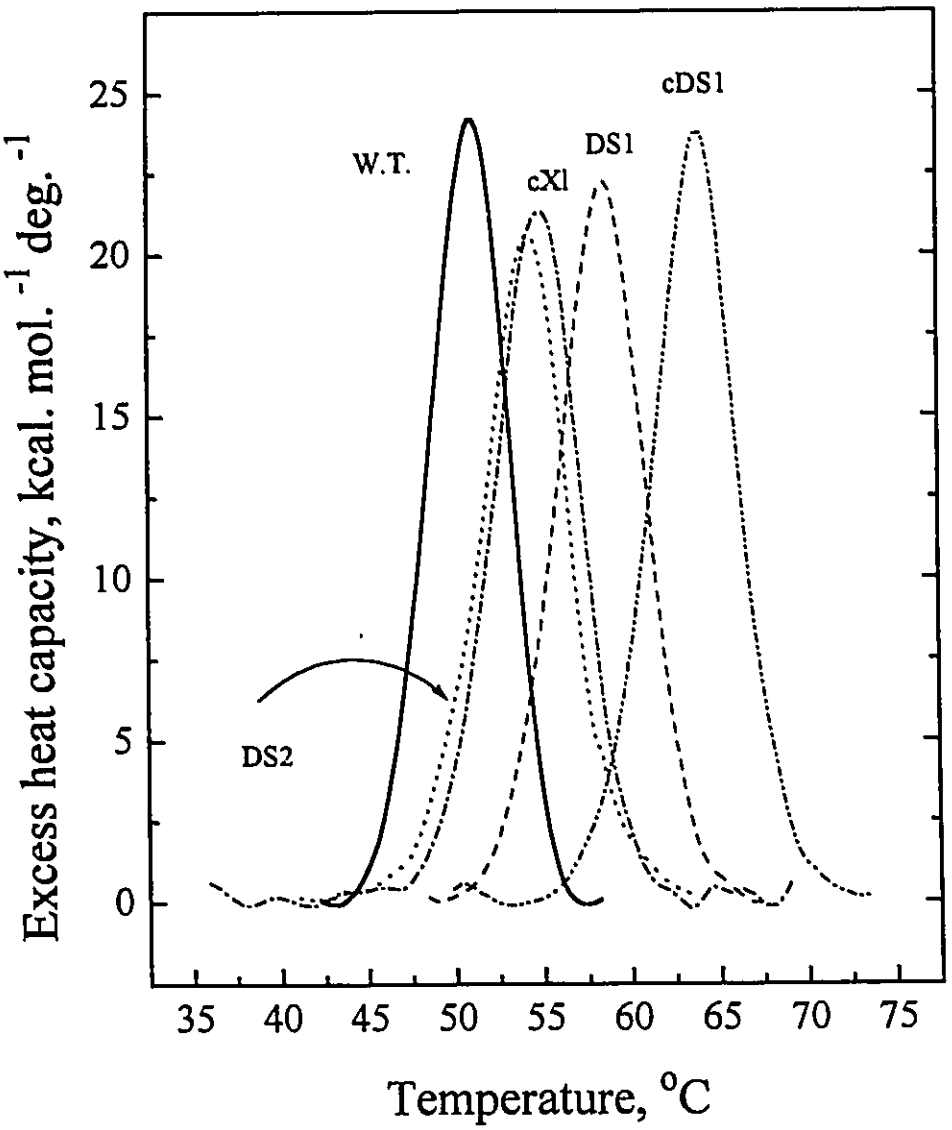

Fig.III.12. Differential scanning calorimetry thermograms of the wild type xylanase and its disulphide bond variants at pH 6.0 in ammonium acetate buffer in the presence of 2.5 M urea concentration.

or any of its variants, no consistent change between heat capacity of the native form and denatured form was observed, ΔC_p was considered to be zero. Since, the van't Hoff enthalpies of all of the mutants are essentially identical to their calorimetric enthalpy, thermal denaturation of the proteins obeys a two state reversible model (Freire & Biltonen, 1978). The values of $\Delta(\Delta G)$ are listed in Table.III.3. A comparison of the melting temperature and $\Delta(\Delta G)$ of the wild type with those of the mutants shows a moderate stabilization effect of the V98C, A152C (DS2) and A1GC, G187, C188 (cXI) mutations. The increase of the melting point due to introduction of the disulphide bond in the DS1 protein is considerably more than in cXI and DS2. A similar trend can be observed from the comparison of the free energy of stabilization of mutants with respect to wild type (Table.III.3). The DS1 mutant with 3.1 kcal/mol free energy of stabilization, is more stable than DS2 or cXI with 1.1 and 1.7 kcal/mol stabilization energies, respectively (Table.III.3). The sum of the $\Delta(\Delta G)$ of stabilization for cXI and DS1 is equal to 4.8 kcal/mol which is 1.3 kcal/mol less than that of the cDS1 mutant. It is therefore suggested that the combination of the two disulphide bonds stabilizes the protein in a cooperative rather than an additive manner.

Table.III.3. Thermodynamic parameters of the wild type xylanase and its disulphide bond mutants obtained from differential scanning calorimetry under reversible conditions (in the presence of 2.5 M urea).

Protein	ΔH_{cal}, kcal/mol	t_m(°C)	Δt_m(°C)	$\Delta(\Delta G°)$, kcal/mol
Wild type	133	51.2	0	0
DS1	138	58.6	7.4	3.1
DS2	132	54.4	3.2	1.1
cXI	136	55.1	3.9	1.7
cDS1	146	63.9	12.7	6.1

III.6. GUANIDINIUM CHLORIDE DENATURATION OF THE WILD TYPE XYLANASE AND ITS MUTANTS

In order to gain further insight into the thermodynamic stabilization achieved by various mutations, chemical denaturation experiments were carried out using guanidinium chloride as a denaturant. To follow the effect of increasing concentration of guanidinium chloride on the structure of the proteins, far-UV circular dichroism spectroscopy was applied (Fig.III.13). Maximal change in the spectrum of the wild type and mutant xylanase occurs in the wavelength range 222-230 nm (data is shown for wild type only). Hence, any wavelength in this range can be used to follow the decrease of the secondary structure as a function of guanidinium chloride concentration. The reversibility of denaturation was verified by diluting a concentrated GdmHCl solution of protein followed by measuring the CD spectrum (Fig.III.14). Assuming unfolding follows a two state transition model, the equilibrium constant, K, between folded (F) and unfolded (U) states, $K=[U]/[F]$, and the free energy of unfolding, $\Delta G_U=-RT\ln K$, at a given concentration of GdmHCl were calculated from each unfolding curve. The values of m and $\Delta G_d(H_2O)$ were obtained directly by fitting the entire CD data set to the following equation (please refer to Materials and Methods of this chapter to see how Equation III.7 is derived):

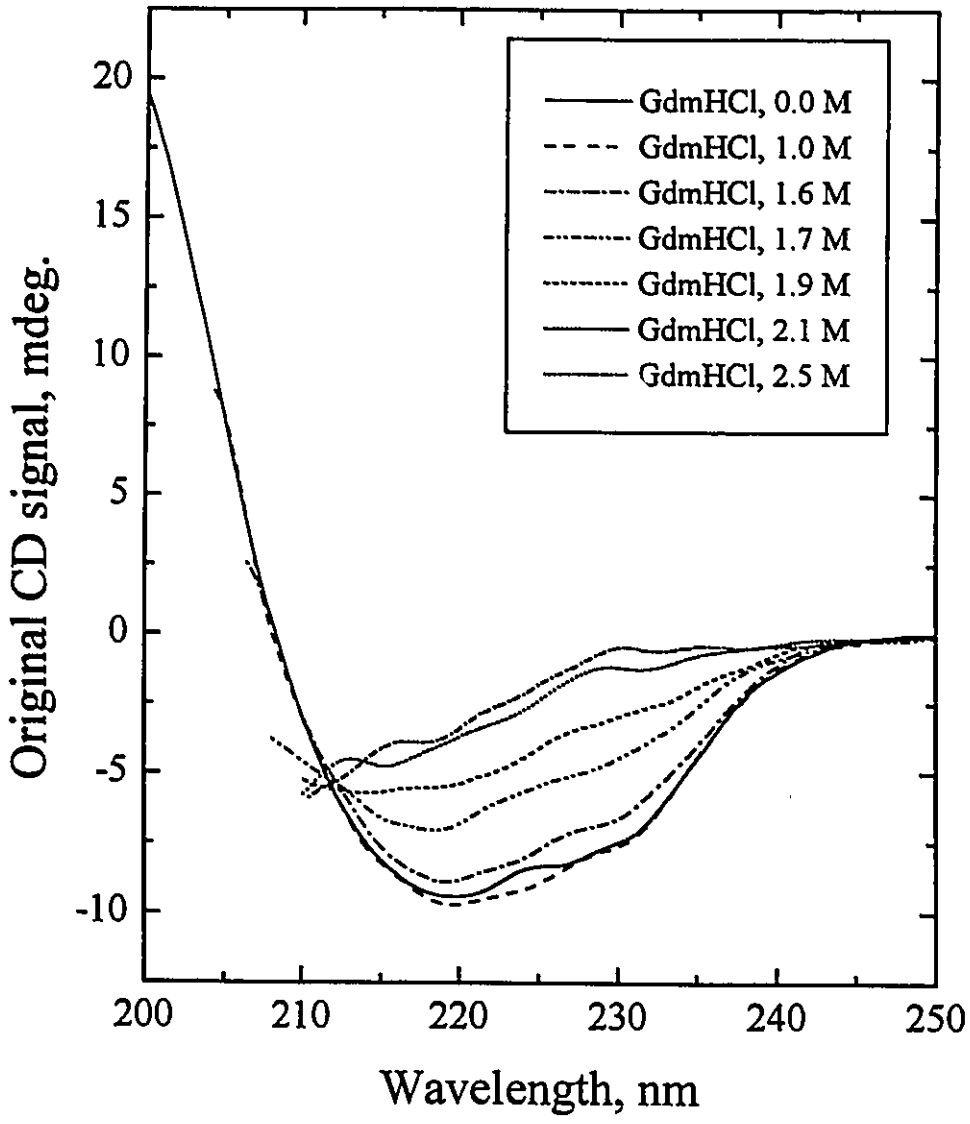

Fig.III.13. Far-UV circular dichroism spectra of the wild type xylanase in various concentrations of guanidinium chloride (GdmHCl) with the protein concentration at about 0.5 mg/mL.

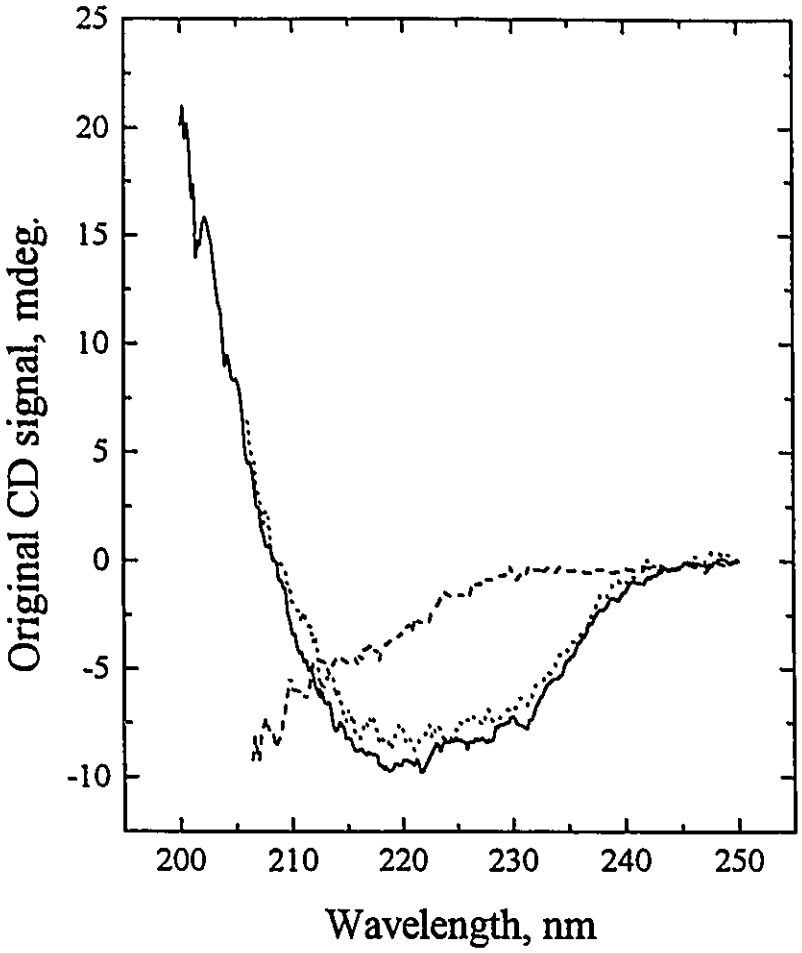

Fig.III.14. Reversibility of guanidinium chloride denaturation of the wild type xylanase verified by far-UV circular dichroism spectroscopy. The solid line is spectrum of the protein in the absence of guanidinium chloride (GdmHCl) with protein concentration of about 0.5 mg/mL, and the dashed line in the presence of 2.7 M GdmHCl measured in a 0.02-cm-path length cylindrical quartz cell. The dotted line is the latter sample after 50 times dilution with 20 mM phosphate buffer measured in a 1 cm pathlength cylindrical quartz cell.

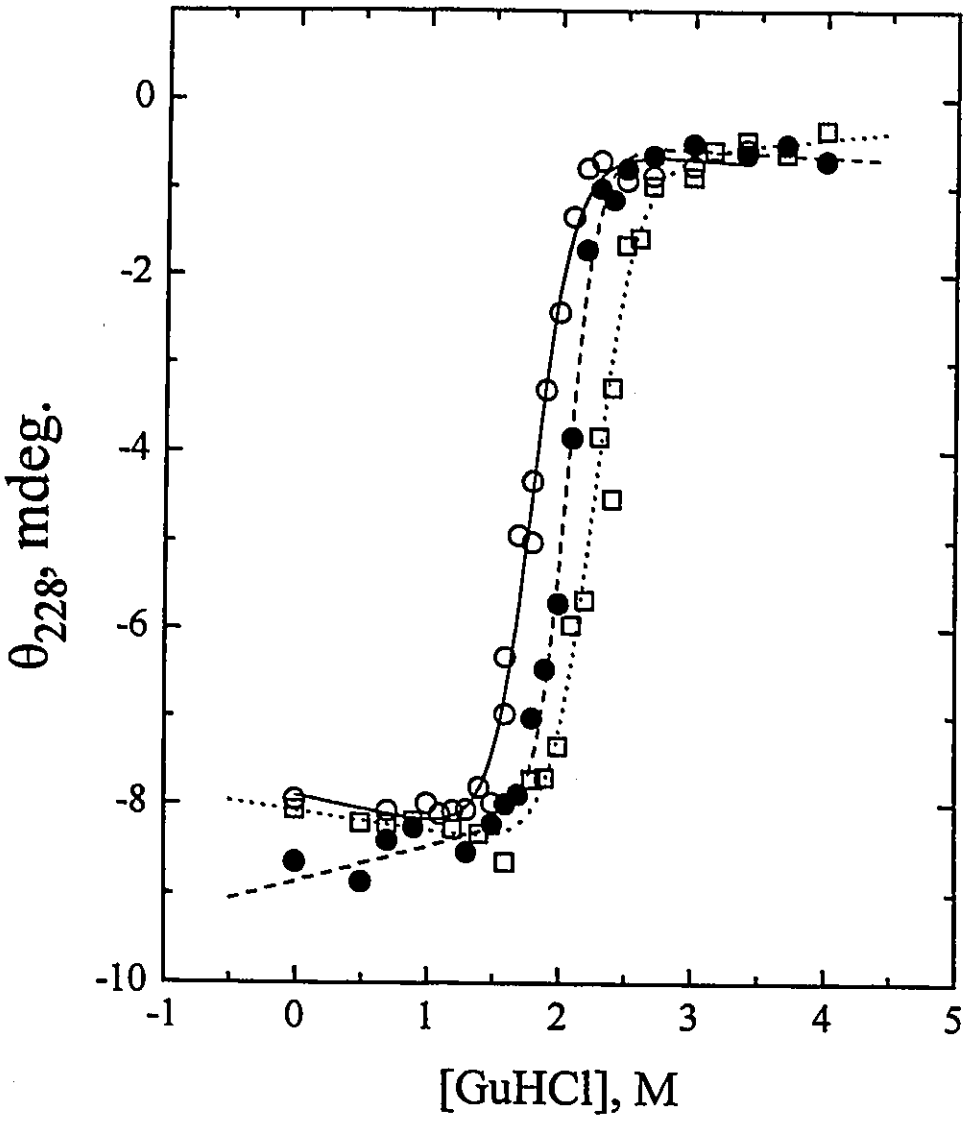

Fig.III.15. Guanidinium chloride denaturation curve of the wild type xylanase (O), DS1 (□), and DS2 (●) mutants. The decrease in secondary structure was monitored at 228 nm wavelength by circular dichroism spectroscopy. The lines show the best fit of experimental data to equation III.7.

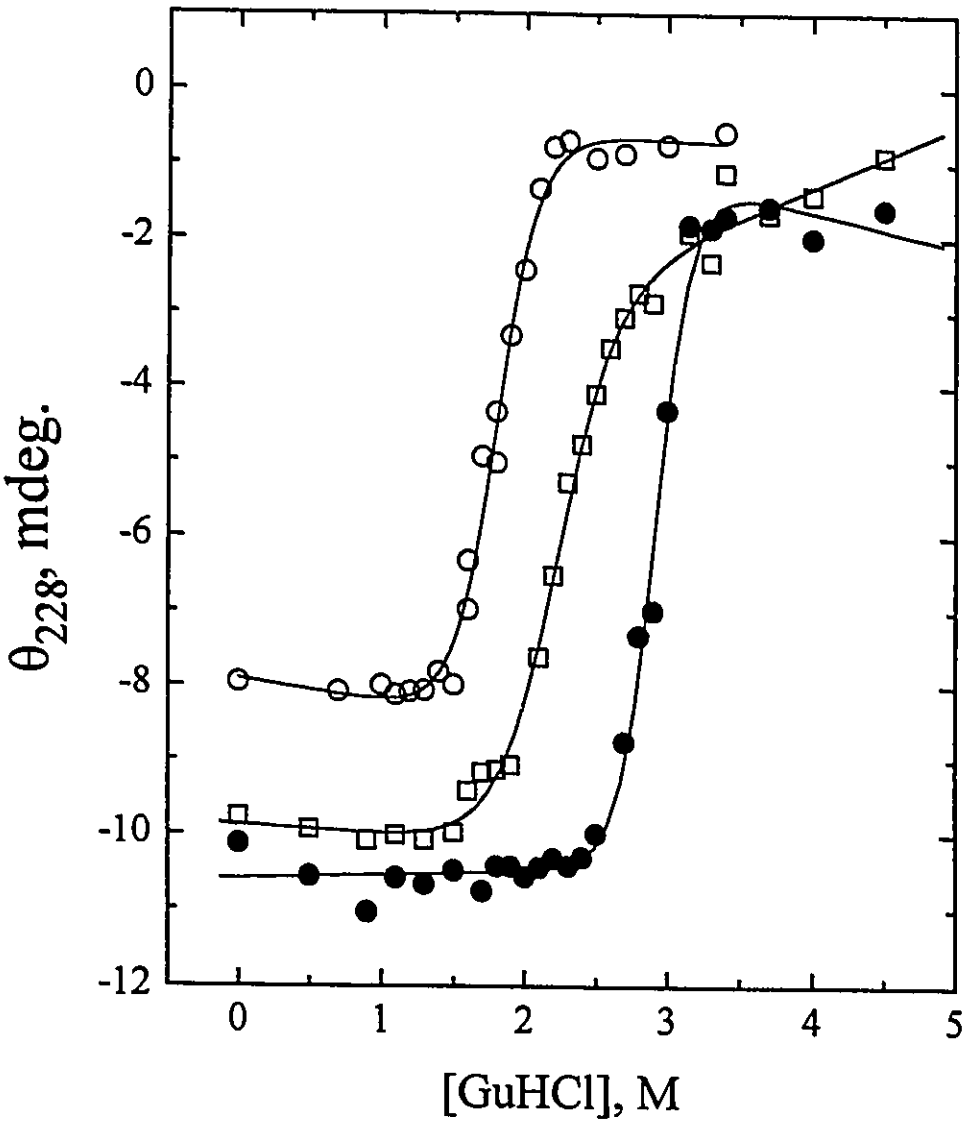

Fig.III.16. Guanidinium chloride denaturation curve of the wild type xylanase (○), cXI (□), and cDS1 (●) mutants. The decrease of secondary structure was monitored at 228 nm by circular dichroism spectroscopy. The lines show the best fit of experimental data to equation III.7.

$$\theta_{228}=\frac{(\alpha_F+\beta_F[D])+(\alpha_U+\beta_U[D])\exp\{\frac{m[D]-\Delta G_d(H2O)}{RT}\}}{1+\exp\{\frac{m[D]-\Delta G_d(H2O)}{RT}\}} \qquad \text{III.7}$$

where $\Delta G_d(H_2O)$ is ΔG of denaturation in the absence of GdmHCl, [D], the concentration of guanidinium chloride, and m is a measure of the dependence of ΔG_U on GdmHCl concentration (Pace *et al.*,1990). In fact, the value of m reflects the cooperativity of the transition and the exposure of the denatured state to solvent relative to the native state (Clarke & Fersht, 1993). The midpoint of denaturation is $[GdmHCl]_{50\%}$, which depends on the mutation. Table.III.4 summarizes these parameters. In comparison to the wild type, the $[GdmHCl]_{50\%}$ values of the mutants are increased. Moreover, positive values of $\Delta\Delta G_d(H_2O)$ for all of the variants (except the cXI mutant) obtained from chemical denaturation experiments support the conclusion from thermodynamic study that all of the mutants have gained increased stability with respect to the wild type. Only the cXI mutant with $\Delta\Delta G_d(H_2O)$ value of -0.91 kcal/mol (Table.III.4) shows a reduction in the stability in comparison to the wild type xylanase. Clearly, because of the reduced slope of ΔG as a function of denaturant concentration, m (Fig.III.17), the estimate of $\Delta G_d(H_2O)$ of cXI mutant is much too low. This can be due to the existence of stable intermediate(s) in the unfolding transition of the cXI mutant that leads to breakdown of a two state

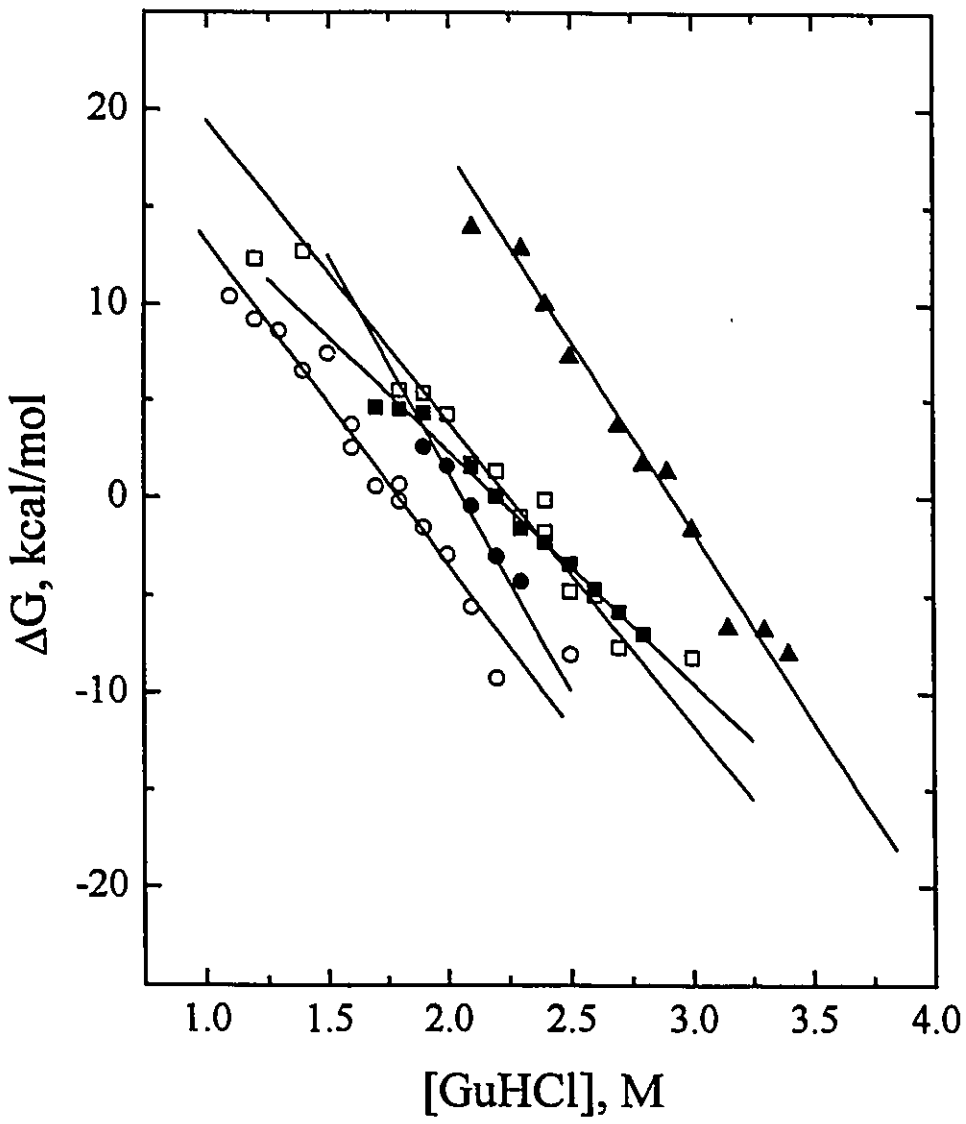

Fig.III.17. Dependence of the ΔG of denaturation upon GdmHCl concentration, m, for the wild type xylanase (O), DS1 (□), DS2 (●), cXI (■), and cDS1 (▲) mutants obtained from GdmHCl denaturation curves as described in Materials and Methods.

assumption (Cupo & Pace, 1983). An alternative possibility is that the degree of exposure of the residues in the unfolded state to solvent may well be different in the disulphide bond mutants in comparison to the wild type protein (Pace, *et al.*, 1990). Furthermore, the introduction of the disulphide bonds is accompanied by variations in the m values in respect with the wild type. This phenomenon further complicates the interpretation of chemical denaturation experiments. Nevertheless, the problem can be partially circumvented, and a reasonable estimate of the difference in the stability among the different mutants can be made. Pace and Vanderburg (1979) tested the validity of linear extrapolation and found that deviations of as much as 30% can occur near zero molar denaturant. It has also been shown that, using urea as a denaturant, $\Delta\Delta G$ is best determined directly if the transition regions of mutants overlap (Serrano, *et al.*, 1990, Kellis, *et al.*, 1989). Therefore, $\Delta\Delta G_d$ was determined in 2.2 M GdmHCl concentration where transitions of all variants overlap and no extrapolation is required to obtain $\Delta\Delta G_d$ values. Similar to the thermal denaturation results, the DS1 mutant shows higher stability against chemical denaturation in comparison to the DS2 and cXI variants. Interestingly, the comparison of the sum of $\Delta\Delta G_d$ in 2.2 molar guanidinium chloride concentration for DS1, 1.8 kcal/mol, and cXI, 1.6 kcal/mol, with that of cDS1, 5.0 kcal/mol, provides further proof that the two disulphide bonds stabilize the cDS1 variant in a cooperative manner.

Table.III.4. A comparison of free energy of denaturation of the disulphide bond mutants with that of wild type *B. circulans* xylanase obtained from fitting experimental data to equation III.7 in GdmHCl denaturation experiments.

Protein	$[GdmHCl]_{50\%}$* [M]	m kcal/mol/ M	ΔG_d (H_2O)	$\Delta\Delta G_d$ (H_2O)	ΔG_d& (GdmHCl)	$\Delta\Delta G_d$ (GdmHCl)
Wild type	1.80	3.99 ±0.24	7.16 ±0.62	0.00	-1.6	0.0
DS1	2.25	3.71 ±0.17	8.37 ±0.71	1.21	0.2	1.8
cXI	2.20	2.84 ±0.11	6.25 ±0.60	-0.91	0.0	1.6
cDS1	2.92	4.68 ±0.20	13.7 ±1.0	6.54	3.4	5.0
DS2	2.07	5.36 ±0.37	11.1 ±0.9	3.94	-0.7	0.9

*$[GdmHCl]_{50\%}$ is the concentration of guanidinium chloride where 50% of protein is denatured.

&Free energy of denaturation in the presence of 2.2 M guanidinium chloride.

III.7. DISCUSSION

The inherent instability of proteins seems to be a major obstacle in the application of enzymes in industry (Matsumura & Matthews, 1991). This limitation also applies to *Bacillus circulans* xylanase as a potential candidate for bleaching kraft pulp. It is of considerable interest, therefore, to increase its stability by modifying a few amino acids in the primary sequence. This appears to be possible as the net free energy of stabilization of native proteins is unexpectedly small. This is due to the fact that the factors contribute to the stability of the folded protein are very large but are offset by almost equally large factors that favour the unfolded form (Matsumura & Matthews, 1991).

It has been shown that removing naturally occurring disulphide bonds can substantially decrease the stability of proteins (Pace, *et al.*, 1988; Radford, *et al.*, 1991; Cooper, *et al.*, 1992). Consequently, the opposite process, the introduction of new disulphide bonds, should provide a powerful tool for protein stabilization. For example, introduction of three disulphide bonds into T4 lysozyme has led to 23.4 °C increase in the melting point of the protein (Matsumura, *et al.*, 1989). Thus, in the present work disulphide bonds are introduced into *B. circulans* xylanase in order to enhance its stability. Circular dichroism spectra demonstrate that all of the mutations posses the same conformation as the wild type protein (Fig.III.4 and Fig.III.5). Only the DS2 mutant shows a somewhat altered tertiary structure. Presumably, introduction

of the disulphide bonds, except in the DS2 variant, was not accompanied by induction of any considerable strain in the structure of protein. This is a particularly important factor in designing disulphide bonds, as introduction of a strained disulphide can offset the stabilizing effect of the cross-link (Matsumura & Matthews, 1991). The lack of structural change, monitored by far and near-UV CD, is consistent with an X-ray crystallographic study of the DS1 mutant showing that its structure is completely isomorphous with wild type enzyme (Wakarchuk, *et al.*, 1994b). Thus, it seems that 100C-148C mutation duly satisfies the geometric and stereochemical requirements for a disulphide bond formation. On the other hand, tertiary structure of the DS2 mutant was affected by the V98C, A152C mutations (Fig.III.5). It is, therefore, anticipated that the DS2 mutant should show decreased stability in comparison to DS1 mutant as some of the stabilizing interactions are distorted due to strain introduced into structure. This notion is supported by $\Delta\Delta G$ values obtained from thermal and guanidinium chloride denaturation experiments (Tables III.3 and III.4). However, all of the mutants have acquired considerable stability against both chemical and thermal denaturation. When the denaturation of the *B. circulans* xylanases was investigated under reversible conditions (guanidinium chloride denaturation or thermal denaturation in the presence of 2.5 molar urea), the stability of the variants decreased in the order of cDS1 > DS1 > cXI > DS2 > W.T. As expected, the stability of DS2 mutant was

found to be less than that of the DS1 mutant.

Often a combination of single point mutations leads to an additive increase in stability, i.e. the sum of the free energy changes derived from single mutations is nearly equal to the free energy change measured in the multiple mutant (Wells, 1990). The cumulative nature of this phenomenon indicates that the structural stability effects of amino acid replacements are strictly local. On the other hand, noncomulative effects imply that either there are some interactions between mutational sites, by direct contact or indirectly through electrostatic interactions or structural perturbation (Wells, 1990, Margarit, *et al.*, 1992). In such cases, a combination of substitutions results in either a more or less stable protein, than if each substitution were to act independently. The term "cooperative" is used when stability achieved by a combination of mutations is more than expected. Mathematically, it can be expressed as (Hurley *et al.*, 1992):

$$\Delta\Delta G_{coop}=\Delta\Delta G-\Sigma\Delta\Delta G_i \qquad \text{III.8}$$

The energy of cooperativity, $\Delta\Delta G_{coop}$, can be defined as the difference between the actual $\Delta\Delta G$ and the sum of the $\Delta\Delta G$ values of the individual changes, $\Sigma\Delta\Delta G_i$. $\Delta\Delta G$ values of various mutants obtained from differential scanning calorimetry

experiments are listed in Table III.3. The cDS1 variant has a ΔΔG value of 6.1 kcal/mol, which shows stability higher than sum of ΔΔG values (4.8 kcal/mol) for the combination of DS1 and cXI mutations. The difference, 1.3 kcal/mol, represents the energy of cooperativity, $\Delta\Delta G_{coop}$, in 2.5 M urea. The energy of cooperativity can also be calculated from guanidinium chloride denaturation experiments. As listed in Table III.4, $\Delta\Delta G_d$ in 2.2 M GdmHCl for the cDS1 mutant equals 5.0 kcal/mol which is 1.6 kcal/mol more than the sum of ΔΔG values (3.4 kcal/mol) of the individual single disulphide bond mutants. These data provide further proof that the combination of two disulphide bonds cooperatively stabilizes *B. circulans* xylanase. The importance of this finding can be realized when it is compared to other cases where cooperativity of stabilization has been reported. First of all, in quite a few cases a combination of two single point mutations has resulted in cooperative stabilization but this has been quantitatively small (Hurley, *et al.*, 1992; Ishikawa, *et al.*, 1993). The ΔΔG of 0.8 kcal/mol for ribonuclease HI is opposed to 6.1 kcal/mol for the *B. circulans* xylanase (Ishikawa, *et al.*, 1993), or in the case of T4 lysozyme stability of the variant containing combination of mutations was not more than wild type (Hurley, *et al.*, 1992).

Theoretical treatments predict that a cross-link should stabilize a polymer according to the length of the primary chain bridged by the link due to a decrease in the chain entropy of the unfolded state of the cross-linked form

(Poland & Scheraga, 1965; Pace, *et al.*, 1988). If this assumption holds true, we should then expect higher stability for the cXI mutant in comparison to DS1, because the number of residues encompassed by the cross-link in the cXI mutant is much greater than DS1, 187 *versus* 49 residues. $\Delta\Delta G$ in 2.2 M guanidinium chloride obtained from chemical denaturation experiments shows similar values for DS1 and cXI variants. Moreover, it was found, from differential scanning calorimetry under reversible conditions, that DS1 with $\Delta\Delta G$ of 3.1 kcal/mol is more stable than the cXI mutant with $\Delta\Delta G$ of 1.7 kcal/mol. Since no structural change can be observed in the circular dichroism spectrum of cXI mutant compared to the wild type enzyme, the reduced thermal stability of the cXI mutant in comparison to the DS1 cannot be attributed to any considerable strain induced by the disulphide bond. Perhaps, it can be suggested that, after a certain point, increase in the number of residues forming a loop does not lead to enhanced stability.

As mentioned above, the stabilizing effect of disulphide bonds is usually assumed to arise from its destabilizing effect on the unfolded state by reducing its conformational entropy (Creighton, 1988; Matsumura & Matthews, 1991; Betz, 1993). The comparison of calorimetric enthalpy under reversible condition (Table III.3) shows no major differences among mutants, while their $\Delta\Delta G$ values were found to be very different. Thus, the stabilizing effect of the disulphide bonds appears to be entropic.

The m value, in the chemical denaturation study, showed considerable dependence upon mutation ranging from 2.84 kcal/mol/M in the case of the cXI mutant to 5.36 kcal/mol/M in the DS2 mutant. The m values of the wild type and DS1 proteins remained similar, while cXI showed 0.87 kcal/mol/M decrease and cDS1, 1.69 kcal/mol/M increase in comparison to the wild type. Two possibilities can be taken into account to explain the variation of m upon mutation; firstly, deviation from the two state model; and secondly, the effect of mutation on accessability of the residues of the unfolded conformation of protein to guanidinium chloride. The cXI mutant is the only one showing a decrease in m. One possibility seems to be the fact that A1GC, G187, C188 mutation in cXI somehow leads to stabilization of an intermediate form and consequently a break down of the two state assumption. As suggested earlier (Greene & Pace, 1974; Pace, 1975) the number and location of disulphide bonds can also affect the exposure of residues in urea and guanidinium chloride solutions. Thus, it appears that introduction of the disulphide bond into cXI mutant would probably decrease the exposure of some residues of the unfolded form to guanidinium chloride leading to a reduced m value. however, the m values for DS1 remained similar to wild type value; and cDS1, which has the combination of cXI and DS1 mutations revealed a considerable increase in m (Table.III.4). This means that the combination of two disulphide bonds increases the cooperativity of unfolding, probably by destabilizing intermediate(s). No

matter what the reason for a change in m values is (affecting the population of the intermediate form or affecting the accessability of the residues in the unfolded conformation), the cooperative stabilization obtained by the combination of two disulphide bonds in cDS1 mutant should be attributed to the effect of disulphide bonds in the unfolded protein. This is consistent with circular dichroism and differential scanning calorimetry studies of cXI, DS1, and cDS1 variants as their structures remained similar to wild type and the stabilization effect of the disulphide bonds was found to be entropic.

In the previous chapter it was shown that a comparison of the scan-rate dependence of the melting points under irreversible conditions to those under reversible conditions can be used as a criterion to determine if the disulphide bond alters the rate limiting step on the thermal denaturation pathway. Scan-rate dependence of the melting points under reversible and irreversible conditions (in the presence and absence of urea) remained similar for the wild type, while in the case of DS1 mutant, the scan-rate dependence under the reversible conditions was found to be much less than that for the irreversible one. Therefore, it was concluded that the introduction of the S100C, N148C disulphide bond changes the rate limiting step in thermal denaturation pathway probably by partially blocking the exposure of putative elements required for aggregation. A similar strategy was used to determine the effect of introduction of disulphide bonds at various locations in the thermal denaturation pathway of

the protein. Accordingly, the melting point, t_m, of each mutant was determined in the presence and absence of 2.5 M concentration of urea at two scanning rates (Table.III.5). Since, the location of the disulphide bond in the DS2 mutant, V98C, A152C, is similar to that in DS1 (with the S100C, N148C mutation) a similar effect of disulphide bond on the rate-limiting step of thermal denaturation pathway is expected. This notion is supported by the fact that dependence of the melting point of the DS2 mutant upon scanning rate under reversible conditions is less than for the irreversible case. A similar observation was made for the cDS1 variant, which consists of S100C, N148V, A1GC,G187,C188 mutations. On the other hand the A1GC,G187,C188 disulphide bond did not change the rate limiting step indicating that the effect of disulphide bonds on the rate-limiting step of the thermal denaturation pathway is dependent on the location of the cross-link. These findings further support the notion that the presence of disulphide bonds in the DS1 and DS2 mutants, linking α-helix to the β-strand, restricts the exposure of hydrophobic surface and putative elements that are required for the initiation of aggregation. Taken together, the results support the attractive hypothesis (Wetzel, *et al.*, 1988) that cross-linking may provide a general means by which some conformational modes of inactivation may be blocked.

Table.III.5. A comparison of the melting points of the various mutants of *B. circulans* xylanase under reversible conditions with those under irreversible conditions obtained by differential scanning calorimetry, at two scanning rates of about 10 and 60 °C/hr.

	t_m(v = 10) (Buffer)	t_m(v = 60) (Buffer)	Δt_m* (Buffer)	t_m(v = 10) (Urea)	t_m(v = 60) (Urea)	Δt_m (Urea)
wild type	57.4	59.6	2.2	51.1	54.0	2.9
DS1	61.6	64.5	2.9	58.6	59.4	0.8
DS2	61.1	63.8	2.7	54.4	55.9	1.5
cXI	60.7	63.5	2.8	55.3	58.1	2.8
cDS1	69.2	72.0	2.8	63.7	65.5	1.8

*Δt_m is equal to difference between the melting points, t_m, at two scanning rates of 10 and 60 °C/hr.

III.8. SUMMARY AND CONCLUSION

The introduction of disulphide bonds has been used as a strategy to enhance the stability of *Bacillus circulans* xylanase. Three different locations were selected based on comparison of the xylanase sequence from *Bacillus circulans* with xylanase A from *Schizophyllum commune* as well as the proximity of the N and C termini. A combination of two disulphide bonds led to a 12 °C increase in the melting point while enzymatic activity was decreased only 32%. Importantly, an increase in the melting point and $\Delta\Delta G$ values of the cDS1 mutant (in comparison to the wild type, DS1, and cXI variants) due to the simultaneous introduction of two disulphide bonds, was more than expected. Therefore, the stabilization effect of two disulphide bonds appears to be cooperative rather than additive. Such cooperativity in enhancing the stability of *B. circulans* xylanase seems to result from the influence of disulphide bonds on the unfolded state and the present study supports previous findings that stabilizing effect of the disulphide bonds is a consequence of decreased conformational entropy of the unfolded state. Finally, these results favour the notion that the presence of a disulphide bond in a particular position restricts the exposure of some elements required for aggregation, leading to a change of the rate limiting step on the thermal denaturation pathway.

CHAPTER IV

ON THE ROLE OF CERTAIN ACTIVE SITE RESIDUES OF *Bacillus circulans* XYLANASE

IV.1. INTRODUCTION

The reaction mechanism of glycosidases is based on acid catalysis by acidic amino acid side chains (Sinnott, 1990). Hen egg-white lysozyme, the best characterized glycosidase, contains a glutamic acid at position 35 and an aspartic acid at position 52. It is generally accepted that the carboxyl group of Glu 35 in its un-ionized form serves as a general-acid catalyst and that of Asp

52 stabilizes, by electrostatic interaction, the oxocarbonium ion intermediate (Phillips, 1967; Chipman & Sharon, 1969). The unusual feature of Glu 35 is its abnormally high pK_a of 6-6.5 (Imoto, *et al.*, 1972). This high pK_a has been originally attributed to two factors: the hydrophobic environment of Glu 35 (Blake, *et al.*, 1967; Rupley, *et al.* 1967) and the electrostatic interaction of two proximal carboxylate anions, Glu 35 and Asp 52 (Kuramitsu, *et al.*, 1974). More recently, however, Inoue *et al.* (1992a) have shown that the hydrophobic environment plays the dominant role in establishing the high pK_a of Glu 35. Elevated pK_as for carboxyl groups have also been observed for other glycosidases. For example, using chemical modification and kinetic experiments Bray & Clarke (1990) have demonstrated the presence of an essential carboxyl group with a pK_a of 6.6 in the xylanase A of *S. commune*. Furthermore, on the basis of detailed kinetic studies of an exoglucanase/xylanase from *Cellulomonas fimi*, it has been postulated that glutamic acid 127 with a pK_a of 7.7 may act as an acid-base catalyst (Tull & Withers 1994; MacLeod *et al.*, 1994). This is consistent with recent crystallographic data that suggest that glutamic acids 127 and 233 act as an acid catalyst and nucleophile, respectively (White, *et al.*, 1994).

B. circulans xylanase has two glutamic acid residues, Glu 78 and Glu 172. These glutamic acid residues are conserved in the entire family of small molecular weight xylanases (the G family xylanases) and have been found to

point into the active site cleft (Wakarchuk, *et al.*, 1994a; Fig. IV.1). The active site cleft spans the whole width of the molecule and appears to be sufficiently long to bind five or six xylose residues. In the complex of inactive enzyme with xylotetraose substrate, the orientation of the substrate suggests that Glu 78 or Glu 172 would be in a position to act as the nucleophile and the acid-base catalyst, respectively (Fig. IV.2., Wakarchuk, *et al.* 1994a). The distance from the oxygen atom of the Glu 78 carboxyl group to the anomeric carbon of the reducing end of the xylotetraose is similar to the distance of oxygen atom of the nucleophile (Asp 52) to the anomeric carbon, C1 atom, of a trisaccharide complexed with hen egg-white lysozyme (Wakarchuk, *et al.* 1994a). The crucial role of the Glu 172 and Glu 78 in catalysis is further supported by site directed mutagenesis as no activity was detected for E172Q and E78Q (Wakarchuk, *et al.* 1994a). In order to act as an acid-catalyst, Glu 172 must be protonated in the neutral pH range where the enzyme is active. It is thus of considerable interest to determine the pK_as of glutamic acid residues in xylanase. This study indicates that Glu 172 has a pKa of 6.8 and that this abnormally high pKa is largely caused by the electrostatic repulsion between the carboxylate anions of Glu 78 and Glu 172.

Fig.IV.1. A side view of the active site cleft of the *B. circulans* xylanase.

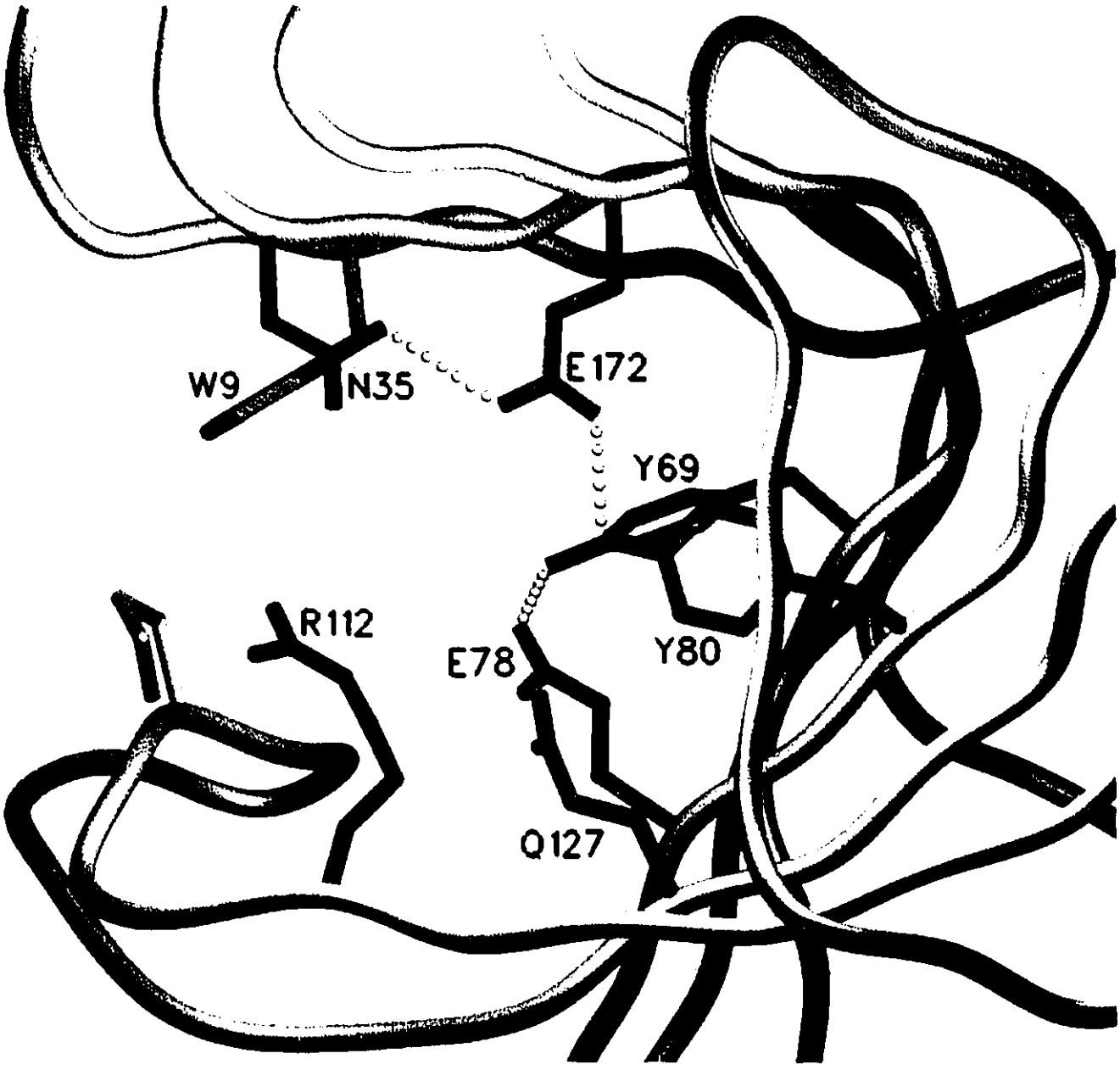
W9
N35
E172
Y69
R112
E78
Y80
Q127

Fig.IV.2. The active site cleft of the E172C mutant in complex with xylotetraose from two views.

a) b)

IV.2. MATERIALS AND METHODS

Site directed mutagenesis experiments were performed by Dr. Warren Wakarchuk at the NRC as described elsewhere (Wakarchuk, *et al.*, 1994a). Purification of the wild type xylanase and its variants, circular dichroism spectroscopy, and differential scanning calorimetry studies were performed according to the procedures described in Chapter II.

IV.2.1. Kinetics studies

Measurements of the enzymatic activity were based on the reaction of reducing sugars with hydroxybenzoic acid hydrazide reagent (Lever, 1972), as described in chapter II, with the following modifications. Instead of citrate, a mixture of tris and maleic acid, 50 mM, was used as the assay buffer between the pH range of 4 to 9. The final concentration of the enzyme was 0.77 μg/mL, while the concentration of the soluble fraction of birchwood xylan as substrate varied from 0.2 to 21 mg/mL. This roughly corresponds to molar concentrations of 0.01 and 1.2 mM, respectively. The plot of absorbance at 420 nm versus moles of the reducing end of the xylose molecules was used as a standard curve (data not shown). These curves were employed to obtain molar concentrations of the substrate and product. Since the natural substrate of the enzyme, the soluble fraction of birchwood xylan, is a heterogeneous solution containing different molecular weights of xylan, kinetic parameters should be

considered apparent values. The progress of the reaction was monitored for 10 minutes by periodic withdrawal of 50 μL of the assay solution followed by addition of 1 mL 10 mM NaOH (Fig.IV.3). Addition of the NaOH solution increases the pH of the solution to 10 or higher to ensure that the hydrolysis reaction is quenched. The initial slope of the product concentration against time provides the initial rate, V_o, by which Lineweaver-Burk and Eadie-Hofstee plots can be constructed (Fig.IV.4)

IV.2.2. Fourier-transform infrared spectroscopic studies

Samples for infrared spectroscopy were prepared in 10 mM phosphate buffer in D_2O at a protein concentration of approximately 15 mg/mL. Protein solutions were incubated at room temperature for at least 24 hours to ensure high levels of hydrogen/deuterium exchange. Each pH titration was performed by addition of very small aliquots of concentrated NaOD or DCl. In order to avoid dissolving water vapour in sample solutions, the exact values of pH were determined after FTIR measurements. Readings of the pH meter are uncorrected for the deuterium effect. Infrared spectra were recorded with a FTS-40A BIO-RAD instrument.

Typically 256 scans were co-added. To minimize spectral contributions of atmospheric water vapour, the instrument was continuously purged with dry nitrogen. Samples were assembled between two calcium fluoride windows

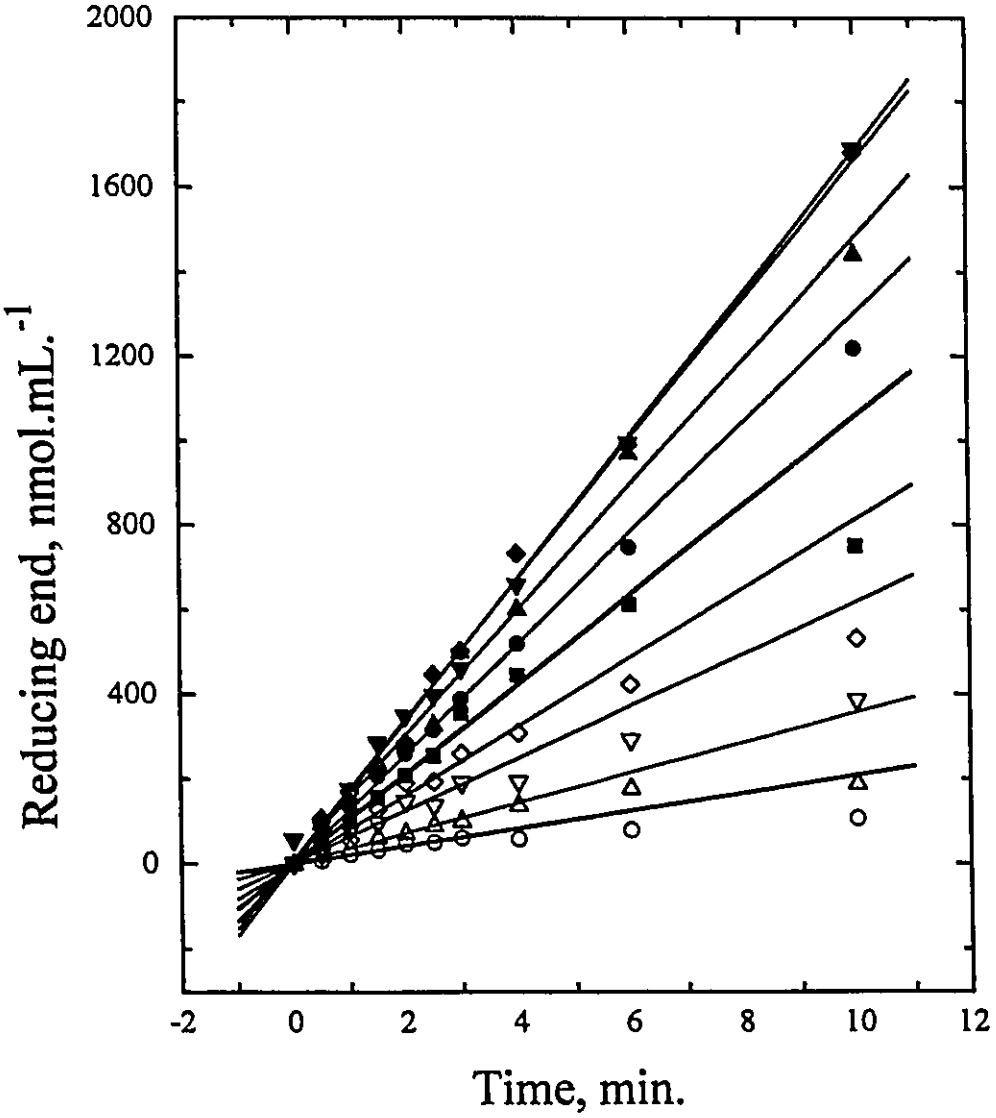

Fig.IV.3. Hydrolysis rate of soluble fraction of birchwood xylan at pH 6.0 with molar concentrations of 0.012 (○), 0.023 (△), 0.046 (▽), 0.069 (◊), 0.116 (■), 0.231 (●), 0.463 (▲), 0.810 (▼), and 1.157 mM (◆).

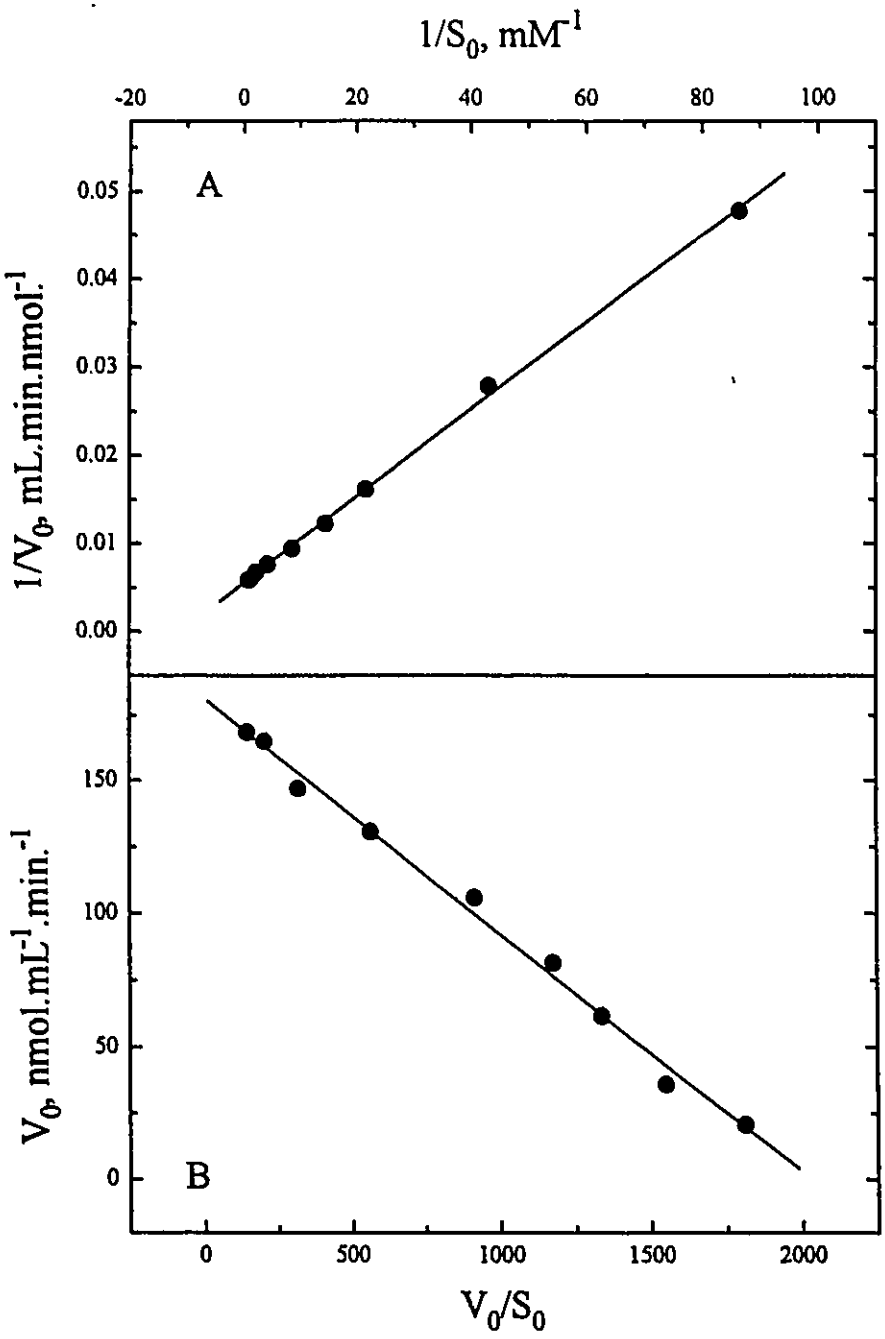

Fig.IV.4. Lineweaver-Burk, A, and Eadie-Hofstee, B, plots of the hydrolysis of soluble fraction of birchwood xylan at pH 6.0.

separated by a 50-μm-thick spacer. The intensities of the carboxylate band at 1574 cm^{-1} and of the amide I band at 1635 cm^{-1} were determined after subtracting the spectrum of 10 mM phosphate in D_2O and making a baseline correction (Fig.IV.5). Even with these precautions, the concentration of protein varied slightly from one sample to another. Therefore the intensity of the band at 1574 cm^{-1} was normalized to the intensity of the amide I band.

IV.2.3. Isothermal reaction calorimetric studies

All experiments were carried out using an Omega titration calorimeter (Microcal, Inc.). In a typical experiment 20 to 50 injections of 5 to 10 μL of the substrate were injected into 1.396 mL of inactive mutant of the enzyme solution while rapidly mixing at 400 rpm. The duration of each injection was normally 10 seconds with a 5 minute interval between injections to allow the instrument to become equilibrated. After normalizing raw data to the concentration of protein and ligand, heats of reaction were determined by integration of the observed peaks. The experimental temperature was 26 °C and the buffer was 50 mM ammonium acetate at pH 6.0. Baseline corrections for the heat of dilution were based on the results of control experiments in which aliquots of the substrate were injected directly into buffer. Data analyses were performed using Origin software provided by Microcal Inc (Northampton MA).

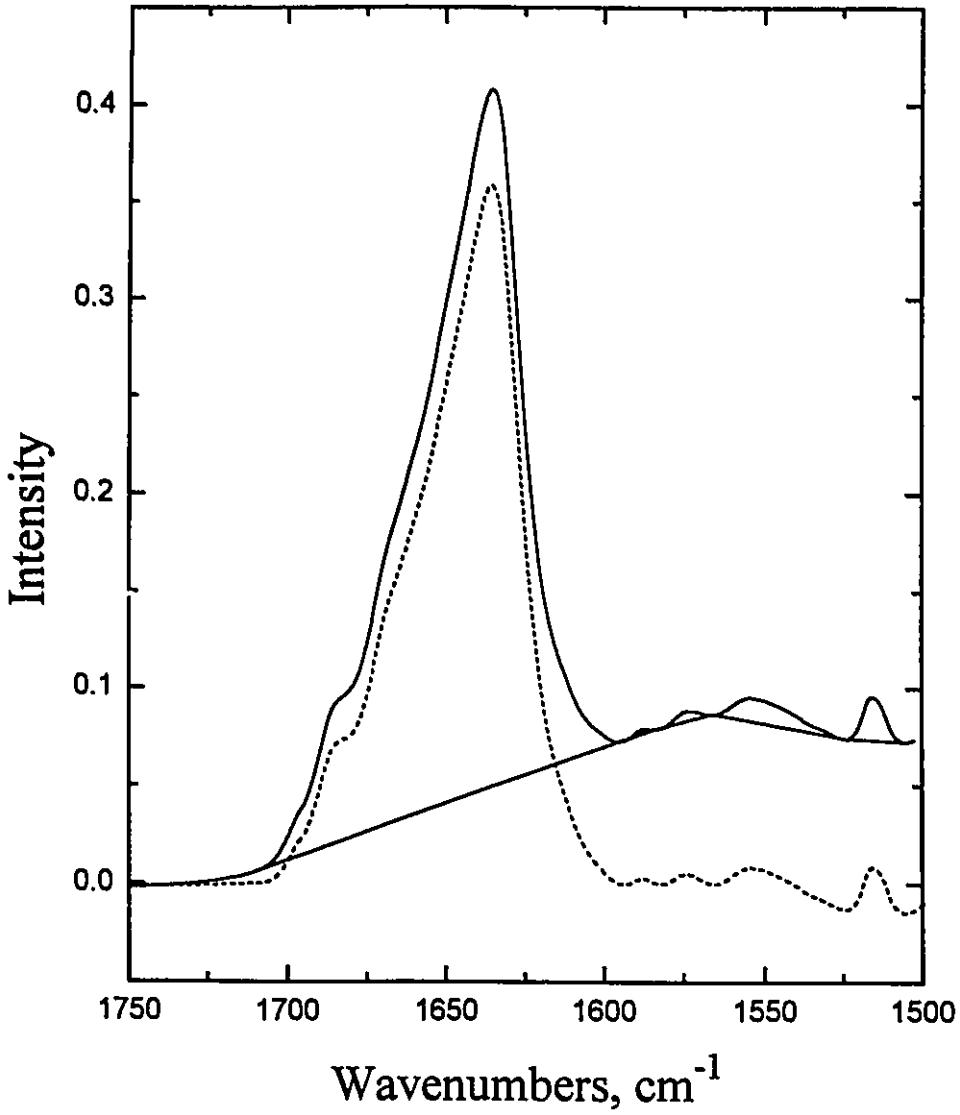

Fig.IV.5. Fourier-transform infrared spectrum of wild type xylanase at pH 7.0 in the region between 1750 and 1500 cm^{-1} before, solid line, and after, dashed line, subtracting baseline.

IV. 3. RESIDUES INVOLVED IN CATALYSIS

A comparison of the primary structure of the 15 G family xylanases (Fig.I.1) shows that some of the residues are absolutely conserved within the family. This probably indicates that at least some of these residues play an important role in catalysis. This notion is confirmed by site-directed mutagenesis experiments (Wakarchuk, *et al.* 1994a,b) showing that the presence of glutamic acids 78 and 172, and tyrosines 69 and 80 is essential for catalysis (Table IV.1).

Table IV.1. The comparison of the enzymatic activity of the wild type (WT) *B. circulans* xylanase and a number of mutant proteins.

Enzyme	WT	E78D	E78Q	E78C	Y69F	Y80F
Relative activity	100	0.045	0	0	0	0.042
Enzyme	E172D	E172Q	E172C	E172H	R112N	R112K
Relative activity	0.2	0	0	0	35*	83*

* Obtained from Wakarchuk *et al.* (1994a)

The structure of the E172C mutant Co-crystallized with the xylotetraose substrate suggested that glutamic acid 78 should be able to act as nucleophile (Campbell, *et al.* 1993; Wakarchuk, *et al.* 1994ab). Furthermore, calculation of the Glu 172 position relative to xylotetraose based on superimposition of the native structure onto that of the complex reveals the essential role of the Glu 172 as an acid catalyst. Accordingly, it is clear why mutation of glutamic acids

78 and 172 to other residues has such a profound effect in the enzymatic activity. It has to be realized that the reduced activity of E172D and E78D mutants cannot be attributed to any gross structural changes as no major changes of the secondary (data not shown) and tertiary structure can be detected by far and near-UV circular dichroism spectroscopy (Fig.IV.6).

Tyrosines 69 and 80 are involved in binding of the enzyme to substrate as they form hydrogen bonds with the hydroxyl groups of the xylose rings. However, binding constants of the xylohexose substrate to Y69F mutant (Fig IV.7) did not differ from that of the E172C (Fig IV.8) or E78C (data not shown) mutants as measured by isothermal reaction calorimetry. Therefore it seems that hydrogen bond established between hydroxyl group of xylose ring and tyrosine 69 does not play significant role in increasing binding affinity of the substrate to enzyme. Then why does the mutation Y69F completely inactivate the protein? Tyrosine 69 forms two hydrogen bonds, one with substrate and another with Glu 78. It seems therefore that the former helps to position the substrate, while the latter may help orient the nucleophile for the reaction. Similarly, tyrosine 80 forms a hydrogen bond with glutamic acid 172 suggesting a role in positioning the proposed acid base catalyst. An alternative explanation may be the involvement of the tyrosine residues in stabilizing the transition state.

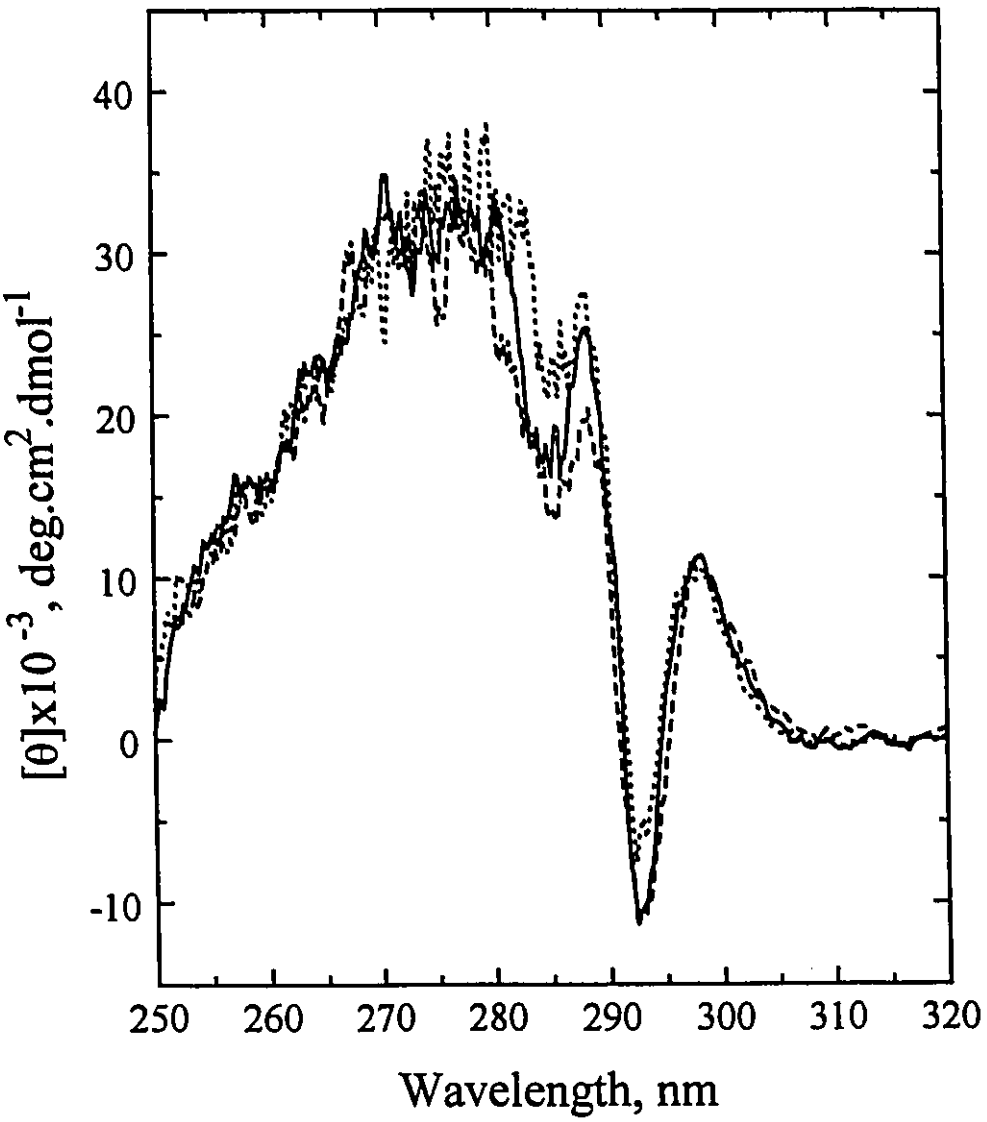

Fig.IV.6. Near-UV circular dichroism spectra of the wild type xylanase, solid line, E172D, dashed line, and E78D, dotted line.

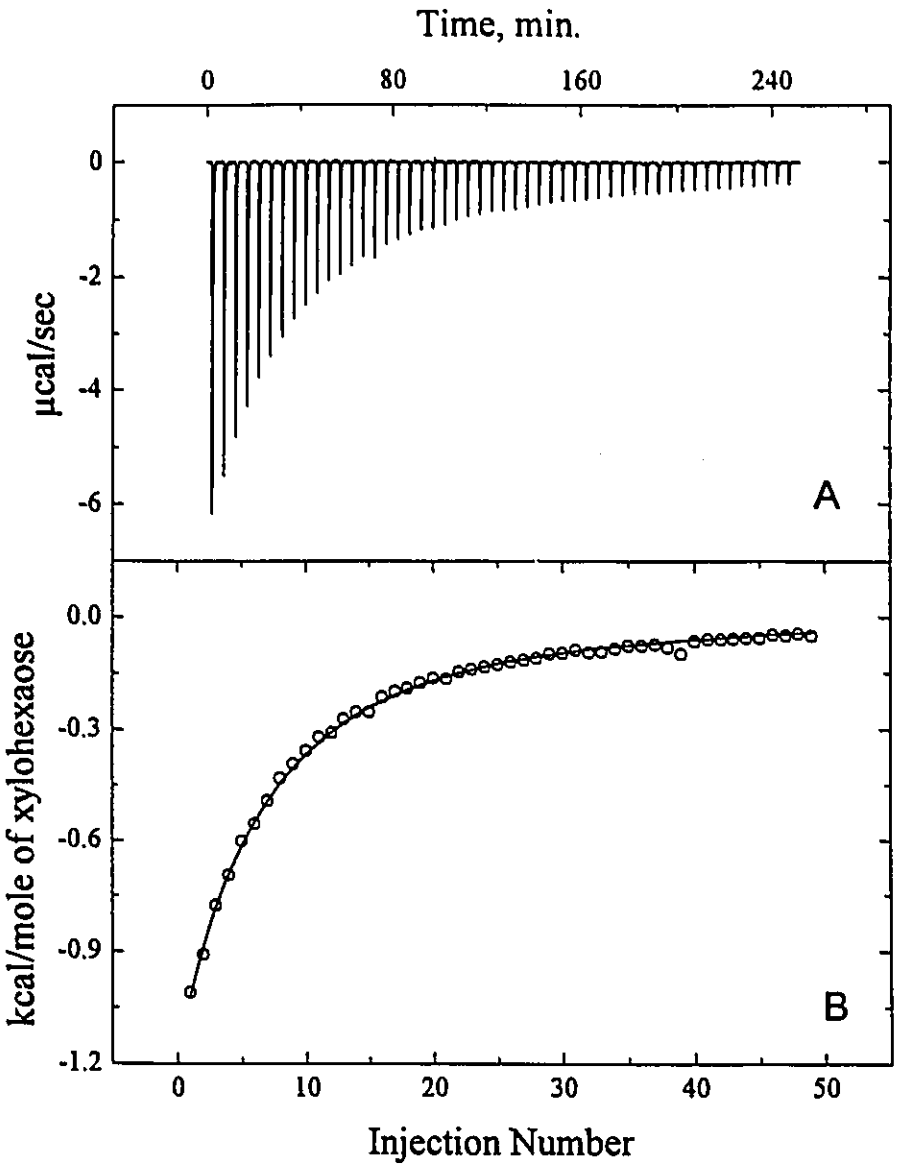

Fig.IV.7. Isothermal titration of Y69F mutant with xylohexaose at pH 6.0 in ammonium acetate buffer. The saccharide solution (34.3 mM) was injected in small increments into the protein solution in the cell (0.123 mM). The area under each peak is equal to the amount of heat released by the binding of the substrate at a given degree of saturation, A. The plot of processed data corresponding to raw data of Fig.IV.7.A, B. The points are experimental and the solid line corresponds to the best fit curve obtained by least square deconvolution. The best values of the fitting parameters are 1 for n, $588 \pm 8\ M^{-1}$ and 16229 cal/mol for ΔH.

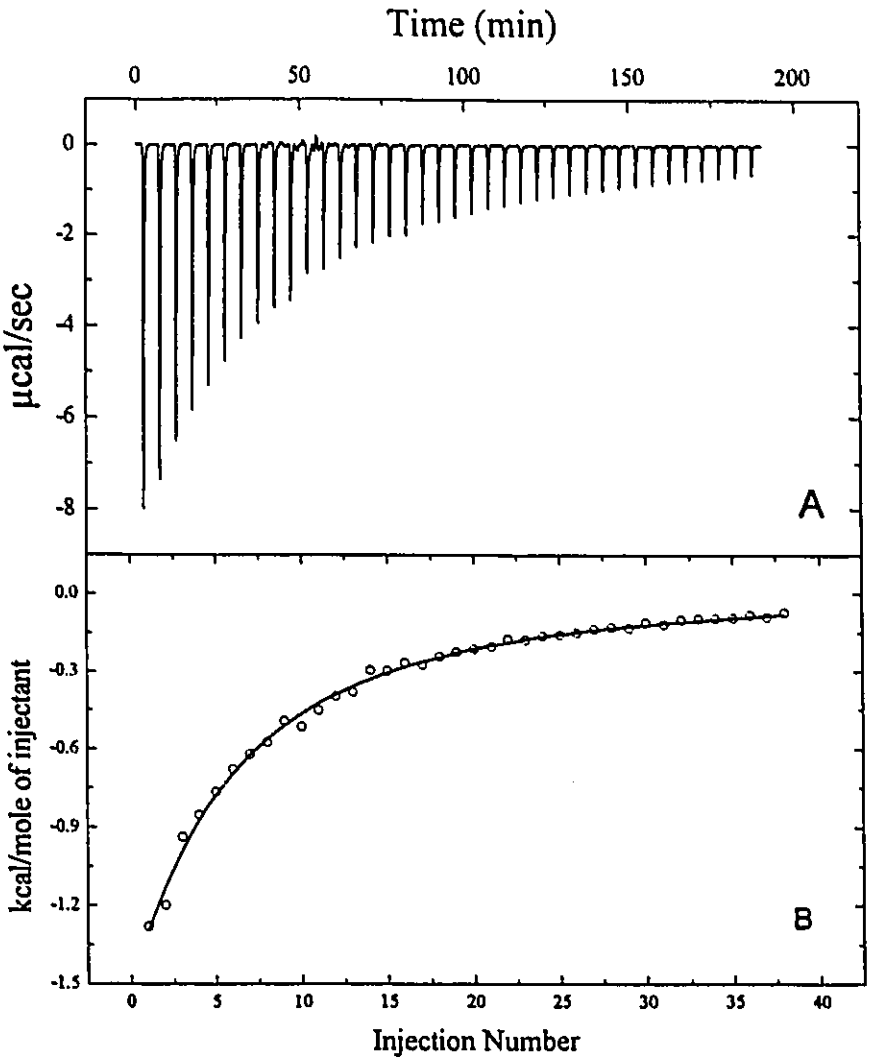

Fig.IV.8. Isothermal titration of E172C mutant with xylohexaose at pH 6.0 in ammonium acetate buffer. The saccharide solution (34.3 mM) was injected in small increments into the protein solution in the cell (0.116 mM). The area under each peak is equal to the amount of heat released by the binding of the substrate at a given degree of saturation, A. The plot of processed data corresponding to raw data of Fig.IV.8.A, B. The points are experimental and the solid line corresponds to the best fit curve obtained by least square deconvolution. The best values of the fitting parameters are 1 for n, 587 ± 13 M^{-1} and 21815 cal/mol for ΔH.

IV.4. DEPENDENCE OF THE ENZYME ACTIVITY UPON pH

Enzymatic activity of the *B. circulans* xylanase was measured between pH 4 and 9 (Fig.IV.9). K_m values show a dependence upon pH, K_m increases as pH rises. Moreover, the V_{max}/K_m values appear to be pH dependent with a steeper curve at lower pH values. The V_{max} profile as a function of pH shows a bell shape curve with minimal activity at the extreme pH values. The optimal activity of the enzyme occurs in the pH range of 5.5 to 7.5 (Fig.IV.9). The decrease of enzymatic activity at extreme pH values can be attributed to a change in the ionization state of the residues that are involved in the enzyme activity and/or local or global change of the enzyme conformation. Interpretation of such data, therefore, requires additional information obtained by other techniques to monitor conformational changes of the structure as a function of pH and also ionization state of the active site residues. Far and near-UV circular dichroism spectroscopy was used to follow structural variation of the wild type protein and its variants. Furthermore, considering the crucial role of two acidic residues in the active site, all of the carboxyl groups present in the protein were titrated using FT-IR spectroscopy.

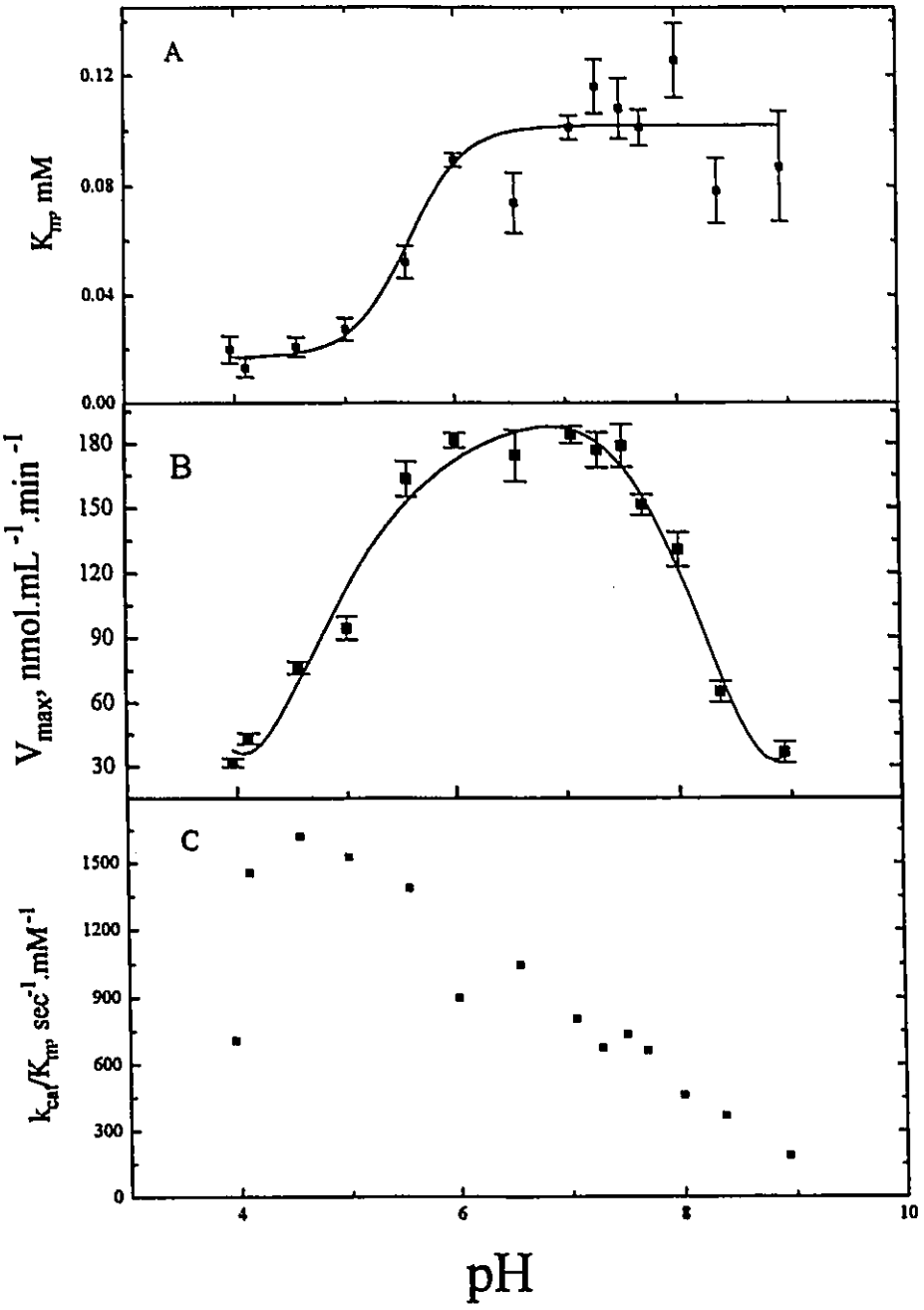

Fig.IV.9. Dependence of the kinetic parameters of the hydrolysis of soluble fraction of birchwood xylan upon pH. Confidence levels are the averages of the standard deviation as calculated by "Origin software".

IV.4.1. Structural variation OF *B. circulans* xylanase as a function of pH

The secondary and tertiary structure of proteins can be studied by circular dichroism spectroscopy. This technique is specially useful when conformational changes of a protein resulting from the ionization of amino acid side chains, the binding of ligands, or a variation in temperature are being investigated (Campbell & Dwek, 1984).

The CD spectrum of the wild type protein in the far-UV region revealed that the secondary structure content of the enzyme essentially remains unchanged in the pH range of 4 to 9 (Fig.IV.10). The tertiary structure of the protein, however, appears to be sensitive to pH as reflected in the spectrum between 250-300 nm (Fig. IV.11). A plot of the CD signal at 275 nm versus pH shows a midpoint structural transition at pH value of about 4.9 (Fig.IV.12). Since this structural transition coincides with the pH range where ionization/deionization of acidic residues occurs, it seems to be reasonable to attribute this pH sensitive structural alteration to a change in the ionization state of one or more acidic residues. The structural transition (Fig.IV.12) accompanied by the activity change (Fig.IV.9) suggests that the local structure of the active site is altered due to a change of the protonation state of an acidic residue in or near the active site. Obviously, glutamic acid 78, which plays the role of nucleophile/charge stabilizing residue, should be considered as the first candidate responsible for these variations. In order to verify this possibility, a

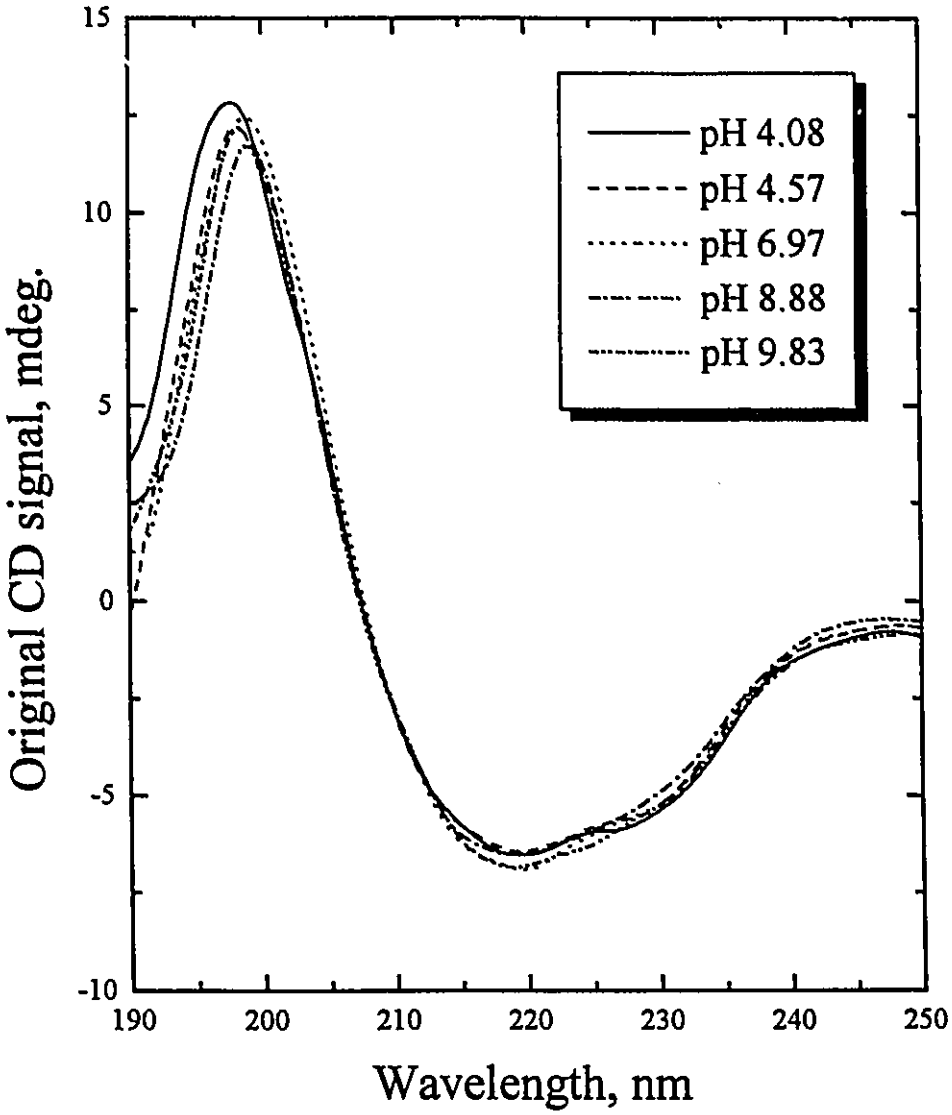

Fig.IV.10. Far-UV circular dichroism spectra of the wild type xylanase with protein concentration of about 0.34 mg/mL at various pH conditions.

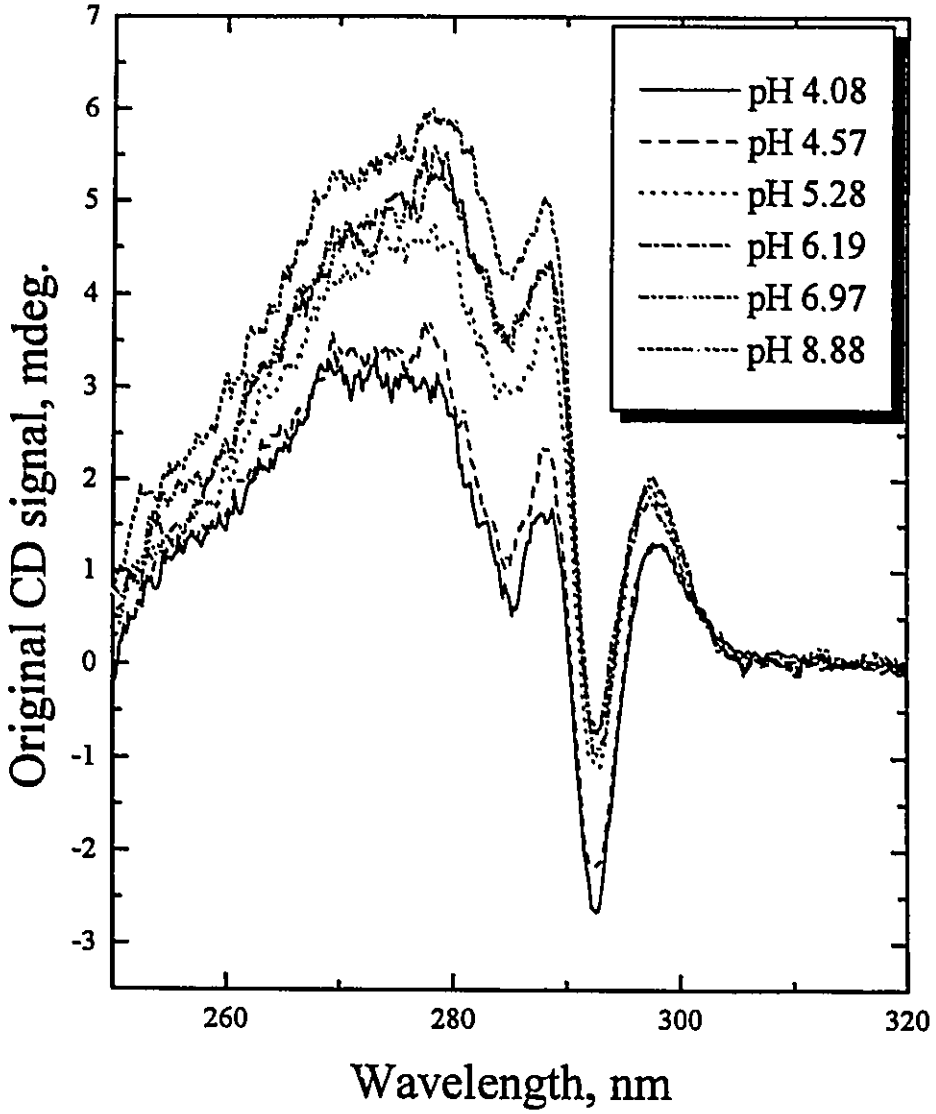

Fig.IV.11. Near-UV circular dichroism spectra of the wild type xylanase with protein concentration of about 0.34 mg/mL at various pH conditions.

similar structural study was carried out for a mutant in which Glu 78 is replaced with a cysteine, E78C (Fig.IV.13). In the case of this mutant, unlike the wild type enzyme, the change of CD spectrum in the near-UV region is limited to the wavelength range of 285-300 nm (Fig.IV.13; Fig.IV.12). It is therefore concluded that changes of the CD signal in the region of 250-285 nm mostly originate from aromatic residues affected by ionization state of glutamic acid 78. Hence, structural alteration monitored at 275 nm can be used to determine the pK_a of glutamic acid 78. Accordingly, the pK_a of this residue in the wild type enzyme is determined to be 4.9. This is consistent with very recent NMR study (McIntosh, *et al.* unpublished data) that shows a pK_a of 4.7 for glutamic acid 78 in the wild type enzyme. It is also supported by a recent report demonstrating that, by using electrospray tandem mass spectrometry, Glu 78 acts as a nucleophile in *Bacillus subtilis* xylanase (Miao, *et al.*, 1994).

Detailed inspection of the residues surrounding Glu 78 suggests that tyrosine 69 and tryptophan 71 are likely the residues whose orientation depend upon the ionization of Glu 78. Tyrosine 69 forms a hydrogen bond with the carboxyl side chain of Glu 78, and a hydrogen bond with tryptophan 71. Consequently, it seems to be reasonable to assume that the relative orientation of tyrosine 69 and tryptophan 71, and therefore their near-UV CD signal, is affected by protonation/deprotonation of glutamic acid 78.

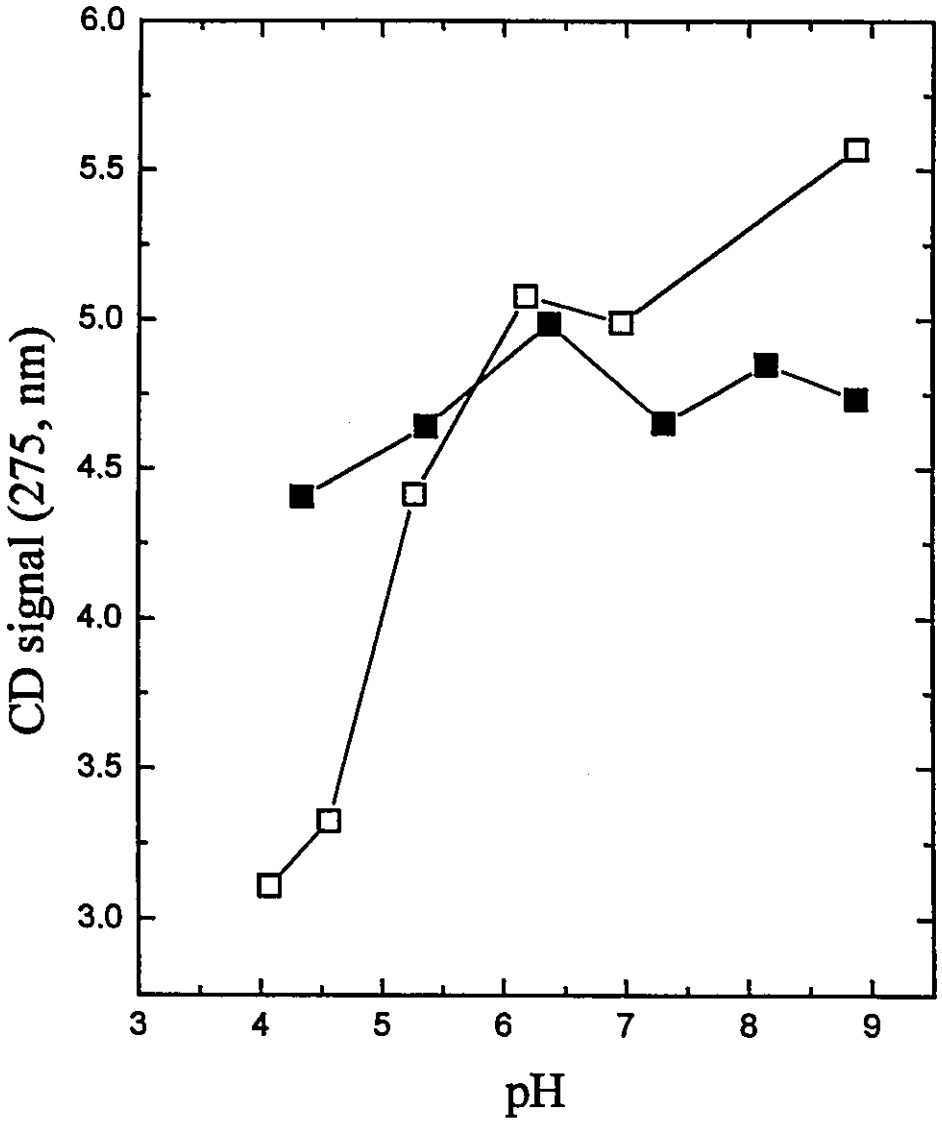

Fig.IV.12. The change of the CD signal of the wild type xylanase (□) and E78C mutant (■) at 275 nm as a function of pH.

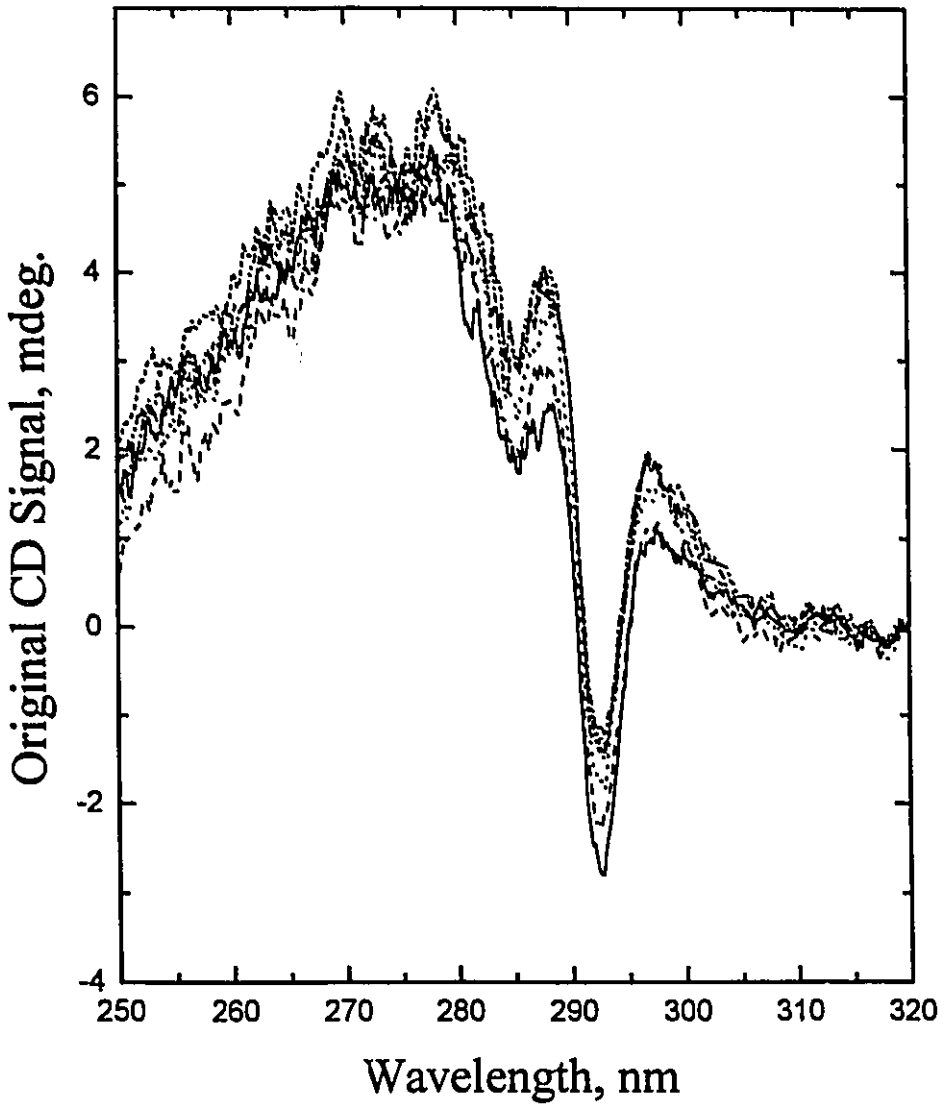

Fig.IV.13. Near-UV circular dichroism spectra of the E78C mutant with protein concentration of about 0.26 mg/mL at different pH conditions.

IV.4.2. An abnormally high pK_a for Glu 172; FTIR evidence

Since the vibrational bands representing the stretching vibrations of carboxyl groups are sensitive to the ionization state, protonation-deprotonation reactions of the carboxyl groups of amino acid side chains of proteins can be conveniently studied by infrared spectroscopy (Chirgadze, *et al.* 1975; Koeppe, & Stroud 1976; Tonge, *et al.* 1989). The FT-IR spectrum in the 1750-1550 cm^{-1} region of *Bacillus circulans* xylanase is dominated by the amide I band with a maximum at 1635 cm^{-1} (Fig.IV.14). The position of this band is highly characteristic of a β-sheet structure (Surewicz, & Mantsch 1988). This is consistent with recent crystallographic data which showed that the secondary structure of *B. circulans* xylanase consists largely of β-strands (Campbell, *et al.* 1993). Next to the amide I band there are two weaker bands at approximately 1588 and 1574 cm^{-1} (Fig.IV.14). Previous studies with model compounds have suggested that the COO^- groups of glutamic acid and aspartic acid should give rise to infrared bands around 1570 and 1585-1590, respectively (Chirgadze, *et al.* 1975). Titration of xylanase in the pH range between 9 and 2 resulted in clearly visible changes in the intensity of the 1574 cm^{-1} band. However, the band at 1587 cm^{-1} remained unaffected by the titration, even when pH was lowered below 2 (data not shown). Based on this observation, it is concluded that in the infrared spectrum of xylanase the relatively broad band contour with a maximum at 1574 cm^{-1} represents COO^- groups of both aspartic and glutamic

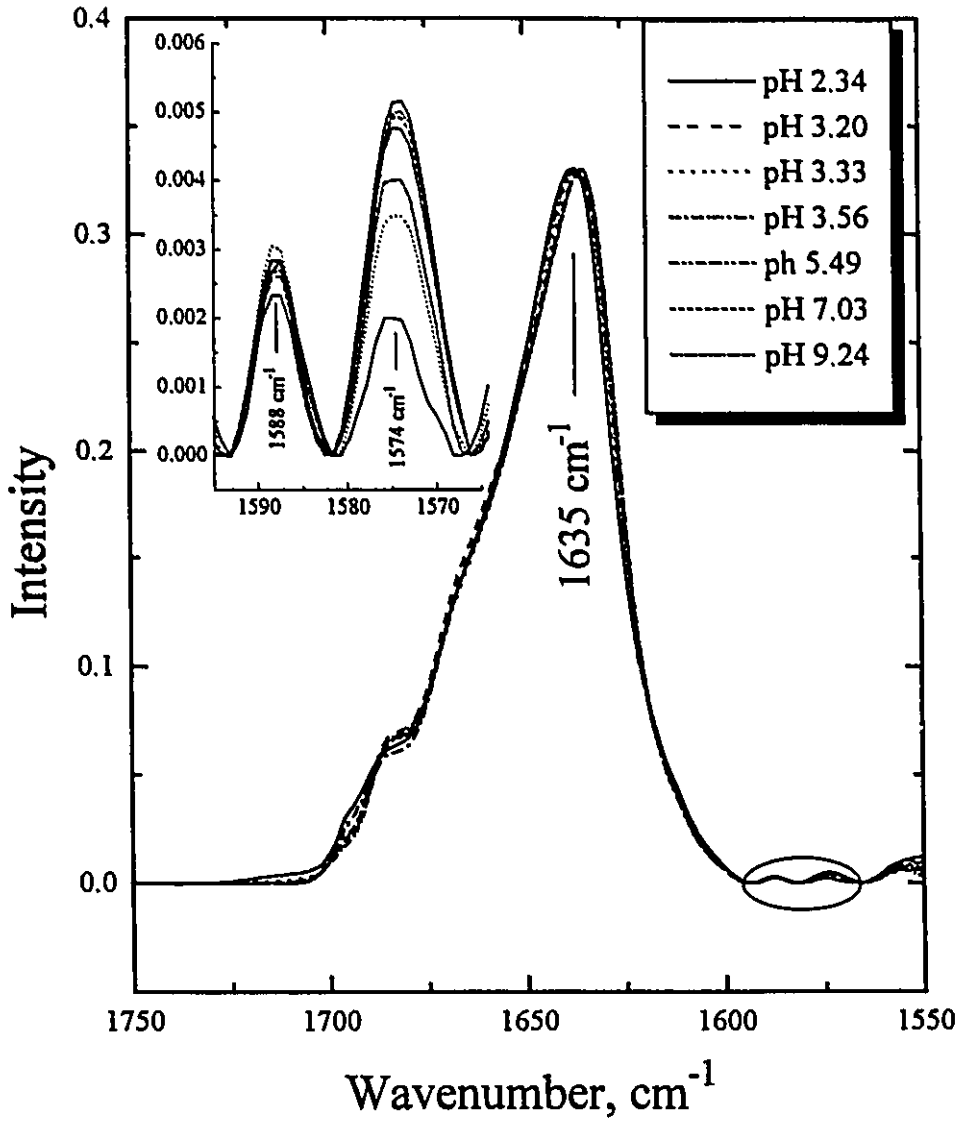

Fig.IV.14. Fourier-transform infrared spectrum of wild type xylanase in the region between 1750 and 1500 cm^{-1} at different pH values. Expansion of spectral region between 1595 and 1565 cm^{-1} is shown in the upper portion of the figure.

acid residues. This is also confirmed by calculating the number of the carboxyl groups that are ionized during the titration. Since the change in the relative intensity in the pH range of 5 to 9 due to ionization corresponds to one carboxyl group, Glu 172, (Fig.IV.15), the total number of carboxyl groups ionized in the whole titration can be calculated. Calculation shows that roughly 10 carboxyl groups are titrated which is exactly the same as number of the acidic residues present in the protein, seven aspartates, two glutamates, plus the C-terminus. The lack of perfect correspondence between the position of COO^- bands in model compounds and in *B. circulans* xylanase likely reflects the effect of environmental factors on the infrared bands of the amino acid carboxyl groups. The bands at 1587 and 1515 cm^{-1} in the spectrum of xylanase (Fig.IV.5) may be tentatively assigned to the side chains of arginine and tyrosine, respectively (Chirgadze, *et al.*, 1975), and the feature at 1551 cm^{-1} represents an amide II band due to residual amide groups which did not undergo hydrogen-deuterium exchange.

The protonation of carboxyl groups is also accompanied by a band at 1708 cm^{-1} that, due to its broad nature, can only be observed if a difference spectrum is obtained (data not shown). The intensity of the valleys of the peaks located between 1500 and 1600 cm^{-1} (Fig.IV.5) is sensitive to the weighting factor used to subtract the spectrum of the buffer; over-subtraction or under-subtraction of the buffer spectrum shifts the whole spectrum to higher

or lower values. Therefore, the buffer subtracted spectrum, as it is, cannot be used to assess the variation of the intensity of the band at 1574 cm^{-1} from one pH value to another. Consequently, a baseline was drawn that connects the minimum points of the peaks (Fig.IV.5). This baseline correction eliminates the buffer subtraction artefacts and also partially removes the contribution of the overlapping residual amide II band which is sensitive to pH. Fig.IV.15 shows the pH titration curves for wild type xylanase and its two variants, E172Q and E78Q. For the wild type protein the plot of the absorbance of carboxyl groups at 1574 cm^{-1} (normalized to the intensity of the amide I band) versus pH shows a pronounced transition with pK_a of 2.8. A second, much weaker but easily detectable and reproducible transition, appears in the pH range between 8 and 5. Without considering the deuterium effect, the apparent pK_a of this transition is 6.8. Importantly, the latter transition disappears upon replacement of either of the two glutamic acids with an uncharged glutamine. This clearly indicates that the transition with pK_a of 6.8 is due to either Glu 172 or Glu 78. It also indicates that, the electrostatic repulsion between two carboxyl groups plays an important role in shifting the pK_a of one of the glutamic acid residues to an abnormally high value. Useful hints regarding the mechanism of this pK_a shift may be obtained by detailed inspections of the crystal structure of xylanase. As in the case of lysozyme, two major factors should be considered as potential sources of carboxylate pK_a shift. These factors are electrostatic interactions of

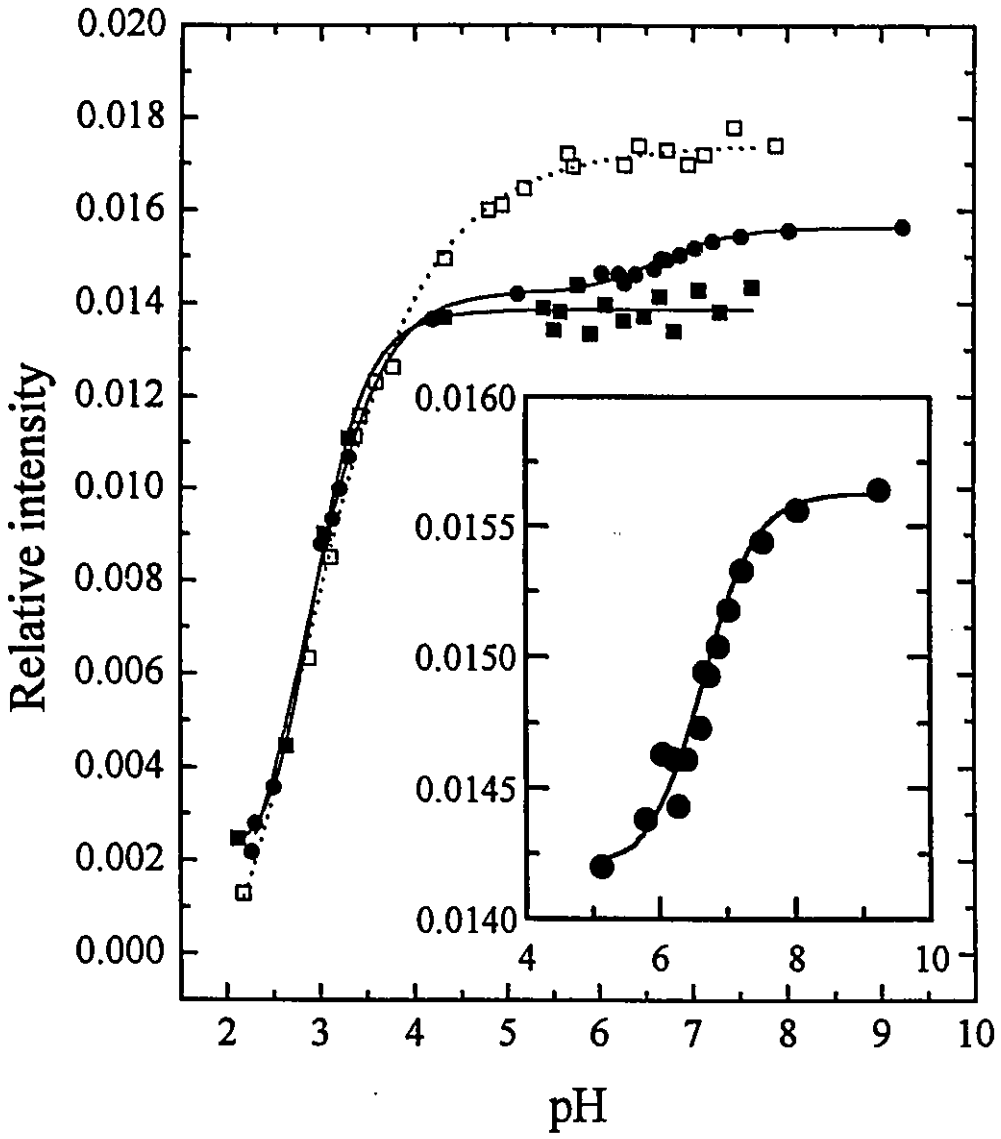

Fig.IV.15. FT-IR titration curve for the wild type xylanase (●), E78Q (□), and E172Q (■) variants. The Y axis represents the intensity of the COO^- band at 1574 cm^{-1} normalized to the intensity of the amide I band. The insert shows the expansion of the titration curve for the wild type protein in the pH range between 9 and 5.

proximal carboxylates (Kuramitsu, *et al.*, 1974) and hydrophobic interactions of carboxyl moieties with nearby chemical groups (Blake, *et al.*, 1967; Rupley, *et al.*, 1967; Inoue, *et al.*, 1992a). Analysis of the glutamate residues in the active site of xylanase reveals that the exposures of Glu 78 and Glu 172 to the aqueous medium are essentially identical. Also the number and type of hydrogen bonds formed between Glu 78 and its surrounding residues are very similar to those experienced by Glu 172 (Davoodi, *et al.* 1995). Thus, glutamic acid at position 78 is hydrogen bonded to Gln 127 and Tyr 69 while Glu 172 forms hydrogen bonds with Asn 35 and Tyr 80 (Fig. IV.1). Furthermore, no major differences can be found in hydrophobic interactions of Glu 78 and Glu 172 with their respective neighbouring groups. The above similarities indicate that it is highly unlikely that hydrophobic interactions are responsible for the carboxylate's abnormally high pK_a value. On the other hand, significant differences can be observed between electrostatic interactions of glutamic acids at position 78 and 172. Glu 78 is involved in strong electrostatic interactions not only with the second glutamic acid but also with Arg 112. The latter residue is located only 5 Å apart from Glu 78. The distance between Glu 172 and active site arginine is much larger, 6.7 Å (Davoodi, *et al.*, 1995), and thus the electrostatic interaction between these residues should be considerably weaker. Glutamic acid 78 in close proximity to positively charged arginine 112 is expected to have a lower pK_a than the more distant Glu 172. All these

factors provide a strong indication that the carboxyl group with a pK_a of 6.8 should be attributed to Glu 172. This is in good agreement with recent NMR study demonstrating that Glu 172 with a pK_a of 6.6 acts as an acid catalyst in *Bacillus subtilis* xylanase (McIntosh, *et al.* unpublished data).

The relative intensity of the FTIR titration curve for the E78Q mutant is slightly higher than that of the wild type protein. This is probably due to an altered tertiary structure of this mutant compared to the wild type protein as indicated by the near UV CD spectroscopy (Fig.IV.16). It is of note that the baseline correction method employed in this study can only be used to follow the variations of the intensity of the band in question when overlapping bands do not change dramatically as a function of pH. Therefore, the FTIR data obtained at extreme pH values are unreliable as the intensity of the residual amide II band that partially overlaps with the band at 1574 cm^{-1} is altered . This offers an explanation as to why the pK_a value of 4.9 for the Glu 78 was not observed in FTIR studies.

IV.5. DESTABILIZING EFFECT OF THE RESIDUES WITH ABNORMAL pK_a VALUES

It is known that the presence of an acidic group with an abnormally high pK_a may result in a decreased stability of the protein structure (Inoue, *et al.*, 1992a; Wyman, 1964). To gain further insight into the molecular interactions

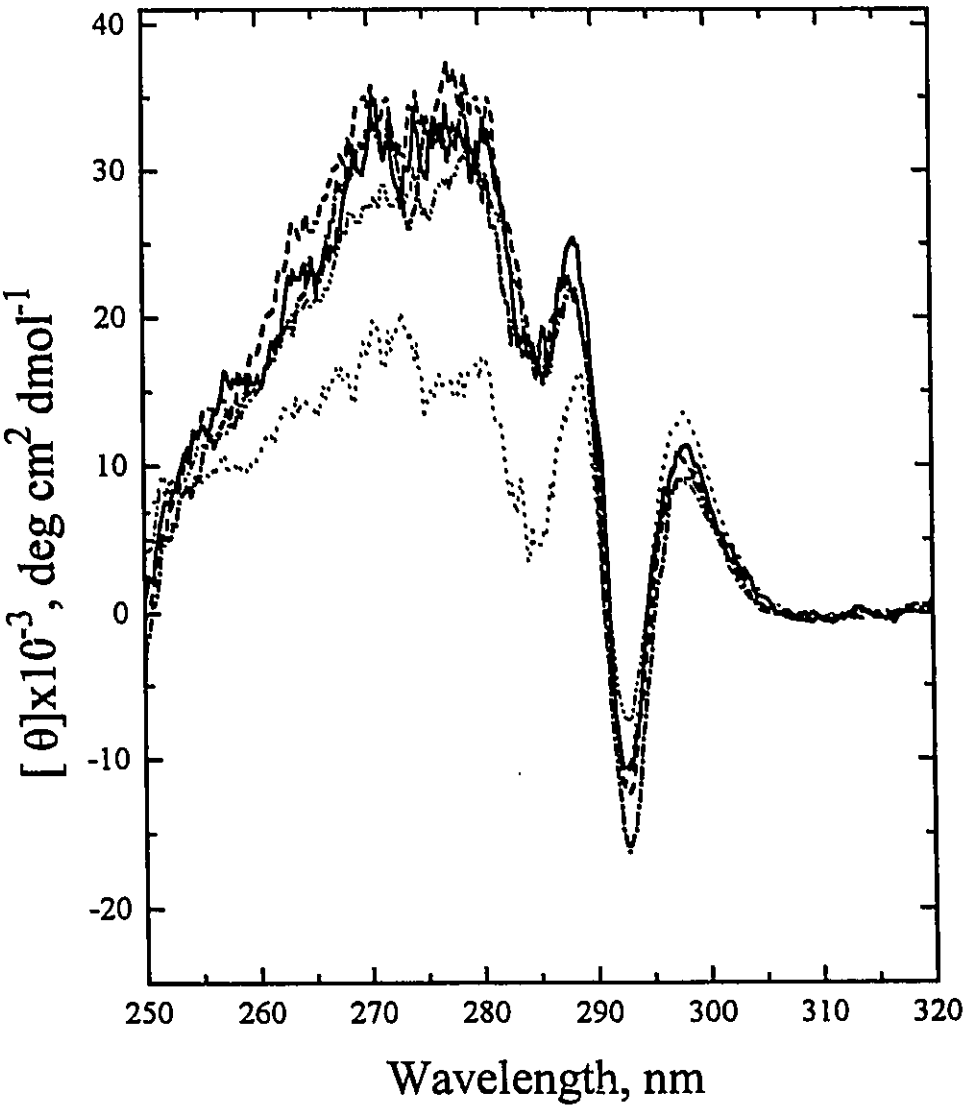

Fig.IV.16. Near-UV circular dichroism spectra of the wild type xylanase (————), E172Q (– – – – –), E78Q (.....), E172C (.__ .__ .__ .__ .__), and E78C (..__ ..__ ..__ ..__) at pH 6.0.

within the active site of *B. circulans* xylanase, the pH dependence of the thermal stability of the wild type enzyme and various mutants in which glutamic acid at position 172 was replaced by other residues was examined. The near-UV circular dichroism spectrum of the E78Q mutant is different from the wild type xylanase (Fig.IV.16) indicating that the E78Q mutant used in the FTIR study might have a somewhat altered tertiary structure. Therefore, to avoid ambiguities in data interpretation arising from potential effects of tertiary structure differences on the stability of xylanase mutants, thermal denaturation experiments were performed using E172C and E78C variants instead of E172Q and E78Q enzymes. Circular dichroism spectra in the near (Fig.IV.16) and far-UV (Wakarchuk, *et al.* 1994a) indicate that the tertiary and secondary structure of both cysteine containing mutants (as well as of the E172D variant used in this study) are essentially identical to that of the wild type protein.

The thermal stabilities of xylanase and its mutants were probed by differential scanning calorimetry. For all proteins studied, the calorimetric denaturation was apparently irreversible. After cooling from the first run, no transition could be detected in a second heating cycle. Furthermore, the calorimetric traces were somewhat scan-rate dependent (data not shown), suggesting that the denaturation process is, at least to some extent, controlled by kinetic factors (Sanchez-Ruiz, *et al.*, 1988; Freire, *et al.*, 1990). The above features preclude the interpretation of our present calorimetric data in terms of

equilibrium thermodynamics. For the purpose of this study, from calorimetric curves, the midpoint denaturation temperatures, t_m, were determined (Fig.IV.17). The t_m values at a given scan rate can be used as a reliable empirical parameter to compare thermal stabilities of various mutant proteins (Kallwass, *et al.*, 1992). The data in this figure show that the replacement of Glu 172 with an uncharged cysteine results in substantial stabilization of the protein. At pH 8, the t_m for the E172C mutant is 7.3° higher than that for the wild type xylanase. Stabilization, although to a considerably smaller degree (4.1° at pH 8), was also observed for the E78C variant. The lesser degree of stabilization of the E78C in comparison to the E172C mutant can be explained in terms of the electrostatic interactions in the active site. Substitution of the Glu 172 with cysteine is accompanied by removal of destabilizing electrostatic repulsion between Glu172 and 78, while the stabilizing attraction between Glu78 and arginine 112 remains intact. In the E78C mutation, however, not only is the destabilizing repulsion between Glu172 and 78 removed, but also the stabilizing attraction between Glu78 and arginine 112 is no longer present. Therefore, the E172C mutant should show a larger increase in stability in comparison to E78C mutant.

The theory originally proposed by Wyman (1964) predicts that the presence of an acidic group with abnormally high pK_a (or a basic group with abnormally low pK_a) should destabilize the protein. Our calorimetric data with

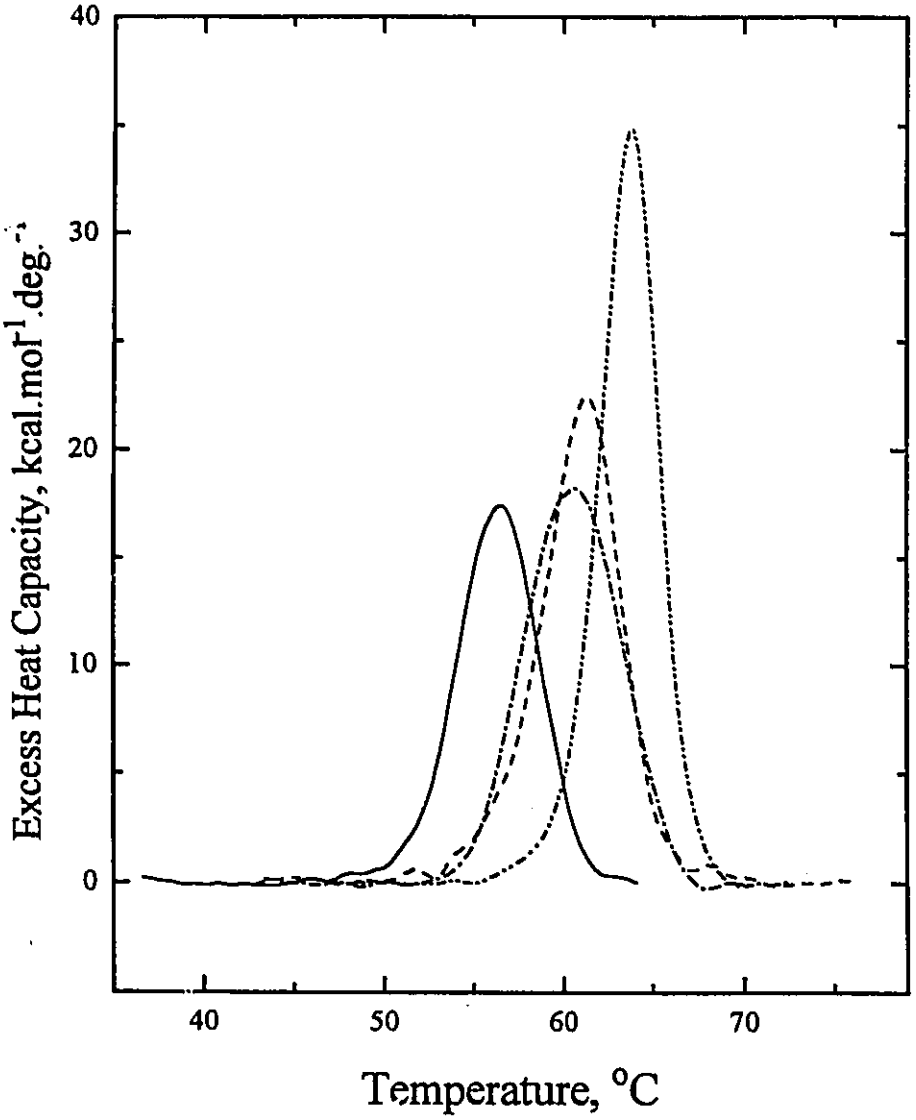

Fig.IV.17. Differential scanning calorimetry thermograms of the wild type xylanase (————), DS1 (– – – – –), E78C (_ _ _ _ _), and E172C (.. .. .. ..), mutants at pH 8.0.

mutant xylanases provide further confirmation of this prediction. Furthermore, they support the notion that the replacement of residues with abnormally high pK_a by site directed mutagenesis may provide very efficient method for stabilization of a protein. Off course, such an strategy is applicable when residues with abnormal pK_a are not created for mechanistic purposes. In this context, it is notable that the substitution of a single residue in the E172C mutant increases the denaturation temperature of the protein by as much as 7.3 degree which is almost twice the increase in the thermal stability in comparison to that of the single disulphide bond mutants at pH 8.0 (Fig.IV.17).

IV.6. DEPENDENCE OF THE STABILITY OF THE WILD TYPE AND MUTANT XYLANASES UPON pH

Calorimetric data reveal that in the pH range between 5 and 8 the stability of wild type xylanase is remarkably sensitive to variations in pH (Fig.IV.18). This pH-dependent stability (see the bell type curve in Fig. IV.19) apparently requires the presence of two carboxylate-containing residues in the active site as it persists for the E172D mutant but the high pH dependent limb disappears when either of the glutamic acids is replaced with an uncharged cysteine residue. The t_m versus pH plot for the wild type xylanase has a bell-type shape, with the t_m at pH 8 being about 3 degrees lower than at pH 5. Taken together, these data clearly suggest that electrostatic repulsion between

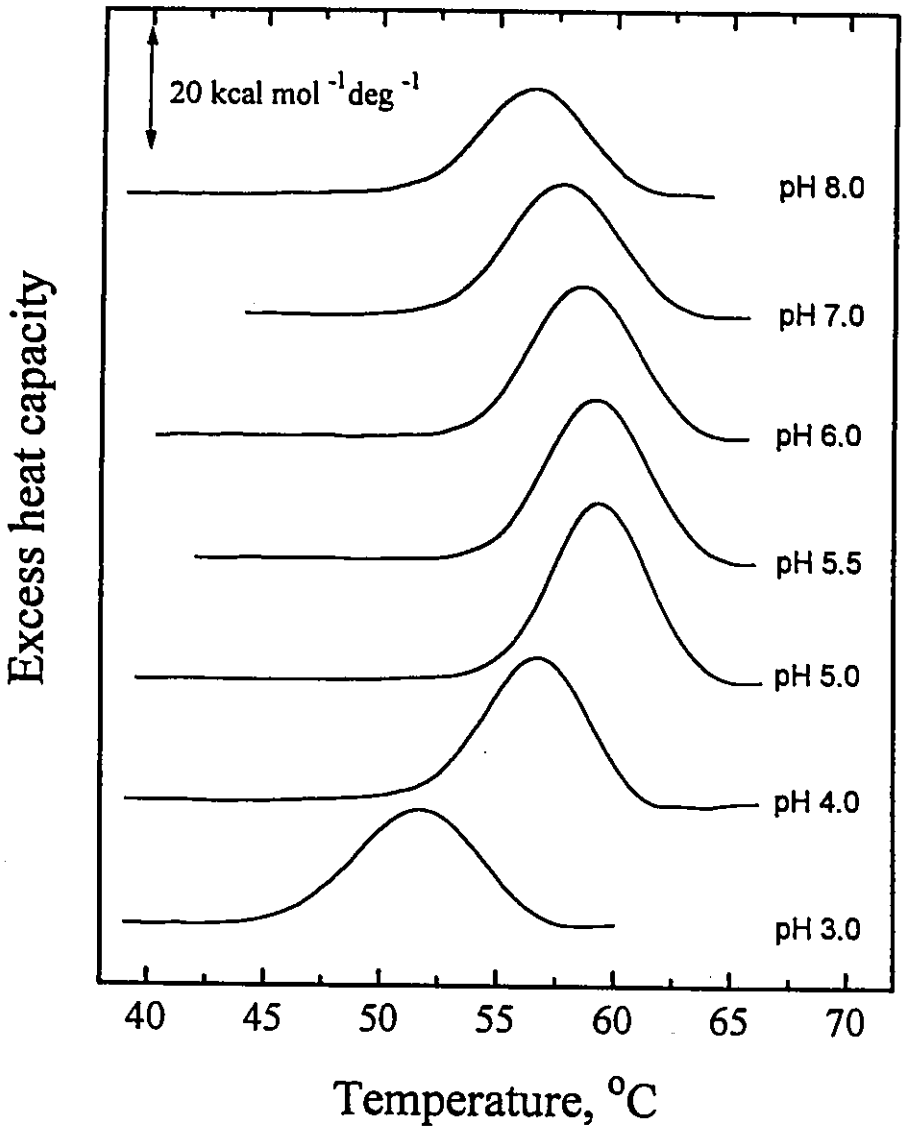

Fig.IV.18. Differential scanning calorimetry thermograms of the wild type xylanase at different pH values.

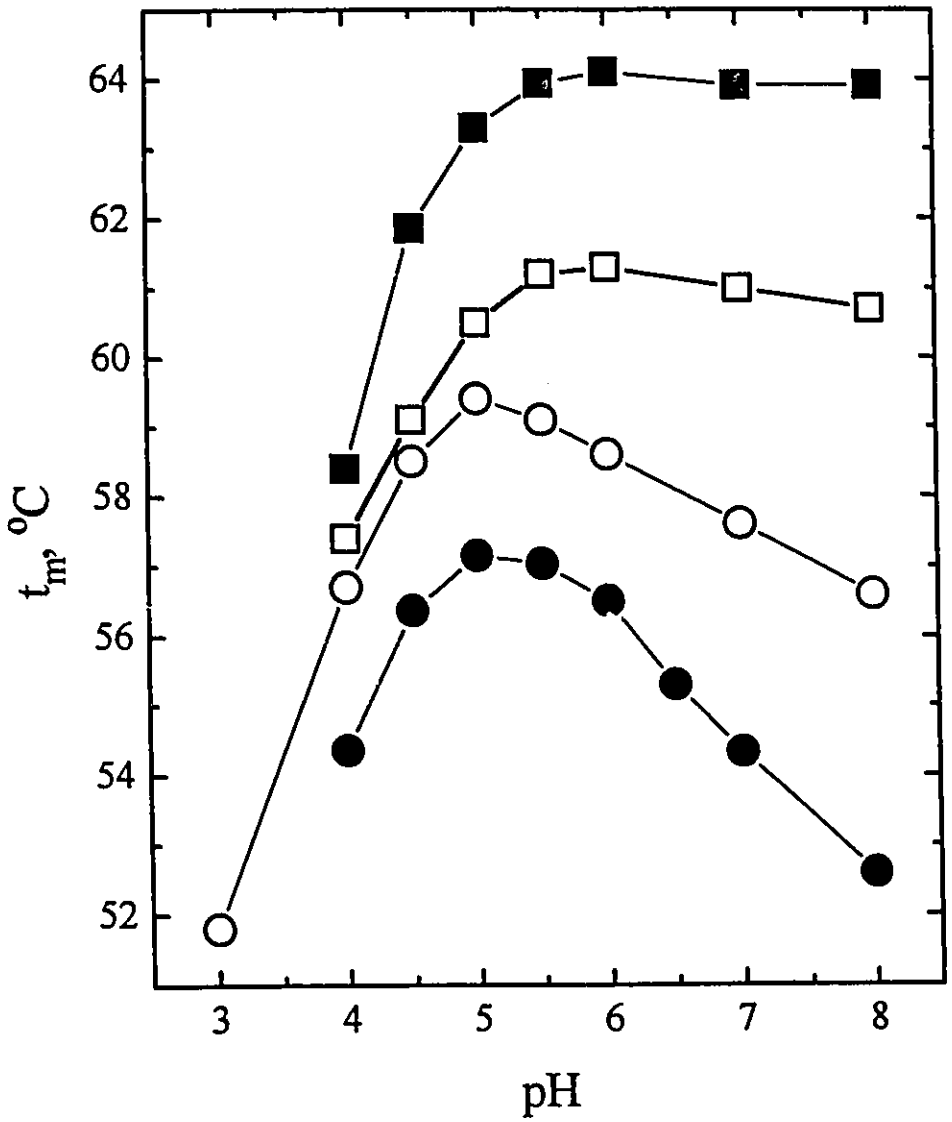

Fig.IV.19. pH dependence of the midpoint denaturation temperature, t_m, for the wild type xylanase (○), E172D (●), E78C (□), and E172C (■) variants.

nearby carboxylate groups (which diminishes as pH is lowered from 8 to 5) is responsible for the decreased stability of wild type xylanase and the E172D mutant at slightly alkaline pH. Thus the calorimetric data provide further support for energetically important interactions between Glu 172 and Glu 78 which can account for the raised pK_a of Glu 172.

Another example of a glycosidase in which glutamic acid acts as an acid catalyst is hen egg-white lysozyme (Phillips, 1967; Chipman & Sharon 1969; Blake, *et al.*, 1967). In the latter enzyme, the active-site Glu 35 has pK_a of 6-6.5 (Imoto, *et al.*, 1972). Despite this general similarity, different factors appear to be responsible for an abnormally high pK_a of active site glutamic acids in lysozyme and *B. circulans* xylanase. In contrast to xylanase, in lysozyme the electrostatic interactions between the two corresponding active site carboxylates are relatively weak and there is no basic residue in the proximity of the carboxylate groups. The abnormally high pK_a of Glu 35 in lysozyme is believed to result largely from a hydrophobic environment of this residue (Inoue, *et al.*, 1992a). From a comparison of these two glycosidases it may be concluded that the enzymes employ two different strategies to raise the pK_a of an active-site glutamic acid in order that it may act as an acid catalyst near neutral pH.

IV.7. SUMMARY AND CONCLUSION

The active site of *Bacillus circulans* xylanase contains two glutamic acids, Glu 78 and Glu 172, which are crucial for catalytic activity of the enzyme. FT-IR and circular dichroism spectroscopy were used to determine the ionization state of these residues as a function of pH. Near-UV CD data of the wild type enzyme showed a structural transition with pK_a of 4.9 which is absent in the E78C mutant. This transition, therefore, is attributed to a change in the protonation state of the glutamic acid 78. Furthermore, for the wild type enzyme, a titration of a carboxylate group occurs at pH 6.8 as monitored by FT-IR. This titration is absent in the E78Q and E172Q variants of the enzyme. These findings taken with previous crystallographic data (Campbell, *et al.* 1993; Wakarchuk, *et al.* 1994a) indicate that glutamic acid at position 172 has an abnormally high pK_a of 6.8. The high pK_a value of Glu 172 is caused largely by electrostatic interactions of this residue with a proximal glutamic acid at position 78. The presence of two nearby negatively charged side chains destabilizes the protein as evidenced by calorimetric measurements. Decreasing pH from 8 to 5.5 or removing either Glu172 or Glu 78 enhances protein stability by decreasing or removing this electrostatic repulsion.

REFERENCES

Ahern, T.J., Casal, J.I., Petsko, G. A., & Klibanov, A. (1987) Control of Oligomeric Enzyme Thermostability by Protein Engineering *Proc. Natl. Acad. Sci. USA* 84, 675-679.

Ahern, T.J.& Klibanov, A. (1987) Analysis of Processes Causing Thermal Inactivation of Enzymes. *Methods of Biochmical Analysis*. 33: 91-127.

Arriaga, P., Menendez, M., Villacorta, J. M.; and Laynez, J., (1992) Differential Scanning Calorimetry Study of the Thermal Unfolding of β-Lactamase I from *Bacillus cereus Biochemistry,* 31, 6603-6607.

Azuma, J. I. & Tetsuo, K. (1988) Lignin-carbohydrate Complexes from Various Sources *Methods in Enzymology* 161, 12-18.

Brems, D. N. (1988) Solubility of Different Folding Conformers of Bovine Growth Hormone *Biochemistry* 27, 4541-4546.

Betz, S.F. (1993) Disulphide Bonde and the Stability of Proteins. *Protein Science*. 2:1551-1558.

Biely, P. (1985) Microbial Xylanolytic Systems. *Trends Biotechnol*. 3, 286-290.

Biely, P. (1991) Biotechnological Potential and Production of Xylanolytic Systems Free of Cellulases *ACS Symp. Ser*. 460, 408-416.

Blake, C. C. F., Johnson, L. N., Mair, G. A., North, A. C. T., Phillips, D. C., & Sarma, V. R. (1967) Crystallographic Studies of the Activity of Hen Egg-White Lysozyme. *Proc. R. Soc. London, Ser.* B 167, 378-388.

Bray, M. R., & Clarke, A. J. (1990) Essential Carboxy Groups in Xylanase A, *Biochem. J*. 270, 91-96.

Campbell, R., Rose, D., Wakarchuk, W., To, R., Sung, W., and Yaguchi, M. (1993) In Proceedings of the Second TRICEL Symposium on *TRICHODERMA REESEI* CELLULASES AND OTHER HYDROLASES, Espoo, Finland, 1993, (Suominen, P. and Reinikainen, T., ed.) Foundation for Biotechnical and Industrial Fermentation Research 8, 63-72.

Cantor, C. R., & Schimmel, P. R. (1980) Conformational Equilibria of

Polypeptides and Proteins: Reversible Folding of Proteins. In *Biophysical chemistry*, Vol. 3, W. H. Freeman and Company, page 1086.

Chipman, D.M. & Sharon, N. (1969) Mechanism of Lysozyme Action. *Science*. 165:454-465.

Chirgadze, Y. N., Fedorov, O. V., & Trushina, N. P. (1975) Estimation of Amino Acid Residue Side-chain Absorption in the Infrared Spectra of Protein Solutions in Heavy Water, *Biopolymers* 14, 679-694.

Clarke, J. & Fersht, A. (1993) Engineered Disulfide Bonds as Probes of the Folding Pathway of Baranase: Increasing the Stability of Proteins Against the Rate of Denaturation. *Biochemistry* 32:4322-4329.

Cleland, J. L., & Wang, D. I. C. (1990) Refolding and Aggregation of Bovine Carbonic Anhydrase B: Quasi-Elastic Light Scattering Analysis *Biochemistry* 29, 11072-11078.

Cooper, A., Eyles, S. J., Radford, S. E., & Dobson, C. M. (1992) Thermodynamic Concequence of the Removal of a Disulphide Bridge from Hen Lysozyme. *J. Mol. Biol.* 225, 939-943.

Creighton, T.E.(1988) Disulphide Bonds and Protein Stability. *BioEssays.* 8:57-63.

Cupo, J. F., & Pace, C. N. (1983) Conformational Stability of Mixed Disulphide Derivatives of β-Lactoglobulin B. Biochemistry 22, 2654-2658.

Davoodi, J., Wakarchuk, W. W., Campbell, R., Carey, P. R., & Surewicz, W. K. (1995) Abnormally High pK_a of an Active-site Glutamic Acid Residue in *Bacillus circulans* Xylanase; The Role of Electrostatic Interactions *Eur. J. Biochem.* 232, 839-843.

Dekker, R. F. H., and Richards G. N. (1976) Hemicellulases: Their Occurrence, Purification, Properties, and Mode of Action *Adv. Carbohydr. Chem. Biochem.* 32, 277-352.

Dekker, R. F. H. (1989) Biodegradation of the Hetero-1,4-linked Xylans, *ACS symp. Ser.* 399, 619-629.

Farrell, R. L., & Skerker, P. S. (1992) Chlorine Free Bleaching with Cartazyme™

HS Treatment. In Visser J. et al eds. *Xylans and xylanases* Amesterdam: Elsevier Science B. V. pp315-324.

Flory, P.J. (1956) Theory of Elastic Mechanisms in Fibrous Proteins. *J. Am. Chem. Soc*. 78:5822-5835.

Freire, E., & Biltonen, R. L. (1978) Statistical Mechanical Deconvolution of Thermal Transitions in Macromolecules. I. Theory and Application to Homogeneuos Systems. *Biopolymers* 17, 463-479.

Freire, E.; Murphy, K.P.; Sanchez-Ruiz, J.M.; Galisteo, M.L.; and Privalov, P.L. (1992) The Molecular Basis of Cooperativity in Protein Folding. Thermodynamic Dissection of Interdomain Interactions in Phosphoglycerate Kinase. *Biochemistry*. 31: 250-256.

Freire, E., van Osdol, O. L., Mayorga, O. L. & Sanchez-Ruiz, J. M. (1990) Calorimetrically Determined Dynamics of Complex Unfolding Transitions in Proteins, *Annu. Rev. Biophys. Biophys. Chem*. 19, 159-188.

Galisteo, M.L., Mateo, P.L. and Sanchez-Ruiz, J.M.(1991) Kinetic Study on the Irreversible Thermal Denaturation of Yeast Phosphoglycerate Kinase *Biochemistry* 30, 2061-2066.

Gebler, J., Gilkes, N. R., Cleayssens, M., Wilson, D. B., Beguin, P., Wakarchuk, W. W., Kilburn, D. G., Miller, R. C., Warren. A. J., & Withers, S. G. (1992) Stereoselective Hydrolysis Catalysed by Related β-1,4-Glucanases and β-1,4-Xylanasese *J. Biol. Chem*. 267, 12559-12561.

Gilbert, J. H. & Hazlewood, G. P. (1993) Bacterial Cellulases and Xylanases. *J. Gen. Microbiol.* 139, 187-194.

Gilkes, N. R., Henrissat, B., Kilburn, D.G., Miller, R. C.Jr, Warren, R. A. J. (1991) Domains in Microbial β-1,4-Glycanases: Sequence conservation, Function, and Enzyme Families *Microbiol. Rev.* 55, 303-315.

Greene, R. F., & Pace, C. N. (1974) Urea and Guanidine Hydrochloride Denaturation of Ribonuclease, Lysozyme, α-Chymotrypsin, and β-Lactoglobulin. *J. Biol. Chem*. 249, 5388-5393.

Gupta, M.N. (1991) Thermostabilization of Proteins *Biotechnology and Applied Biochemistry*. 14, 1-11.

Henrissat, B. (1992) Analysis of Hemicellulases Sequences. Relationship to Other Glucanases. In Visser J. et al eds. *Xylans and xylanases* Amesterdam: Elsevier Science B. V. pp 97-110.

Henrissat, B., Callebaut, I., Fabrega, S., Lehn, P., Mornon, J. P., & Davies, G (1995) Conserved Catalytic Machinery and the Prediction of a Common Fold for Several Families of Glycosyl Hydrolases; Proc. Natl. Acad. Sci. USA 92, 7090-7094.

Hurley, J. H., Baase, W. A., & Matthews, B. W. (1992) Design and Structural Analysis of Alternative Hydrophobic Core Packing Arrangements in Bacteriophage T4 Lysozyme. *J. Mol. Biol.* 224, 1143-1159.

Imoto, T., Johnson, L. N., North, A. C. T., Phillips, D. C., & Rupley, J. A. (1972) Vertebrate Lysozymes, in: *The Enzymes*, vol. r7l (Boyer, P. D., ed.) 665-868.

Inoue, M.; Yamada, H.; Hashimoto, Y.; Yasukochi, T.; Hamaguchi, K.; Miki, T.; (1992a) Stabilization of a Protein by Removal of Unfavourable Abnormal pK_a: Substitution of Undissociable Residue for Glutamic Acid-35 in Chicken Lysozyme; *Biochemistry*; 31:8816-8821.

Inoue, M., Yamada, H., Yasukochi, T., Kuroki, R., Miki, T., Horiuchi, T., & Imoto, T. (1992b) Multiple Role of Hydrophobicity of Tryptophan-108 in Chicken Lysozome: Structural Stability, Saccharide Binding Ability, and Abnormal pKa of Glutamic Acid-35, *Biochemistry* 31, 5545-5553.

Ishikawa, K., Nakamura, H., Morikawa, K., Kimura, S., & Kanaya, S. (1993) Cooperative Stabilization of *Escherichia coli* Ribonuclease HI by Insertion of Gly-80b and Gly-77→Ala Substitution *Biochemistry* 32, 7136-7142.

Kallwass, H. K., Surewicz, W. K., Parris, W., Mcfarlane, E. L. A., Luyten, M. A., Kay, C. M., Gold, M. & Jones, J. B. (1992) Single Amino Acid Substitutions Can Further Increase the Stability of a Thermophilic L-Lactate Dehydrogenase, *Protein Engineering* 5, 769-774.

Kanaya, S., Katsuda, C., Kimura, S., Nakai, T., Kitakuni, E., Nakamura, H., Katayanagi, K., Morikawa, K., & Ikehara, M. (1991) Stabilization of *Escherichia coli* Ribonuclease H by Introduction of an Artificial Disulphide Bond *J. Biol. Chem.*266, 6038-6044.

Kellis, J., Nyberg, K., Fersht, A. R. (1989) Energetics of Complementary Side-Chain Packing in a Protein Hydrophobic Core. Biochemistry 28, 4914-4922.

Ko, E. P., Akatsuka, H., Moriyama, H., Shinmyo, A., Hata, Y., Katsube, Y., Urabe, I., & Okada, H. (1992) Site Directed Mutagenesis at Aspartate and Glutamate Residues of Xylanase from *Bacillus pumilus Biochemical J.* 288, 117-121.

Koeppe, R. & Stroud, R. M. (1976) Mechanism of Hydrolysis by Serine Proteases: Direct Determination of the pKa's of Aspartyl-102 and Aspartyl-194 in Bovine Trypsin Using Difference Infrared Spectroscopy, *Biochemistry* 15, 3450-3458.

Lepock, J.R., Rithcie, K.P., Kolios, M.C., Rodahl, A.M., Heinz, K.A., and Kruuf, J. (1992) Influence of Transition Rates and Scan Rate on Kinetic Simulations of Differential Scanning Calorimetry Profiles of Reversible and Irreversible Protein Denaturation *Biochemistry* 31, 12706-12712.

Lever, M. (1972) A New Reaction for Colorimetric Determination of Carbohydrates, *Anal. Biochem.* 47, 273-279.

Lumry, R., and Eyring, H., (1954) Conformational Changes of Proteins *J. Phys. Chem.*58, 110-120.

Maat, J., Roza, M., Verbakel, J., Stam, H., Santose da Silva, M. J., Bosse, M., Egmond, M. R., & Hagemans, M. L. D. (1992) Xylanases and Their Application in Bakery. In Visser J. et al eds. *Xylans and xylanases* Amesterdam: Elsevier Science B. V. pp349-360.

MacLeod, A. M., Lindhorst, T., Withers, S. G., & Warren, R. A. J. (1994) The Acid Base Catalyst in the Exoglucanase/Xylanase from *Cellulomonas fimi* is Glutamic Acid 127: Evidence from Detailed Kinetic Studies of Mutants *Biochemistry* 33, 6371-6376.

Margarit, I.; Campagnoli, S.; Frigerio, F.; Grandi, G.; Filippis, V.D.; Fontana, A. (1992) Cumulative Stabilization Effets of Glycine to Alanine Substitutions in *Bacillus subtilis* Nuetral Protease. *Protein engineering*. 5:543-550.

Mathews, B. W., (1987) Genetic and Structural Analysis of the Protein Stability Problem *Biochemistry* 26, 6885-6888.

Matsumura, M., Becktel, W. J., Levitt, M., & Matthews, B. W. (1989) Stabilization of Phage T4 Lysozyme by Engineered Disulphide Bonds *Proc. Natl. Acad. Sci. USA* 86, 6562-6566.

Matsumura, M. and Matthews, B.W. (1991) Stabilization of Functional Proteins by Introduction of Multiple Disulphide Bonds. *Methods in Enzymology*. 202:336-356.

Matsumura, M., Signor, G., & Matthews, B. W. (1989a) Substantial Increase of Protein Stability by Multiple Disulphide Bonds *Nature* 342, 291-293.

Matsumura, M., Becktel, W. J., Levitt, M., & Matthews, B. W. (1989b) Stabilization of Phage T4 Lysozyme by Engineered Disulphide Bonds *Proc. Natl. Acad. Sci. USA* 86, 6562-6566.

Mayorga, O.L. & Freire, E. (1987) Dynamic Analysis of Differential Scanning Calorimetry Data *Biophysical Chemistry* 87, 87-96.

Miao, S., Ziser, L., Aebersold, R. & Withers, S. G. (1994) Identification of Glutamic Acid 78 as the Active Site Nucleophile in *Bacillus subtilis* Xylanase Using Electrospray Tandem Mass Spectrometry, *Biochemistry* 33, 7027-7032.

Mitchinson, C. & Baldwin, R. L. (1986) The Design and Production of Semisynthetic Ribonuclease with Increased Thermostability by Incorporation of S-Peptide Analogues With Enhanced Helical Stability *Proteins: Struct. Funct. Genet.* 1, 23-33.

Mitraki, A., Haase-Petingell, C., & King, J. (1991) Mechanisms of Inclusion Body Formation *ACS Symposium Series, Protein Refolding* 470, 35-49.

Nissen, A. M., Anker, L., Munk, N., & Lange, N. K. (1992) Xylanases for the Pulp and Paper Industry. In Visser J. et al eds. *Xylans and xylanases* Amesterdam: Elsevier Science B. V. pp325-337.

Nosoh, Y. & Sekiguchi, T.(1990) Protein Engineering for Thermostability *TIBTECH* 8, 16-20.

Oku, T., Roy, C., Watson, D., Wakarchuk, W., Campbell, R., Yaguchi, M., Jurasek, L., Paice, M. (1993) Amino Acid Sequence and Thermostability of Xylanase A from *Schizophyllum commune. FEBS* 334, 296-300.

Pace, C.N. (1975) The Stability of Globular Proteins. *CRC Crit. Rev. Biochem.* 3:1-43.

Pace, C.N., Grimsley, G. R., Thomson, J. A., & Barnett, B. J. (1988) Conformational Stability and Activity of Ribonuclease T_1 with Zero, One, and Two Intact Disulfide Bonds. *The Journal of Biological Chemistry* 263, 11820-11825.

Pace, C. N., Laurents, D. V., & Thomson, J. A. (1990) pH Dependence of Urea and Guanidine Hydrochloride Denaturation of Ribonuclease A and Ribonuclease T1. *Biochemistry* 29; 2564-2572.

Pace, C. N., & Vanderburg, K.E. (1979) Determining Globular Protein Stability, Guanine Hydrochloride Denaturation of Myoglobin. *Biochemistry* 18, 288-292.

Paice, M. G., Gurnagul, N., Page, D. H., and Jurasek, L. (1992) Mechanism of Hemicellulose-Directed Prebleaching of Kraft Pulp *Enzyme Microb. Technol.* 14, 272-276.

Phillips, D. C. (1967) The Hen Egg-White Lysozyme Molecule, *Proc. Natl. Acad. Sci. USA*, 57, 484-495.

Poland D.C.& Scheraga H.A. (1965) Statistical Mechanics of Noncovalent Bonds in Poly Amino Acids. VIII. Covalent Loops in Proteins. *Biopolymers* 3:379-399.

Privalov, P.L.;(1982) Stability of Proteins: Proteins That Do Not Present a Single Cooperative System *Advances in Protein Chemistry* 35, 1-104.

Privalov, P.L.;(1989) Thermodynamic Problems of Protein Structure *Annu. Rev. Biophys. Biophys. Chem.* 18, 47-69.

Puls, J., Borchman, A., Gottschalk, D., & Weigel, J., (1989) Xylobiose and Xylooligomers, *Methods in Enzymology* 160, 528-536.

Radford, S. E., Woolfson, D. N., Martin, S. R., Lowe, G., and Dobson, C. M. (1991) A Three Dissulphide Derivative of Hen Lysozyme; Structure, Dynamics and Stability *Biochem. J.* 273, 211-217.

Rupley, J. A., Butler, L., Gerring, M., HartdegenF. J., and Pecoraro, R. (1967)

Studies on the Enzymatic Activity of Lysozyme, III. The Binding of Saccharides. *Proc. Natl. Acad. Sci. USA*, 57, 1088-1095.

Sanchez-Ruiz, J.M.(1992) Theoretical Analysis of Lumry-Eyring Models in Differential Scanning Calorimetry *Biophysical Journal* 61, 921-935.

Sanchez-Ruiz, J. M., Lopez-Lacomba, J. L., Cortijo, M. & Mateo, P. (1988) Differential Scanning Calorimetry of the Irreversible Thermal Denaturation of Thermolysin, *Biochemistry* 27, 1648-1652.

Schleif, R. F., & Wensink, P. C. In Practical Methods in Molecular Biology, Springer, Berlin, 1981.

Sears, W. D. & Beychok, S. (1973) Circular Dichroism in *Physical principles and techniques of protein chemisrty*, Part C, Leach, S. J. Ed., Academic, New York, pp. 446-585.

Serrano, L., Horovitz, A., Avron, B., Bycroft, M., & Fersht, A. R. (1990) Estimating the Contribution of Engineered Surface Electrostatic Interactions to Protein Stability by Using Double-mutant Cycles. *Biochemistry* 29, 9343-9352.

Sinnott, M. L. (1990) Catalytic Mechanisms of Enzymic Glycosyl Transfer, *Chem. Rev.* 90,1171-1202.

Strickland, E. H., (1974) Aromatic Contributions to Circular Dichroism Spectra of Proteins, *CRC Review in Biochemistry*, 2, 113-175.

Sung, W. L., Luk, C. K., Zahab, D. M., and Wakarchuk, W. (1993). Overexpresion and Purification of the *Bacillus subtilis* and *Bacillus circulans* Xylanases in Eschericia coli. *Protein Express. Purif.* 4, 200-216.

Surewicz, K. W. & Mantsch, H. H. (1988) New Insight into Protein Secondary Structure from Resolution-Enhanced Infrared Spectra, *Biochim. Biophys. Acta* 952, 115-130.

Takagi, H., Takahashi, T., Momose, H., Inouye, M., Maeda, Y., Matsuzawa, H., & Ohta, T. (1990) Enhancement of the Thermostability of Subtilisin E by Introduction of a Disulphide Bond Engineered on the Basis of Structural Comparison with a Thermophilic Serine Protease *J. Biol. Chem.* 265, 6874-6878.

Timell, T. E. (1967) Recent Progress in the Chemistry of Wood Hemicelluloses, *Wood Sci. Technol.* 1, 45-70.

Tonge, P., Moore, G. R. & Wharton, C. W. (1989) Fourier-Transform Infra-Red Studies of the Alkaline Isomerization of Mitochondrial Cytochrome c and the Ionization of Carboxylic Acids, *Biochem. J.* 258, 599-605.

Tull, D., & Withers, S. G (1994) Mechanism of Cellulases and Xylanases: a Detailed Kinetic Study of the exo-β-1,4-Glycanase from *Cellulomonas fimi Biochemistry* 33, 6363-6370.

Wakarchuk, W. W., Campbell, R., Sung, W., Davoodi, J., and Yaguchi, M. (1994a) Mutational and Crystallographic Analysis of the Active Site Residues of the *Bacillus circulans* Xylanase *Prot. Science* 3, 467-475.

Wakarchuk, W. W., Methot, N., Lanthier, P., Seligy, V., Yaguchi, M., To, R., Campbell, R., Rose, D., & Rose, D. (1992) The 20 kDa Xylanase of *Bacillus subtilis*: A Structure/Function Analysis. In Xylanase and Xylanases Amesterdam: Elsevier Science B. V. pp 439-442.

Wakarchuk, W. W., Sung, W., Campbell, R., Cunningham, A., Watson, D. C., & Yaguchi, M. (1994b) Thermostabilization of the *Bacillus circulans* Xylanase by the Introduction of Disulfide Bonds. *Protein engineering* 7, 1379-1386.

Wells, J.A. (1990) Additivity of Mutational Effects in Proteins. *Biochemistry* 29, 8509-8517.

Wetzel, R. (1987) Harnessing Disulphide Bonds Using Protein Engineering *Trends biochem. Sci.* 12, 478-482.

Wetzel,R., Perry, L.J., Baase, W.A., and Becktel, W.J.(1988) Disulphide Bonds and Thermal Stability in T4 Lysozyme *Proc. Natl. Acad. Sci. USA* 85, 401-405.

White, A., Withers, S. G., Gilkes, N. R., & Rose, D. R. (1994) Crystal Structure of the Catalytic Domain of the 1,4-Glycanase Cex from *Cellumonas fimi Biochemistry* 33, 12546-12552.

Wong, K.K.Y., & Saddler, J.N.,(1992) Trichoderma Xylanases, Their Properties and Application *CRC Rev. Biotechnol.* 12, 413-435

Wyman, J. (1964) Linked Functions and Reciprocal Effects in Hemoglobin: a Second Look *Adv. Protein Chem.* 19, 223-286.

Yaguchi, M., Roy, C., Ujiie, M., Watson, D. C., & Wakarchuk, W. (1992) Amino Acid Sequence of the Low-Molecular-Weight Xylanase from *Trichoderma viride*. In Visser J. *et al* eds. *Xylans and xylanases* Amesterdam: Elsevier Science B. V. pp149-154.

Yang, R.C.A., MacKenzie, C.R., & Narang, S.A. (1988) Nucleotide Sequence of a *Bacillus Circulans* Xylanase Gene *Nucleic Acids Research* 16, 7187.

Yang, R.C.A.; MacKenzie, C.R.; Bilous, D.; and Narang, S.A.;(1989) Hyperexpression of a *Bacillus circulans* Xylanase gene in *Escherichia coli* and Characterization of the Gene Product. *Appl. Environ. Microbiol.* 55:1192-1195.

Zeikus, J. G., Lee, C., Lee, Y.E., & Saha, B. c.(1991) Thermostable Saccharidases. New Sources, Users, and Biodesigns, ACS Symp. Ser. 460, 36-51.

APPENDIX

We know from calorimetry experiments in the presence and absence of urea that protein aggregation is mostly responsible for the observed irreversibility of thermal denaturation. It is therefore reasonable to assume that the enthalpy of this step is negligible in comparison to the reversible step of protein denaturation. Based on this assumption we can say that;

$$Q=\{[U]+[I]\}\Delta HV \qquad \text{A-1}$$

where Q is the heat evolved at any temperature, [U] and [I] are the concentrations of the unfolded state and irreversibly denatured state, ΔH is the total heat (enthalpy) of the process, and V is the volume of the DSC cell. we know that [N] + [U] + [I] = c, where c is the total molar concentration of the protein in the sample cell, thus;

$$Q=\{c-[N]\}\Delta HV \qquad \text{A-2}$$

Differentiation of this equation against temperature (T) leads to;

$$\frac{dQ}{dT}=-\Delta HV\frac{d[N]}{dT} \qquad \text{A-3}$$

A) Wild type xylanase

Thermal inactivation studies show that thermal denaturation of the wild type xylanase obeys a first order rate law. Therefore;

$$\frac{d[N]}{dt} = -K_{app}[N] \qquad \text{A-4}$$

where K_{app} is the apparent kinetic rate constant, which due to the complicated nature of thermal denaturation process cannot be defined in terms of k_1, k_2, and k_3 (see Equation II.4 in Chapter II). Nevertheless, this parameter can be experimentally obtained from thermal inactivation kinetic experiments. Replacement of dt from $\nu = dT/dt$ (ν, the scanning rate, is defined as the rate of temperature increase) in the above equation and its rearrangement results in the following;

$$\frac{d[N]}{N} = -\frac{1}{\nu}K_{app}dT \qquad \text{A-5}$$

Integration of this equation provides the concentration of the native form of the protein as a function of temperature;

$$[N] = [N_o]\exp\{-\frac{1}{\nu}\int K_{app}dT\} \qquad \text{A-6}$$

Differentiation yields

$$\frac{d[N]}{dT} = -[N_o].\frac{K_{app}}{\nu}\exp\{-\frac{1}{\nu}\int K_{app}dT\} \qquad \text{A-7}$$

d[N]/dT from equation A-3 can be replaced with the above equation, therefore;

$$\frac{dQ}{dT} = [N_o]\frac{K_{app}}{\nu}\Delta H.V.\exp\{-\frac{1}{\nu}\int K_{app}dT\} \qquad \text{A-8}$$

Since $Q_t = [N_o]V\Delta H$, we can write;

$$\frac{1}{Q_t}\frac{dQ}{dT} = \frac{K_{app}}{\nu}\exp\{-\frac{1}{\nu}\int K_{app}dT\} \qquad \text{A-9}$$

K_{app} can be obtained from thermal inactivation kinetic experiments. Therefore, it is possible to predict from thermal inactivation kinetics the values of $1/Q_t.dQ/dT$ as a function of temperature and compare it with experimental values obtained from DSC experiments. It is of note that the equation A-9 is concentration independent.

B) DS1 mutant

Thermal inactivation kinetic experiments show that the rate limiting step on the thermal denaturation pathway of the DS1 mutant complies with a second order rate law. Therefore;

$$\frac{d[N]}{dt} = -K_{app}[N]^2 \qquad \text{A-10}$$

Since scanning rate can be defined as $\nu = dT/dt$;

$$-\frac{d[N]}{[N]^2} = \frac{1}{\nu} K_{app} dT \qquad \text{A-11}$$

Integration of the above equation results in;

$$\frac{1}{[N]} - \frac{1}{[N_o]} = \frac{1}{\nu} \int K_{app} dT \qquad \text{A-12}$$

The concentration of the native state as a function of K_{app} can be obtained by rearrangement of this equation;

$$[N]=\frac{[N_o]}{\frac{[N_o]}{\nu}\int K_{app}dT+1} \qquad \text{A-13}$$

Differentiation of this equation provides variation of the concentration of the native state as a function of temperature and K_{app};

$$\frac{d[N]}{dT}=\frac{-\frac{[N_o]^2}{\nu}K_{app}}{\{\frac{[N_o]}{\nu}\int K_{app}dT+1\}^2} \qquad \text{A-14}$$

Replacement of $[N_o]\Delta HV$ with Q_t in equation A-14 and its combination with equation A-3 yields;

$$\frac{1}{Q_t}\frac{dQ}{dT}=\frac{\frac{[N_o]}{\nu}K_{app}}{\{\frac{[N_o]}{\nu}\int K_{app}dT+1\}^2} \qquad \text{A-15}$$

Since the original concentration of the DS1 mutant, the apparent kinetic rate constant (K_{app}), and scanning rate (v) are known, it is possible to predict $1/Q_t.dQ/dT$ from thermal inactivation kinetic experiments and compare it with actual values from differential scanning calorimetry experiments, provided that no other slow step is present on the thermal denaturation pathway of the protein. N_o, the original concentration of protein, appears in the equation which is consistent with thermal inactivation kinetics experiments showing dependence of denaturation rate upon concentration.